IMPLEMENTATION OF A GENERALIZED METHOD FOR THE ANALYSIS OF DEFORMATON SURVEYS

JAMES M. SECORD

October 1985

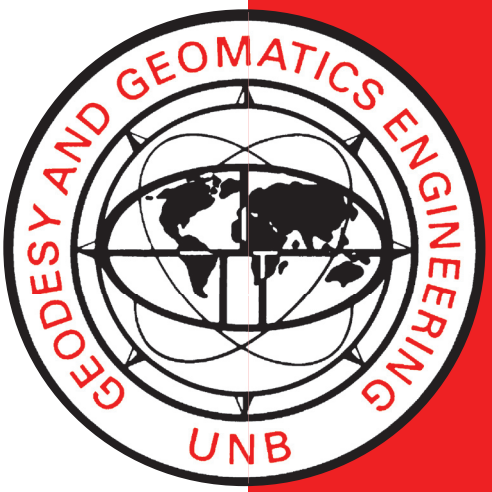

TECHNICAL REPORT
NO. 117

PREFACE

In order to make our extensive series of technical reports more readily available, we have scanned the old master copies and produced electronic versions in Portable Document Format. The quality of the images varies depending on the quality of the originals. The images have not been converted to searchable text.

IMPLEMENTATION OF A GENERALIZED METHOD FOR THE ANALYSIS OF DEFORMATION SURVEYS

James M. Secord

Department of Geodesy and Geomatics Engineering
P.O. Box 4400
Fredericton, N.B.
Canada
E3B 5A3

October 1985
Latest Reprinting May 1996

PREFACE

This report is an unaltered version of the author's M.Sc.E. thesis of the same title which was submitted to the Department in 1984 12.

The thesis advisor for this work was Professor Adam Chrzanowski and financial assistance was in part from the Natural Sciences and Engineering Research Council of Canada.

ABSTRACT

Over the past three years, a generalized method for analysing deformation surveys has been developed at the University of New Brunswick. A number of papers and a Ph.D. thesis have presented a rigorous and unified method which has successfully achieved the ability to apply the same computational procedure to any type of deformation; to be applied to one, two, or three dimensional data with spatial and temporal parameters; to utilize any type of data simultaneously; to be applied to any configuration, even when incomplete or defective; and to allow the use of any type of minimal constraints. The method of analysis follows several steps, from assessing the quality of the observations, through the pursuit of trend and the devising of possible models, to the estimation of model parameters with assessment of the model, its parameters and the choice of the "best" model and its depiction.

Dealing with the implementation of the generalized method, this thesis provides detailed discussion on the inclusion of a variety of non-geodetic observables, on trend analysis, on model selection, and on model parameter estimation using a number of campaigns simultaneously.

In doing so, two main examples are given. One is a reference triangulation network which is isolated with several of the reference stations being unstable. The other is a relative trilateration network for monitoring tectonic movement in California, with 12 years of at least annual campaigns and varying configuration. This method has been found to be flexible and adaptable to an assortment of applications and truly generalized.

TABLE OF CONTENTS

TABLE OF CONTENTS (CONT'D)

LIST OF FIGURES

LIST OF FIGURES (CONT'D)

LIST OF TABLES

ACKNOWLEDGEMENTS

Without the efforts and inspiration of Dr. Chen Yong-qi of the Wuhan Technical University of Surveying and Mapping in the People's Republic of China, there would not have been this method to implement. With the guidance, encouragement, and boundless opportunities for discussion from Dr. Adam Chrzanowski of the University of New Brunswick, there has been much activity, a small part of which has resulted in this thesis.

These graduate studies were made possible through a scholarship from the Natural Sciences and Engineering Research Council of Canada.

Not in the least, Ms. D. Smith is to be commended for her expedient rendering of the author's sinistral script.

1. INTRODUCTION

In order to monitor the deportment of large or complex structures, the reaction of nature to exploitation of its resources, or the behaviour of natural phenomena posing a potential threat to human safety, engineering surveying has encompassed deformation measurements which differ in several aspects from conventional geodetic surveying. The networks are of limited extent or of small aperture, are usually isolated from any external system of coordinates, and must often be considered in a kinematic or a dynamic as well as the usual static sense. In addition to angular, distance, and height difference observables, other measurements in the realm of mechanical, geotechnical, or geophysical engineering are often made about the structure or in the area of interest. The accuracy requirements are likely to be more stringent, especially if the behaviour is of similar magnitude, and there is not usually an opportunity for remeasurement. Consequently, the design, execution, and analysis of such surveys are of particular concern to ensure valid and safe conclusions.

These concerns have been addressed through the objectives of an "ad hoc" committee under Commission 6 of the Fédération Internationale des Géomètres (FIG) -- "Committee on the Analysis of Deformation Surveys" chaired by Dr. Adam Chrzanowski of the Department of Surveying Engineering at the University of New Brunswick since its formation at the FIG 2nd International Symposium on Deformation Measurements by Geodetic Methods at

Bonn in 1978. Originally, there were five centres, known by geographic location, each with its own approach to analysis - Deflt(B-method of testing, data snooping), Fredericton (use of invariant functions of displacements), Hannover (global congruency using analysis of variance), Karlsruhe (analysis of variance, confidence regions for displacement vectors), and Munich (investigation and description considering the datum) (Chrzanowski, 1981). Since then the number of institutes involved has grown to sixteen and the approaches have evolved and expanded.

Born from methods by Lazzarini (1974), Polak (1975, 1978), and Tobin (1983), the Fredericton approach (Chrzanowski, 1981) has recently matured as a "generalized method" through the Ph.D. thesis by Chen (1983). He has tackled many of the concerns in the analysis of deformation surveys. In the development of this approach, several objectives were sought. Earlier discussion (Chrzanowski et al., 1983) has outlined them as follows:

1. applicability of the same computational procedure to any type of deformation,
2. applicability to one, two, or three dimensional data with spatial and temporal parameters,
3. ability to utilize any type of data simultaneously,
4. applicability to any configuration, even when defective or incomplete,
5. ability to allow the use of any type of minimal constraints.

Chen has met these criteria and has gone beyond by presenting a rigorous and unified method for analysis. It is some of the aspects of his thesis and hence the method that are the dealings of this thesis, the author of which has been involved in the development and implementation of the Fredericton approach since 1981.

Activity under the FIG committee has consisted of the sharing of data from several types of networks and of the comparison of the results from the various approaches. In addition to the examples of Chen (1983), recent publications provide discussion of the approach and the results from several networks: Huaytapallana relative network (Chrzanowski et al., 1982c, 1983b), Lohmuehle reference network (Chrzanowski and Secord, 1983a, b), and a simulated relative network (Chrzanowski et al., 1983a).

In the broadest sense, there can be two different intentions for a network - reference and relative. The reference network is intended to create a stable set of stations to which the deformation is referred, and thus, to be situated beyond the influence of the causes of the deformation. Unfortunately, this is not so easily predicted and also, individual station movement may occur from local environmental causes. It is necessary to recognize the ability of the network to serve as a reference and to salvage whatever possible if it fails to do so. On the other hand, the relative network is intentionally established on the deformable body in order to sample the behaviour of the body through the alteration of the configuration. Here, the main problem is with the recognizing, modelling, and substantiating some pattern of behaviour.

Here, particular interest is with two networks. One, the Lohmuehle network, is a reference network in Luxembourg for the monitoring of a hydroelectric power dam. The other is a relative network in California for the monitoring of tectonic plate movement. Applying the generalized method to these examples has prompted a detailed exposition to expand on some of the aspects of Chen's thesis and to clarify the application of others.

To do this, first the method is presented in outline. Next, detailed discussions on trend analysis, model selection, and simultaneous model estimation are given. Following this are the two examples to illustrate the application of the method and then, conclusions and recommendations.

2. OUTLINE OF THE GENERALIZED METHOD

In order that the following chapters can be viewed in their proper context, the generalized method is first presented.

It is intuitive that a successful analysis is one that has resulted in valid conclusions. These can be attained only if the procedures are properly guided by the flow of statistical information through the analysis. As mentioned earlier, the development of the generalized method was aimed at its being able to satisfy several basic criteria. This ability is revealed through an outline of the computational procedures, as taken from Chen (1983) with slight modification. Already mentioned by Chrzanowski et al. (1982c; 1983b), they will be given here in point form by steps, followed by explanation in more detail.

1. establishment of variances and possible correlations among observations within a single campaign of measurement or between campaigns.
2. detection of outliers and systematic errors.
2. a) possible successive iteration of steps 1 and 2.
3. comparison of campaigns for spatial and temporal trend. temporal trend from a series of observations.
4. selection of deformation models.
5. estimation of the parameters for the models of step 4.
6. assessment of the models.
7. possible simultaneous multiple campaign estimation.
7. a) possible successive iteration of steps 4, 5, and 6; 7.

8. choice of the "best" model; computation of deformation characteristics.
9. graphical display of the deformation.

These steps have been depicted in the flowchart of figure 2.1 modified from Chen (1983) and the possible routes that may be followed are shown in figure 2.2.

The quality of any analysis is intimately associated with that of the information used. This is particularly the case when attempting to utilize instrumentation to its limit. With instruments properly calibrated and utilized, knowledge of their variances must be established. In some cases, these may be well known a priori - from previous behaviour and analysis. Otherwise, some method of estimating the variances and possibly correlations must be employed. Chen (1983) has developed the application of the minimum norm quadratic unbiased estimation (MINQUE) to this task quite successfully. However, this method requires that the observations can be reduced to a computational surface, although it may be done in three dimensions as well, since an adjustment or least squares estimation of coordinates is required.

The method of design or preanalysis is especially crucial in deformation monitoring because the parameters are other types of functions of the observables than the conventional coordinates, as discussed in section 4.1. Their magnitudes are likely to be at the same level as the noise of the observations. Hence knowledge of this noise is critical. This has been discussed, with an example, in Chen et al. (1983).

The possibility of correlation between campaigns must be also investigated. If the same instrumentation and observing conditions persist, then such is likely to occur. Consequently, a simultaneous adjustment of the campaigns would be performed (chapter 5). Otherwise,

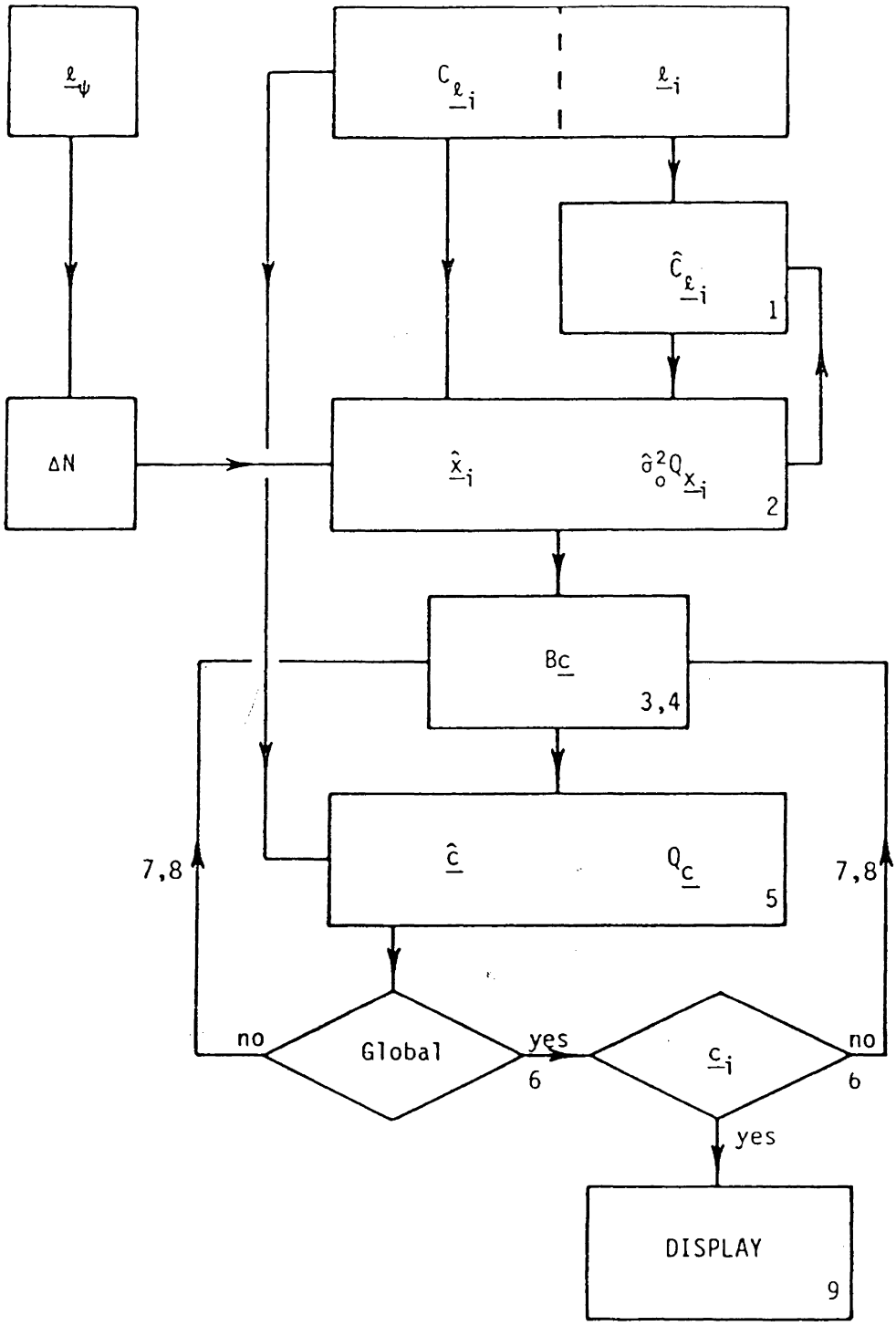

Numerals indicate step numbers

Figure 2.1 Computational Procedures (after Chen(1983))

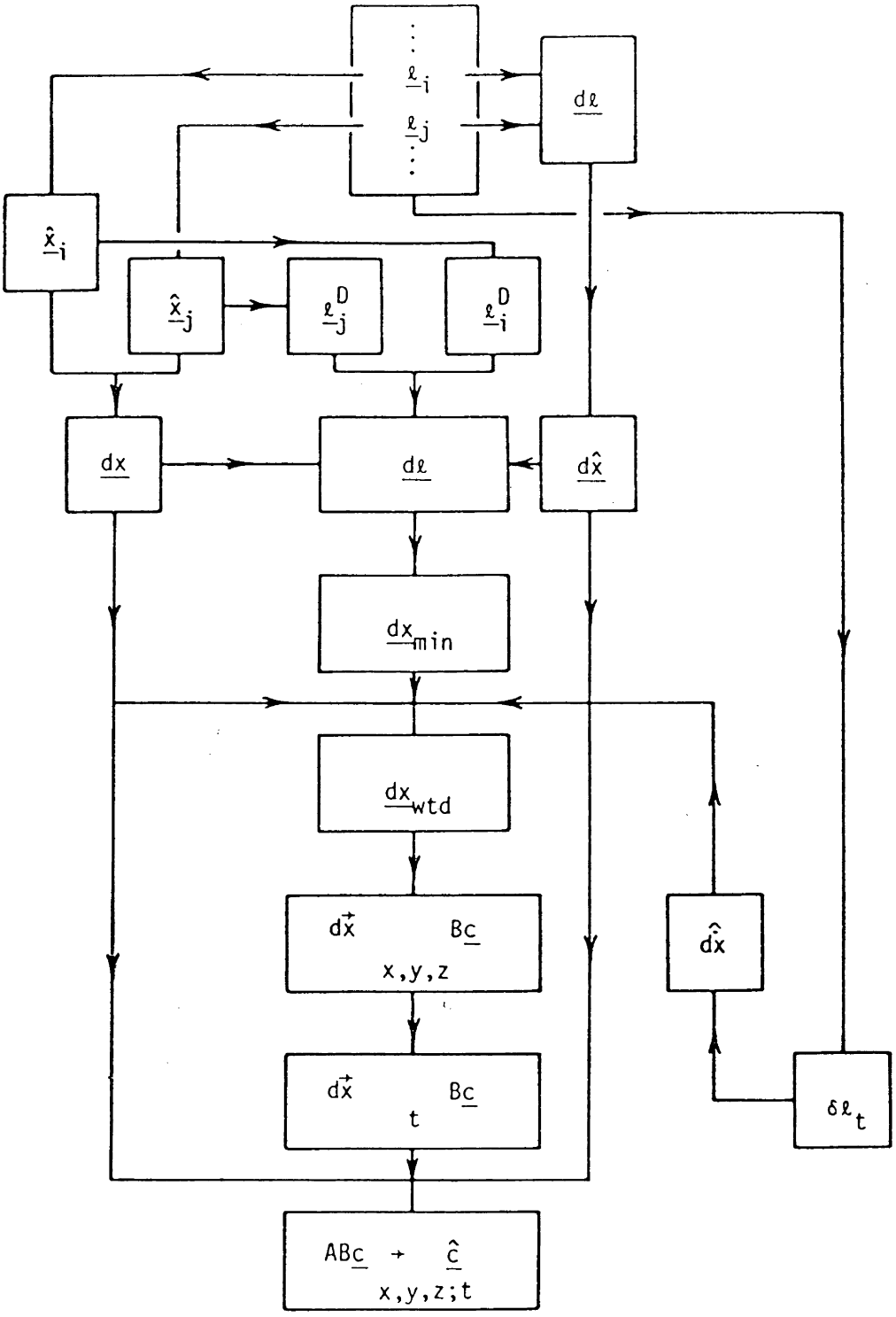

Figure 2.2 Routes through the Generalized Method

separate adjustments would be permitted.

If the observations can be reduced to a computational "surface" (two or three dimensions) and if there is negligible correlation between campaigns, then a least squares estimation of the coordinates for each campaign may be performed. Some useful and necessary byproducts of the estimation or adjustment are the statistical capabilities for detecting outlying observations and systematic errors. This is the purview of conventional geodetic surveying and becomes even more acute due to the stringent accuracy requirements of deformation surveys (Chen, 1983; Vanicek and Krakiwsky, 1982).

Because the outcome of the adjustment has depended on the variances and covariances that were adopted and because the estimated variances and covariances have been affected by the existence of any outliers or systematic errors, then the first two steps may be necessarily successively repeated. The adjustment itself has a rather global indicator of acceptable variance estimates in its estimated variance factor (a posteriori). It is certainly necessary that its compatibility with the a priori value is acceptable before proceeding further.

If, for the above reasons or the observations have been gathered over time intervals that cannot be suitably considered as "instantaneous", then all of the observations would be considered together in a simultaneous estimation of deformation parameters. By consequent necessity, this would include rates or functions of higher orders in time. Hence, any trend would be sought through several campaigns (section 3.2.1).

The actual analysis of the deformation entails the choosing of plausible models and, with statistical guidance, the selection of the "best" model. According to Himmelblau (1970) and as mentioned in

Chrzanowski et al. (1982), the "best" model would possess at least one or a combination of the following:

1. the simplest form or the fewest number of coefficients, either consistent with reasonable error,
2. rationale based on physical grounds,
3. minimal error of fit or between the predicted and empirical values.

The extent to which a model satisfies these criteria is an indication of its "best"-ness.

The supposition of models is guided by information from external sources and by whatever spatial and temporal trend that may be exhibited by the points through the comparisons of campaigns or by the observables through their behaviour through time.

Utilizing the separate adjustments, displacement patterns may be created by comparison of pairs of campaigns, either adjacent or cumulative. Because of the bias and other difficulties associated with the choices in constraining the network to effect the adjustment for each campaign, this comparison warrants special attention, given in section 3.1.

As an alternative, and by necessity if an adjustment is not possible, the changes in each individual observable may be depicted against time. This is very simple when dealing with trilateration, but such a method of trend illustration is not so easily interpreted for angular relationships. If rates of change of angles or distances can be derived, then an estimation of the displacement rates may be performed. However, several conditions are necessary for success, e.g. matching of observations and choice of proper datum, and this is discussed below (sections 3.1.2 and 3.2).

With the attributes of "best" considered, possible or supposed models of the deformation are chosen with regard for the displacement patterns (spatial) and their changes over successive campaigns (temporal) or for the observation change rates and also with regard for any other information e.g. historical or expected behaviour or characteristics of activity obtained from other experts. Depending on the period of the phenomenon, it may be necessary to make the comparisons over time intervals taken by several campaigns to reveal effects over a longer term.

According to the supposed models, parameters are estimated and a measure of the significance of each becomes available. Each model is tested for its global appropriateness and each parameter, group of parameters, or derived parameter, for its significance.

As refinement of the model is likely to follow from this assessment, i.e. a reduction in the number of parameters by removing those that were insignificant and removable, the new model is then considered with estimation and assessment. Hence several iterations of the selection, estimation, and assessment cycle may be executed, with continual regard for the trend displayed through the pairs of campaigns. Some liberty may be taken in order to obtain a model that would be acceptable over a substantial period. However, there is always the danger of having masked long term phenomena. This must be considered with due caution. Although the design of the monitoring scheme had attempted to account for the frequency of the phenomena, there is always the possibility of some unexpected, yet significant, occurrence or the contamination by some systematic effect.

From the comparisons, it may appear that the same spatial model might be considered over several campaigns. Or, from the temporal tendencies of the observables, it may appear that some model in time is appropriate. If so, the coefficients may be estimated using all of the observations simultaneously with index by time. If the observations had been scattered over time so that segregation into campaigns would not be reasonable, then this simultaneous estimation would be mandatory. As with the modelling of the comparisons, the selection, modelling, and assessment cycle may be iterated.

From the successful possibilities, the "best" model is selected with appropriate statistical guidance. The characteristics of the deformation are derived from the estimated parameters, and, if feasible, a graphical display of the deformation is presented.

Through the flowchart of figure 2.1 (after Chen, 1983), the computational steps have been illustrated. Each campaign of measurement results in a vector of observations $\underline{\ell}_i$ which may have an associated dispersion matrix, $C_{\underline{\ell}_i}$, known a priori. If not, the MINQUE principle is followed to estimate the variance components and hence $\hat{C}_{\underline{\ell}_i}$. This requires that, with the model $\underline{\ell} + \underline{v} = A\underline{x}$, a least squares estimation of the coordinates, $\hat{\underline{x}}_i$, must be performed. The outcome of the adjustment, specifically the residuals $\underline{v}_i$, the estimated or a posteriori variance factor $\hat{\sigma}_0^2$, and the possibility of detectable outliers or systematic errors, would affect the MINQUE. Hence, there is a looping or iterative nature to these two steps. In order to alleviate datum defects or configuration defects, pseudo-observations, $\underline{\ell}_\psi$, with corresponding normal equations ΔN, may be inserted. From the displacement

patterns of the comparisons and from a priori information, various models of deformation, $B\underline{c}$, are identified and offered for consideration. The parameters, $\underline{\hat{c}}$ with Q_c, for each of these models are estimated using the adjusted coordinates, $\underline{\hat{x}}_i$ with $\hat{\sigma}_0^2 Q_{\underline{x}_i}$ or the observations $\underline{\ell}_i$ with $C_{\underline{\ell}_i}$ or $\hat{C}_{\underline{\ell}_i}$. Each model is assessed for its global appropriateness under the null hypothesis, H_0: $E\{\underline{\ell}_i\} = \underline{\xi} + A_i B_i \underline{c}$, and for the significance of individual parameters, groups of parameters, or derived parameters under the null hypothesis, H_0: $E\{\underline{c}_i\} \neq 0$. In reaction to the outcome of the testing of the hypotheses, the parameters of revised models may be estimated requiring looping or iteration. From the ultimately acceptable models having only significant parameters, the "best" model is chosen. The estimation and testing may also be done using all of the observations simultaneously, possibly if the campaign comparisons would indicate some suitable tendency and necessarily if the observations cannot be grouped appropriately into campaigns.

Another view of the procedure is given in figure 2.2. A series of "campaigns" has been executed, each resulting in a vector of observations $\underline{\ell}_q$ having n_q individual observations, each being ℓ_{qp}, $p = 1, 2, 3, \ldots, n_q$; $q = 1, 2, 3, \ldots, i, j, k, \ldots$ If possible, the least squares estimates for the coordinates from each campaign, $\underline{\hat{x}}_q$, are obtained with each relative to the same set of minimal constraints on the network, regardless of point stability. From these displacements, $\underline{dx}$, may be derived. If an adjustment is not possible, i.e. if the observations cannot be properly reduced to a computational surface or if the campaigns are too sparsely populated, then observation differences, $\underline{d\ell}$, are taken in the former case, or individual observable values ℓ_{qp} are considered

against time ($\delta \ell_t$) in the latter. The observation differences can be used to estimate displacements $\underline{d\hat{x}}$ by $\underline{d\ell} + \underline{dv} = A\ \underline{dx}$. For stable point analysis, the derived observation differences $\underline{d\ell}$ may be obtained from the displacements $\underline{dx}$ or $\underline{d\hat{x}}$ or from the difference of two sets of observations $\underline{\ell}_i^D$, $\underline{\ell}_j^D$, derived from the adjusted coordinates $\underline{\hat{x}}_i$, $\underline{\hat{x}}_j$. The "best" choice of minimal constraints is made, guided by the stable point analysis and the displacement components $\underline{dx}_{min}$ are estimated under these constraints. This is particularly applicable for a reference network, the stations of which are regarded under the null hypothesis, H_o: $\underline{dx} = 0$. More generally, and especially appropriate to relative networks for which $\underline{dx} \neq 0$, the weighted projection, $\underline{dx}_{wtd}$, may be obtained from any set of minimally constrained displacements. In either case, the displacement components are plotted as vectors $\vec{dx}$ so that a spatial trend might be identified, and with depictions from several campaign comparisons, a temporal trend. From regarding the individual observables against time, $\delta \ell_t$, rates of change of each, $\dot{d\ell}_p$, can be obtained, commonly by linear regression. The same estimation method, $\underline{d\ell} + \underline{dv} = A\ \underline{dx}$, may be used to obtain estimates of displacement velocities $\underline{\hat{dx}}$, which are then regarded in space for both trends. In parallel with the displacement pattern may be several supposed models, $B\underline{c}$. If the tendency would indicate some time dependence, then a simultaneous estimation of the model parameters would be done using all of the observations.

Each stage would flow to the next, provided that the appropriate statistical criteria were met. The campaign adjustments must result in an a posteriori $\hat{\sigma}_o^2$ compatible with the a priori σ_o^2 with due regard for possible outlying observations. Similarly is the case with any of the

estimations of $\underline{d\hat{x}}$ or $\underline{\hat{d\hat{x}}}$. The stable point analysis should yield at least some choice for minimal constraints among the stations not suspected of instability. The displacement vector should be significant at some specified $(1-\alpha)$ level of confidence. Otherwise, statistically, there is no deformation that can be detected by the monitoring scheme. The models should satisfy the global test of appropriateness and also not be unduly littered with ineffective parameters.

Any modelling of deformation must be not only statistically acceptable, but also plausible from the nature of the phenomena involved. Hence, the testing serves as a guide in making decisions along with information from other experts. Symbiotically, the analysis may further enhance knowledge of the phenomena. Hence, there should always be the opportunity for refinement of the monitoring scheme - type, accuracy, and scheduling of observations; location of stations - as well as the modelling.

3. TREND ANALYSIS

The deformation of a body, be it a natural feature or an artificial structure, may be described to some extent by a mathematical modelling of its behaviour over its extent or with respect to its surroundings, i.e. in space, or, in addition, over time. By virtue of its being a function of space and of time, the mathematical model attempts to describe the reaction of an infinitely-membered set of points within the coordinate system. However, the basis for modelling is a very limited, discrete set of points ("stations") at which or among which a finite number of measurements have been made. The supposition of a model leads from any a priori information that is available and, especially, from whatever trend or change is exhibited by the measurements or by the location of the stations. Consequently, it is important that the trend or tendency depicted during the analysis is not biased by systematic error, by inappropriate statements of accuracy, or by datum alteration (shift, rotation, scale change of the "coordinate system") consequent from utilizing unsuitable stations as reference.

With observations having been made during distinct campaigns, pairs of campaigns may be compared using adjusted coordinates if they can be obtained, or using observation differences. Otherwise, the tendency of each observable over time must be considered. Hence, there are two facets of trend analysis - comparison of pairs of campaigns for spatial trend and subsequent temporal trend; and tendency over several campaigns. The pair comparison branches further into either the coordinate approach or the observation approach.

3.1 Trend Analysis Through Comparison of Pairs of Campaigns

The comparison of adjacent and other pairs of compaigns can be made in two ways, depending on the nature of the observations. Rarely is a survey performed in which the vertical and horizontal aspects of the network are compatible in both accuracy and time. Usually the height difference information, if it is gathered at the same time as distances and horizontal angles, is sufficient only for the reduction of the observations to a computational surface and is not of comparable accuracy to resolve the third dimension.

If the observations can be reduced without undue error or if the height differences are known well enough to allow consideration in three dimensions and, at the same time for either, if the network can be considered without multiple configuration defects, i.e. if a two or three dimensional adjustment can be performed, then the coordinate approach may be followed and is advised for several reasons as given below. Otherwise, the observation approach must be used, provided that there is some knowledge of the configuration (e.g. approximate coordinates of observation stations are known).

Under some circumstances, mainly associated with the correlation between campaigns, these two approaches are equivalent. The effect of this correlation and its neglect is discussed after the two approaches have been presented.

3.1.1 Coordinate Approach

In following this approach, there are already the same difficulties that plague conventional geodetic surveys: poorly defined or incomplete connection to a system of coordinates - datum defect; incomplete connection among the stations within the network - configuration defect; and the possible existence of systematic errors or outlying observations. Their impact is even more pronounced in engineering surveys. Usually the network is isolated from any system of coordinates that could serve as an external reference. Consequently the definition of a datum is strongly dependent on the stability of several stations within the network. It can also happen that some of the observations, e.g. a hanging distance or line of sight, although repeated in each campaign, cannot furnish sufficient information on the position of a station because there is no other connection to it. Hence, there is more likely to be configuration defects involving single stations or the joining between sections of a network. The nature and magnitude of movement associated with the phenomena will likely require the ultimate in measurement accuracy making the impact of systematic errors or outliers more contaminative. Also, there is the danger that, when undetected, they would be interpreted as part of the behaviour.

Compensating for the datum and configuration defects allows the estimation of coordinates and, along with it, the pursuit of systematic errors and outliers and the estimation of variance components. Subsequent to such a so-called special solution, the weighted projection may be applied to obtain displacements independent of the choice of datum.

3.1.1.1 Defect of Datum and Configuration

A single campaign of n_{ℓ_i} observations may be represented by the vector $\underline{\ell}_i$ each element of which holds a functional relationship with the position of a pair or triplet of points. Each observation, $\ell_j \in \underline{\ell}_i$ has an associated variance, $\sigma_o^2 q_{jj}$, which is a measure of the dispersion of $\underline{\ell}_i$ by $D\{\underline{\ell}_i\} = \sigma_o^2 Q_i$ so that $P_i = (\sigma_o^2 Q_i)^{-1}$. The position of each point in some three-dimensional Cartesian coordinate system is represented by a vector $(x, y, z)^T$ as illustrated in figure 4.2. Each of these three-element vectors is a hyper-element of the hyper-vector of unknown parameters, $\underline{x}$, which has 3p elements if there are p stations in the network. The functional relationship may be expressed in matrix form by

$$\underline{\ell} + \underline{v} = A\underline{x} \quad \text{or} \quad \underline{v} = A\underline{x} - \underline{\ell} \tag{3.1}$$

in which the n_{ℓ_i} by 3p matrix A is the first-order design matrix or configuration matrix, i.e. $A = \left[\frac{\partial \underline{v}}{\partial \underline{x}}\right]$.

In an isolated network, this fully dimensioned matrix will be rank defective according to the number of datum parameters or degrees of freedom of movement of the configuration in space that have not been accounted plus the number of configuration defects. Hence, the matrix of normal equations, $N = A^T PA$, will be singular and a regular inverse cannot be obtained. That is, the system of equations, $N\underline{x} = \underline{u}$ with $\underline{u} = A^T P\underline{\ell}$, has an infinite number of solutions, $\underline{x} = N^g\underline{u}$, N^g being the generalized inverse of N, and the $\underline{x}$ are not estimable.

These datum parameters express the connection between the configuration of stations in the network and the system of coordinates in which the $\underline{x}$ are described. If totally isolated, the configuration can have any position and any orientation with respect to the axes of the system and, if no distance has been measured, also any scale. For a three

dimensional network, the maximum number of datum defects is seven: δx, δy, δz; ω_x, ω_y, ω_z; k for translation parallel to each axis; rotation about each axis; and scale. For two dimensions there could be as many as four: δx, δy; ω_z; k with rotation only in the x, y plane. For a one dimensional, vertical or levelling, network there could be the one shift or translation, δz. Thus, the two- and one-dimensional networks are subsets of the three-dimensional and dealing with them can be extracted from what follows.

In conjunction with its being singular, the matrix N shares the same null space as the matrix A, i.e. $NH = 0$ following from $AH = 0$. The matrix H expresses the datum defects of the configuration described by A and is used later in the weighted projection. For a fully defective network, the matrix H would be $3p$ by 7, i.e.

$$H = \begin{array}{c} \begin{matrix} \delta_x & \delta_y & \delta_z & \omega_x & \omega_y & \omega_z & k \end{matrix} \\ \begin{bmatrix} 1 & 0 & 0 & 0 & (z-\bar{z}) & -(y-\bar{y}) & (x-\bar{x}) \\ 0 & 1 & 0 & -(z-\bar{z}) & 0 & (x-\bar{x}) & (y-\bar{y}) \\ 0 & 0 & 1 & (y-\bar{y}) & -(x-\bar{x}) & 0 & (z-\bar{z}) \end{bmatrix} \end{array} \begin{matrix} \\ x \\ y \\ z \end{matrix}$$

with a row for each coordinate and a column for each defect. The coordinate values have been reduced to the centroid $(\bar{x}, \bar{y}, \bar{z})^T$ of the network, for which

$$\bar{x} = \frac{1}{p} \sum_{i=1}^{p} x_i \; ; \quad \bar{y} = \frac{1}{p} \sum_{i=1}^{p} y_i \; ; \quad \bar{z} = \frac{1}{p} \sum_{i=1}^{p} z_i \quad .$$

In order to effect a solution to the system $N\underline{x} = \underline{u}$ and, at the same time, to allow the observations to conform among themselves in the least squares sense, the datum defect may be removed by constraining the

freedom of movement of the configuration in only so many ways as would be necessary for both conditions to exist - by minimal constraints. In the convention of geodetic surveys, there are commonly two ways of constraining: explicit and inner minimal constraints. Further, in the context of comparing adjustments, Prescott (1981) has proposed outer minimal constraints.

Whatever constraints are imposed, a datum is defined by the constraint equation $D^T\underline{x} = 0$ affecting certain $x_i \in \underline{x}$, either individually or severally in a functional relationship dictated by some pseudo-observation. The rank of D is the number of defects that have been removed. Each results in a biased form of displacements since the $\underline{x}$ are not estimable. The weighted projection, as proposed by Chen (1983), is independent of the choice of datum and hence is attractive for use as the "best" depiction of displacements.

With the explicit minimal constraints which result in a special solution, $\hat{\underline{x}}_S$, the defects are removed by augmenting the vector of observations and the design matrix with pseudo-observations and by reducing the design matrix and vector of parameters by adopting some of the coordinates as known. The pseudo-observations are given values that would conform with the a priori approximate coordinates to ensure compatibility with and convergence to the solution. Theoretically, these pseudo-observations would be ascribed infinite weight, i.e. zero variance, but for computational stability they are assigned values which as standard errors would be two orders of magnitude smaller than that of the real observations in order that the variance propagation is not distorted by noise from them. For example, if directions were $\pm$ 2", then an azimuth constraint would be $\pm$ 0.01" and if the coordinates were considered to be

0.001 m, then a distance would be $\pm$ 0.00001 m or smaller. The variety of choice comes from the assortment of real observations. The measurement of a distance would remove k. An azimuth would remove ω_z while two zenith angles, in planes ideally perpendicular, would remove ω_x and ω_y. By adopting one set of coordinates as known, the translation components could be removed. As an alternative to the zenith angles, two other z coordinates, suitably located, could account for any tilt.

The system is now somewhat altered from the original and may be considered as

$$\begin{bmatrix} \underline{\ell} \\ \underline{\ell}_\psi \end{bmatrix} + \begin{bmatrix} \underline{v} \\ \underline{v}_\psi \end{bmatrix} = \begin{bmatrix} A_{11} & A_{12} \\ A_{21} & A_{22} \end{bmatrix} \begin{bmatrix} \underline{x}_s \\ \underline{x}_c \end{bmatrix} \tag{3.2}$$

with

$$\begin{bmatrix} P & 0 \\ 0 & P_\psi \end{bmatrix}$$

and originally

$$A = [A_{11}\ A_{12}],\ \underline{x} = \begin{bmatrix} \underline{x}_s \\ \underline{x}_c \end{bmatrix}$$

There are now the additional pseudo-observations $\underline{\ell}_\psi$ of azimuth, zenith angle, or distance with pseudo-weight matrix P_ψ. Some of the original $x_i \in \underline{x}$ have been "fixed", $\underline{x}_c$, so that the only unknowns considered are in the smaller vector, $\underline{x}_s$, the special solution. So,

$$\hat{\underline{x}}_s = N_s^{-1} \underline{u}_s,\quad C_{x_s} = \sigma_o^2 N_s^{-1},\quad \hat{\sigma}_o^2 = \frac{1}{\nu} [\underline{v}^T\ \underline{v}_\psi^T] \begin{bmatrix} P & 0 \\ 0 & P_\psi \end{bmatrix} \begin{bmatrix} \underline{v} \\ \underline{v}_\psi \end{bmatrix}$$

with

$$N_s = \begin{bmatrix} A_{11} \\ A_{21} \end{bmatrix}^T \begin{bmatrix} P & 0 \\ 0 & P_\psi \end{bmatrix} \begin{bmatrix} A_{11} \\ A_{21} \end{bmatrix} \; ; \; \underline{u}_s = \begin{bmatrix} A_{11} \\ A_{21} \end{bmatrix}^T \begin{bmatrix} P & 0 \\ 0 & P_\psi \end{bmatrix} \begin{bmatrix} \underline{\ell} \\ \underline{\ell}_\psi \end{bmatrix}$$

$$\nu = n_\ell - d - n_x = (n_\ell + n_{\ell_\psi}) - n_{\ell_\psi} - \dim(\underline{x}_c) - \dim(\underline{x})$$

As shown in the examples of chapter 6, the result at any station of the propagation of variance through the network from the fixed stations varies noticeably with the choice of those stations. This is also true for the displacement vectors.

In the comparison of adjusted coordinates from repeated surveys under the same explicit minimal constraints, the movements of some of the points is restricted. Any coordinate having a stipulated constant value would have a displacement component of zero. If an azimuth had been imposed, the movement of the reference sight (i.e. station Q as shown in figure 4.2) would be constrained to occur along that azimuth. The horizontal components of relative movement between P and Q, i.e. $dx_{PQ} = dx_Q - dx_P$ and $dy_{PQ} = dy_Q - dy_P$, are not independent and are functionally related by $\tan \alpha = \frac{dx_{PQ}}{dy_{PQ}}$. This would be reflected in the equation $D^T \underline{dx}_s = 0$.

Another method which is often used in geodetic surveys is termed inner minimal constraints (Blaha 1971; Brunner, 1979; Brunner et al., 1981; Leick, 1982; Prescott, 1981; Welsch 1979; Vanicek and Krakiwsky, 1982). The centroid, $(\bar{x}, \bar{y}, \bar{z})^T$, rather than a real station is used in the imposition of the constraints. Its coordinates become fixed, rotations about it... are made to zero, and scale emanating from it is dictated. In a horizontal network the displacements are confined through the datum equations $D^T \underline{x}_I = 0$ which are, in effect, the following summations:

1. $\sum_{i=1}^{P} d_{x_i} = 0$ and $\sum_{i=1}^{P} dy_i = 0$, the algebraic sum of the individual displacement components is each zero;
2. $\sum_{i=1}^{P} (y_i dx_i - x_i dy_i) = 0$, the net rotation about $(\bar{x}, \bar{y}) = (0, 0)$ is zero;
3. $\sum_{i=1}^{P} (x_i dx_i - y_i dy_i) = 0$, the net change in scale is zero.

Now, the original system, i.e. $\underline{v} = A\underline{x} - \underline{\ell}$, is maintained, but the solution is obtained through minimizing $\underline{v}^T P \underline{v}$ under the condition that $D^T \underline{x}_I = 0$. So,

$$\hat{\underline{x}}_I = N^g \underline{u}, \quad C_{x_I} = \sigma_o^2 N^g$$

with $N^g = (A^T PA + HH^T)^{-1} - H(H^T HH^T H)^{-1} H^T$ which is a pseudo-inverse of N (Chen, 1983; Leick, 1982).

This method of solution has been advocated (e.g. Brunner, 1979; Leick, 1982) since it may be obtained from any choice of special solution through a similarity transformation and these "inner coordinates" are independent of such a choice (see also section 3.1.1.4 and Chen (1983)). Prescott (1981) similarly recognized their value since they weakly depend on any single station whereas the explicit constraints are very strongly influenced. He went further to propose a method of outer constraints which would favour deformation in a specified direction by rotation of the axis to some more physically suitable orientation as might be desired for a relative network about a strike slip fault. This outer constraints solution can also be obtained from a special solution through a suitable transformation.

Unfortunately, these implicit means of constraining still refer to an artificial datum, the centroid of the network, which is not necessarily really fixed, depending on the deformation phenomena. If there is a great

deal of relative movement among the stations or between sections of a network then the two configurations resulting from two survey campaigns would have different centroids or their movement may not have been primarily along the direction specified. Certainly there would be cases in which either would be suitable. But, this supposes very good knowledge of the phenomena. In order to arrive at some trend without bias, then some general view should be taken, at least to substantiate the choice of constraints. Consequently, the weighted projection was developed by Chen (1983) and is discussed here in section 3.1.1.4.

3.1.1.2 Stable Point Analysis

Due to the possibility of bias being introduced in the depiction of displacements by the change in datum between campaigns, it is desired to establish a datum that can be regarded as stable for the purposes of a monitoring survey. As mentioned in section 3.1.1.4, the weighted projection offers one such method, especially applicable in relative networks. It is a general method that can be applied to any type of network; however, there may be circumstances under which it is desired or necessary to refer to several actual stations, such as for a reference network. The obvious difference is between the two types of network. In a relative network, there is strong suspicion that the stations have moved in some pattern or some grouping, against another, so that the basis for investigation is the assumption that $\underline{dx} \neq 0$. On the other hand, a reference network is intended to serve as some stable basis for monitoring, so H_0: $\underline{dx} = 0$. The Fredericton approach in its earlier form (Chrzanowski et al., 1981) entailed a suitable method by examining the invariant functions of displacements (Tobin, 1983) based on earlier efforts by Polak (1978) and Lazzarini (1974).

Depending on the nature of the information available, this can be done in several ways. Here, it is assumed that the individual campaign network adjustments can be performed. Nonetheless, the observation approach can also be extended to the same type of analysis. Just as the measurement of angles and distances among the stations of a network define the geometric relationships among the stations and hence the configuration but cannot by themselves determine the positions within a system of coordinates, angles and distances that are derived from adjusted coordinates recover the geometric relationships with independence of the choice of datum or definition of the coordinate system (except for possibly scale).

This recovery capability can be utilized to investigate how the geometric relationship among triplets of points (horizontal angles) and between pairs of points (horizontal distances) has changed between campaigns. If the change is significant, it would indicate that the relative stability of the triplet or pair should be suspected. By accounting for the instabilities through a hierarchy of suspected points, the segregation of unstable points can be made with some guidance in the choices of stations that are likely stable enough to be involved in the minimal constraints on the network. The method in the most general sense for horizontal networks is outlined below. The third dimension may also be examined by considering dz as dℓ, a change in the vertical distance between a pair of stations.

Two campaigns of measurement, $\underline{\ell}_i$, $\underline{\ell}_j$ have been adjusted using minimal constraints, not necessarily the same. These adjustments provide sets of coordinates and their respective variance-covariance matrices:

$$\underline{x}_i = \begin{bmatrix} \hat{\underline{x}}_i \\ \underline{x}_{c_i} \end{bmatrix} \text{ with } Q_i = \begin{bmatrix} N_i^{-1} & 0 \\ 0 & 0 \end{bmatrix} \text{ and } \hat{\sigma}^2_{o_i}, \ \nu_i ;$$

$$\underline{x}_j = \begin{bmatrix} \hat{\underline{x}}_j \\ \underline{x}_{c_j} \end{bmatrix} \text{ with } Q_j = \begin{bmatrix} N_j^{-1} & 0 \\ 0 & 0 \end{bmatrix} \text{ and } \hat{\sigma}^2_{o_j}, \ \nu_j .$$

Organization is facilitated if the coordinate components are in the same order in both campaigns. There may be some stations that are in one campaign but not in the other; however, the common station coordinates may be extracted along with the appropriate rows and columns from the cofactor matrices. This can also be done if some stations are to be considered as grouped together, e.g. reference block as opposed to object points.

If there are p_i stations in the network but only p_c common or in the group, then the extraction entails

$$\underline{x}_i^c = S\underline{x}_i \quad \text{with} \quad Q^c = SQ_iS^T$$

with S being a $2p_c$ by $2p$ array of identity matrices, a row for each common coordinate, a column for each coordinate of $\underline{x}_i$.

The derived observations are generated using a model similar to that used in the original adjustment. Now, however, all possible adjacent angles and all possible one-way distances about each station are generated. For a group of p_c stations, this would result in $p_c(p_c-1)$ angles and $\frac{p_c}{2}(p_c-1)$ distances. Hence the design matrix, with elements that are functions of the $\underline{x}^c$, is $\frac{3p_c}{2}(p_c-1)$ by $2p_c$, so

$$\underline{\ell}^D = A\underline{x}^c \text{ with } Q^D = AQ^cA^T$$

for each campaign. Derived from this are the observations ℓ_i^D and ℓ_j^D, each with the same observables in the same order.

From these, the derived observation differences are obtained

$$\underline{d\ell}^D = \underline{\ell}_j^D - \underline{\ell}_i^D \text{ with } Q_{d\ell} = Q_i^D + Q_j^D$$

assuming the two campaigns to be uncorrelated (see section 3.1.3), and with

$$\hat{\sigma}_o^2 = \frac{\nu_i \hat{\sigma}_{oi}^2 + \nu_j \hat{\sigma}_{oj}^2}{\nu_D} \; ; \; \nu_D = \nu_i + \nu_j \; .$$

The triplets and pairs can now be examined under the null hypothesis H_o: $d\ell_h = 0$ versus H_A: $d\ell_h \neq 0$, $d\ell_h \in \underline{d\ell}^D$ by the statistic

$$T^2 = \frac{d\ell_h^2}{\hat{\sigma}_o^2 q_{hh}} < F(1, \nu_D; \alpha); \; q_{hh} \in Q_{d\ell} \qquad (3.3)$$

In order to build a hierarchy of suspicious stations, the testing of T^2 is done at several levels, i.e. $(1-\alpha)$ of 0.90, 0.95, 0.99. The failing observables (the identity of the stations involved in each failing observation difference) are tabulated at each level. The frequency of involvement of each station is tallied for the 0.90 level. The stations are ordered in suspicion by this frequency. Since the most frequently involved station is likely to be unstable, then it has probably been responsible for the failures in which it occurred. Hence, those at the 0.95 level could be explained by the instability of this station. Therefore, the observables involving that station are removed from the lists of failures at 0.90 and 0.95. From the remaining failures at 0.90, a new hierarchy is formed, especially if the frequencies of involvement of the first hierarchy were very nearly the same for some of the stations more frequently involved. This might be the case in a grouping of only a few points in which there is no one point that is isolated from the

effects of the movement of a single station. If the frequencies had been very much different, i.e. with an obvious ordering, the next most frequently involved station could be considered. The remaining involved observables are then removed from the lists at 0.90 and 0.95. This is repeated until all of the failures at 0.95 have been explained. If such cannot be easily done, then there should be the consideration that $\underline{dx} \neq 0$, that there is some form of relative movement occurring or that the network is likely unsuitable as a reference. If the removal has been successful there would now be two sets of stations -- those suspected of being unstable and those remaining. The suspected stations would have to be recognized as being different in each of the two campaigns while the least risk is met when utilizing the least frequently involved stations in the minimal constraints.

If either or both of the original ℓ_i, $\underline{\ell}_j$ had been pure triangulation or if there were some doubt about the maintenance of scale within the two campaigns, then the distance difference could be contaminated by a change in scale and would be considered only after removing a mean change in scale. For each of the distances derived from each campaign, there would be the same scale factor, i.e.

$$\underline{\ell}_j = (1+k)\underline{\ell}_i \quad \text{so} \quad k_h = \frac{\ell_j - \ell_i}{\ell_i} = \frac{d\ell_h}{\ell_h}$$

with

$$d\ell_h \in \underline{d\ell},\ \ell_h \in \underline{\ell}_i^D$$

so,

$$\bar{k} = \frac{2}{p_c(p_c-1)} \sum_{h=1}^{\frac{p_c}{2}(pc-1)} k_h \ ; \ \sigma^2_{\bar{k}} = \frac{1}{\frac{p_c}{2}(p_c-1) - 1}\left[\Sigma k_h^2 - \frac{2k^2}{p_c(p_c-1)}\right] \qquad (3.4)$$

3.1.1.3 Detection of Outliers and Systematic Errors

Because of the bias introduced by the existence of outliers and of the possibility of systematic error being interpreted as behaviour, the detection of both is critical in the analysis of deformation surveys. Some precautions can be taken, such as field checks during the observation process and frequent thorough calibration of instrumentation, especially optical plummets and electronic distance measuring equipment. Nonetheless, the network adjustment allows for testing to be done and this should be a matter of course.

As a global indication of the appropriateness of the model and on the scaling of the weight matrix, there is the customary test on the ratio of the a posteriori, $\hat{\sigma}_0^2$, and the a priori, σ_0^2, variance factors. This is explained very amply in Vanicek and Krakiwsky (1982) from which the following has been taken.

The ratio is acceptable, i.e. H_0: $\hat{\sigma}_0^2 = \sigma_0^2$ is not rejected in favour of H_A: $\hat{\sigma}_0^2 \neq \sigma_0^2$, at the $(1-\alpha)$ level of confidence if

$$\frac{\nu\hat{\sigma}_0^2}{\xi\chi^2(\nu;1-\frac{\alpha}{2})} < \sigma^2 < \frac{\nu\hat{\sigma}_0^2}{\xi\chi^2(\nu;\frac{\alpha}{2})} \qquad (3.5)$$

If this cannot be satisfied, then several circumstances could be the cause.

1. The residuals do not have a normal distribution - this can be easily investigated using the χ^2 goodness of fit test on the histogram of standardized residuals; or there may be outlying observations - these may be detected as mentioned below.

2. The mathematical model expressed by $\underline{\ell} = A\underline{x}$ is incorrect - this is not likely unless position of one or several of the stations is poorly determined (configuration defect). This is a physical problem and cannot be rectified in the analysis. If the station is identified, then its information would be considered by other routes through the analysis. Here, it might be possible to undertake the adjustment omitting that station.
3. Systematic errors may be contaminating the observations - these may be sought as mentioned below.
4. The weight matrix may be improper - this is not likely since either sufficient information or the MINQUE process was used. Nonetheless, both the scale and the relative weighting should be substantiated.

Chen (1983) has proposed a general method for detecting outliers (see also Chen et al., 1984). Of the original vector of observations, there might be n_o of them which are outliers resulting in the bias $\underline{\delta}$. The original model is then partitioned to reflect this by

$$\underline{\ell} + \underline{v} = A\underline{x} \rightarrow \begin{bmatrix} \underline{\ell}_I \\ \underline{\ell}_o \end{bmatrix} + \begin{bmatrix} \underline{v}_I \\ \underline{v}_o \end{bmatrix} = \begin{bmatrix} A_I & 0 \\ A_o & I \end{bmatrix} \begin{bmatrix} \underline{x} \\ \underline{\delta} \end{bmatrix} = [A_1 \; A_2] \begin{bmatrix} \underline{x} \\ \underline{\delta} \end{bmatrix} \qquad (3.6)$$

with

$$D\left\{ \begin{matrix} \underline{\ell} \\ \underline{\ell}_o \end{matrix} I \right\} = \sigma_o^2 Q$$

Testing is performed under the null hypothesis H_o: $\underline{\delta} = 0$ versus H_A: $\underline{\delta} \neq 0$ while the adjustment had been performed without any conscious partitioning, i.e. enforcing that $\underline{\delta} = 0$. In the usual manner, the residuals result from $\hat{\underline{v}} = A\hat{\underline{x}} - \underline{\ell}$ which may be similarly partitioned as

$$\underline{v} = \begin{bmatrix} \underline{v}_I \\ \underline{v}_o \end{bmatrix} \quad \text{with} \quad Q_v = \begin{bmatrix} Q_I & Q_{Io} \\ Q_{oI} & Q_o \end{bmatrix}$$

with $\nu = n_\ell - \text{rank}\,(A) = n_I + n_o - \text{rank}\,(A)$; $\nu_I = \nu + n_o$. So, the test becomes

$$T^2 = \frac{\underline{v}^T Q^{-1} A_2 [A_2^T Q^{-1} Q_v Q^{-1} A_2]^{-1} A_2^T Q^{-1} \underline{v}}{\underline{v}^T Q^{-1} \underline{v}} \leq \frac{\nu_I}{n_o + \nu F(\nu, n_o; 1-\alpha)} \tag{3.7}$$

for which there may be several outliers, n_o, in observations that are correlated (Chen, 1983).

If only a single outlier is suspected, then this test becomes the data snooping of Baarda (Chen, 1983). If, also, the observations are assumed to be uncorrelated, then it further dissolves into the common t-test of Heck (1981) (Chen, 1983) which is given as

$$T^2 = \frac{\hat{v}_h^2}{\sigma_o^2 q_{hh}} \leq \xi_t^2(\nu_I - 1;\ \alpha/2) \tag{3.8}$$

with σ_o^2 having been known. Or, it becomes the τ-test of Pope (1976) (Chen, 1983) as

$$T^2 = \frac{\hat{v}_h^2}{\hat{\sigma}_o^2 q_{hh}} \leq \xi_\tau^2(\nu_I;\ \alpha/2) \tag{3.9}$$

if σ_o^2 had not been known and $\hat{\sigma}_o^2$ was necessary, or if the χ^2-test on $\hat{\sigma}_o^2 : \sigma_o^2$ failed.

In a similar manner, it is possible to pursue the existence of systematic errors. Of the original observations, $\underline{\ell}$, there may be n_s of them which are contaminated by some systematic error represented by a model $A_s \underline{y}$. Thus, the full model becomes

$$\underline{\ell} + \underline{v} = A\underline{x} + A_s \underline{y}$$

with

$$D\{\underline{\ell}\} = \sigma_o^2\, Q\ .$$

Testing is performed under the null hypothesis H_0: $\underline{y} = 0$ against H_A: $\underline{y} \neq 0$. If the adjustment involved the full model as immediately above, then the testing involves the values of the parameters, $\hat{\underline{y}}$, by

$$T^2 = \frac{\hat{\underline{y}}^T Q_y^{-1} \hat{\underline{y}}}{n_s \hat{\sigma}_0^2} \leq F(n_s, \nu; \alpha) \qquad (3.10)$$

with $\nu = n_\ell$ - rank (A).

If the systematic errors had not been modelled, so that the adjustment involved only the original model $\underline{\ell} + \underline{v} = A\underline{x}$, then the testing is of the residuals, $\hat{\underline{v}}$, by

$$T^2 = \frac{\hat{\underline{v}}^T Q^{-1} A_s [A_s^T Q^{-1} Q_v Q^{-1} A_s]^{-1} A_s^T Q^{-1} \hat{\underline{v}}}{\hat{\underline{v}}^T Q^{-1} \hat{\underline{v}} - \hat{\underline{v}}^T Q^{-1} A_s [A_s^T Q^{-1} Q_v Q^{-1} A_s]^{-1} A_s^T Q^{-1} \hat{\underline{v}}} \cdot \frac{\nu}{n_s} \leq F(n_s, \nu; \alpha) \qquad (3.11)$$

or equivalently equation 3.7 with $A_2 = A_s$, $\nu_I = \nu$, $n_o = n_s$ (Chen, 1983).

3.1.1.4 The Weighted Projection

As a means of overcoming the difficulties mentioned in section 3.1.1.1 with regard to datum defect, a weighted projection in the parameter space has been developed by Chen (1983). A full explanation and proofs of its properties are given in Chen (1983), so only a short discussion of its features and application will be given here.

In the original system

$N\underline{x} = \underline{u}$ with $N = A^T Q^{-1} A$, $\underline{u} = A^T Q^{-1} \underline{\ell}$

the configuration matrix, A, is rank deficient by n_r so that N is singular. All possible $\underline{x}$ that satisfy the system lie in a hyperplane $\Psi = N\underline{g}_u + S_H$ of the Euclidean space E^{n_u} having a dimension of n_u, with a subspace S_H spanned by the column vectors of the H matrix (section 3.1.1.1). Another subspace of E^{n_u} is E^{n_v} with $n_v = n_u - n_r$ which is defined by the datum equations $D^T\underline{x} = 0$. The orthogonal complement to E^{n_v} is S_D, dimensional n_r, and spanned by the column vectors of D. By projecting any solution, $\underline{x}_s$, parallel to S_H, onto E^{n_v}, the datum defect problem is alleviated by giving a uniquely projected vector, $\underline{x}_w$. This is done by

$$\underline{x}_w = [I - H(D^TH)^{-1}D^T]\underline{x}_s \tag{3.12}$$

or alternatively

$$\underline{x}_w = [I-H(H^TD(D^TD)^{-1}D^TH)^{-1}H^TD(D^TD)^{-1}D^T]\underline{x}_s \tag{3.13}$$

in which weighting may be applied by $P_w = D(D^TD)^{-1}D^T$.

This has been an oblique projection. As a special case, when the projection is orthogonal, viz. projection parallel to S_H onto S_N the subspace spanned by the column vectors of N, the solution has minimum Euclidean norm which is part of the definition of the inner constraints solution (section 3.1.1.1). Hence,

$$\underline{x}_I = [I - D(D^TD)^{-1}D^T]\underline{x}_s \tag{3.14}$$

which follows the notion that the inner constraints solution may be derived from any special solution, i.e.

$$\hat{\underline{x}}_I = \hat{\underline{x}}_s + H\underline{t}$$

with $\underline{t}$ defined so that $D^T\hat{\underline{x}}_I = 0$. Consequently,

$$0 = D^T\hat{\underline{x}}_S + D^T H\underline{t}$$

making

$$\underline{t} = -(D^T H)^{-1} D^T \hat{\underline{x}}_S \ ,$$

so

$$\hat{\underline{x}}_I = \hat{\underline{x}}_S - H(D^T H)^{-1} D^T \hat{\underline{x}}_S = [I - D(D^T D)^{-1} D^T]\hat{\underline{x}}_S$$

since D = H. All of the points have contributed equally toward the definition of the datum, so $P_w = I$.

The uniqueness of this projector may be seen by considering a second datum defined by $D_2^T\underline{x} = 0$. The double projection has the same effect as the single projection. The two projections dissolve as

$$[I - H(D^T H)^{-1} D^T][I - H(D_2^T H)^{-1} D_2^T]$$
$$= I - H(D^T H)^{-1} D^T - H(D_2^T H)^{-1} D_2^T + H(D^T H)^{-1} D^T H(D_2^T H)^{-1} D_2^T$$
$$= I - H(D^T H)^{-1} D^T$$

Along with the projection of the solution is the projection of its cofactor matrix. So,

$$Q_{x_w} = [I - H(D^T H)^{-1} D^T]\, Q_{x_s} [I - H(D^T H)^{-1} D^T]^T \qquad (3.15)$$

which has the same rank defect as $[I - H(D^T H)^{-1} D^T]$ and $D^T Q_{x_w} = 0$.

In the context of analysing deformation surveys, the circumstances are not so simple. Especially in a relative network, there is likely movement of points sufficient to not allow knowledge of the datum, i.e. to define the elements of D. Intuitively, the stations with the least amount of movement should have the most influence in the definition of a datum. However, since any special solution is already biased, there is then

the problem of how to define the projector. Chen (1983) has revealed a relatively uncomplicated manner for doing so by further refining the projection by making an "iterative weighted projection" which can be very readily utilized.

A two dimensional displacement field has resulted from differing two network adjustments using the same minimal constraints or from the direct solution from observation differences as described in section 3.1.2 below. The vectors and matrices are brought to full dimension by augmenting rows and columns with elements of zero. For a total of p stations with n_d coordinates having been considered as fixed, the information available is:

$$\underline{x} = \begin{bmatrix} \underline{\hat{x}}_s \\ \underline{x}_c \end{bmatrix}$$

a 2p vector of at least approximate coordinates for all of the stations, referred to the centroid of the network. $\underline{\hat{x}}_s$ has $2p-n_d$ elements possibly available from one of the network adjustments;

$$\underline{dx} = \begin{bmatrix} \underline{d\hat{x}}_s \\ \underline{0} \end{bmatrix}$$

similar to $\underline{x}$, except $\underline{d\hat{x}}_s = \underline{\hat{x}}_{s_2} - \underline{\hat{x}}_{s_1}$ or from the direct solution;

$$Q_{dx} = \begin{bmatrix} Q_{dx_s} & 0 \\ 0 & 0 \end{bmatrix}$$

with $Q_{dx_s} = Q_{x_{s1}} + Q_{x_{s2}}$ or directly from the solution for $\underline{d\hat{x}}_s$;

$$\nu_{dx} = \nu_1 + \nu_2$$

$$\hat{\sigma}^2_{dx} = \frac{\nu_1 \hat{\sigma}^2_{o1} + \nu_2 \hat{\sigma}^2_{o2}}{\nu_{dx}}$$

the weighted variance factor or $\hat{\sigma}^2_o$ from $\underline{d\hat{x}}_s$.

For a fully defective network (triangulation), the matrix H is 2p by 4, i.e.

$$H = \begin{array}{c} \begin{array}{cccc} \delta x & \delta y & \omega_{xy} & k \end{array} \\ \begin{bmatrix} \cdot & & & \\ \cdot & & & \\ \cdot & & & \\ 1 & 0 & -y_i & x_i \\ 0 & 1 & x_i & y_i \\ \cdot & & & \\ \cdot & & & \\ \cdot & & & \end{bmatrix} \end{array} \begin{array}{l} \\ \\ \\ dx_i \\ dy_i \\ \\ \\ \\ \end{array}$$

The last column, scale, would be removed and H would be 2p by 3 for trilateration or triangulateration.

The projection is done through several iterations,

$$\underline{dx}_{i+1} = [I - H(H^T P_{w_i} H)^{-1} H^T P_{w_i}] \underline{dx}_i \qquad i = 0, 1, 2, \ldots \qquad (3.16)$$

For $i = 0$, $P_w = I$, $\underline{dx}_0 = \underline{dx}_s$ and $\underline{dx}_1$ is as if using inner constraints. For subsequent projections, $i = 1, 2, 3, \ldots$, the effect of the least displaced stations is given more weight by assigning the elements of P_w as

$$p_{jj} = |dx_j + \delta|^{-1} \qquad dx_j \in \underline{dx}_i$$

The δ is some small amount, such as the criterion for convergence, that remains in the denominator of p_{jj} to maintain numerical stability if some

displacement component approaches zero. The iteration would continue until the updating of the displacement components is less than the criterion, i.e. if all $|dx_{i+1} - dx_i| < \delta$. The result, if at iteration i = w, is the weighted projection $\underline{dx}_w$ with $Q_{dx_w} = [I-(H^T P_w H)^{-1} H^T P_w] \cdot Q_{dx} [I-(H^T P_w H)^{-1} H^T P_w]^T$ from which the submatrices for each of p stations may be extracted so that the displacement may be displayed against its error ellipse at some $(1-\alpha)$ level.

In essence, the weighting $P_w = D(D^T D)^{-1} D^T$ has defined the datum. When $P_w = I$, each component has contributed equally, the inner constraints, and the effect of any one point is absorbed by all the others. When the weighting is inversely proportional to the magnitude of the displacement component, the weighted projection, the contribution to the datum has been by heavier weight by the smaller displacement components, i.e. the stations that have moved the least. The initial projection, as inner constraints, relieves the biased very high weight that would otherwise be carried by the zero displacement components of the stations used as the constraints in the special solution. While the unit weight projection (inner constraints) minimized the Euclidean length of the $\underline{dx}$ vector, i.e. $(\Sigma\, dx_i^2)^{1/2}$ minimum, the weighted projection minimizes the first norm of $\underline{dx}$, i.e. $\Sigma|dx_i|$ minimum.

The process may be visualized as the mating of the two rigid configurations resulting from, or that would have resulted from, the adjustments of the two campaigns - each in itself a rigid undistortable framework with the station points as nodes or junctions. They are initially separated by the displacements resulting from the special solution with the constraint station components coinciding. After its iterations, the weighted projection has brought the coincidence as

nearly as possible through the heavier weighting given to the least moved stations so that the sum of the magnitudes of all the displacement components is minimal.

The procedure may be illustrated by a simple example of the measurement of the distance between two points in a horizontal plane, given in Appendix A.2.

3.1.2 Observation Approach

While the network may suffer from configuration defects, not allowing an adjustment (e.g. the station heights are not known well enough to allow reasonable reduction of the observations), it is still possible to utilize most of the observation data toward some indication of trend. The following employs principles introduced by Lazzarini (1974), used by Tobin (1983), and also discussed by Vanicek and Krakiwsky (1982). The objective is a set of displacement components which can then be handled in the same manner as those derived from the two separate adjustments for coordinates. Again, the discussion is related to a horizontal network, at least with regard to the elements of the design matrix and the displacement components, but this is not a restriction.

Two campaigns of measurement have occurred with $\underline{\ell}_i$ and $\underline{\ell}_j$ with the assumption that the instrument eccentricities, both vertical and horizontal, have been removed and that meteorological corrections have been applied so that the observations can be considered as having been made between the same spatial points. For whatever deformation has occurred between the two campaigns, it is assumed that the result has not moved the stations to the extent that the configuration has appreciably changed, except

for the loss or addition of stations. Another requirement is that the directions be transformed into angles and that the resultant correlations be maintained in the cofactor matrix. These angles may be adjacent about the station or in whatever pattern results in the same observables for each campaign. Thus, the information available is

$$\underline{\ell}_i \text{ with } \sigma_{oi}^2 Q_i \quad \text{and} \quad \underline{\ell}_j \text{ with } \sigma_{oj}^2 Q_j$$

with the observables in the same order in each campaign. In addition, it is necessary to have a set of approximate coordinates, $\underline{x}$, describing the configuration of common stations existing in each of both campaigns.

The common observations are extracted from each campaign by

$$\underline{\ell}_{ci} = S_i \underline{\ell}_i ; \quad Q_{ci} = S_i Q_i S_i^T$$

and

$$\underline{\ell}_{cj} = S_j \underline{\ell}_j ; \quad Q_{cj} = S_j Q_j S_j^T$$

in a manner similar to what was done for common coordinate components (section 3.1.1.2).

The $n_{d\ell}$ differences can be taken by

$$\underline{d\ell} = \underline{\ell}_{cj} - \underline{\ell}_{ci}$$

having

$$\sigma_{d\ell}^2 Q_{d\ell} = \sigma_{oi}^2 Q_{ci} + \sigma_{oj}^2 Q_{cj}$$

assuming no correlation between campaigns (section 3.1.3). These differences can be considered as the observables, so the displacements may be estimated through the model

$$\underline{d\ell} + \underline{v} = A\underline{dx}$$

with

$$A = \left[\frac{\partial \underline{v}}{\partial \underline{x}} \right] \quad ,$$

as if the observables were being used to estimate coordinate components, and with $P_{d\ell} = \sigma_{d\ell}^{-2} Q_{d\ell}^{-1}$. Then,

$$\underline{d\hat{x}} = (A^T P_{d\ell} A)^{-1} A^T P_{d\ell} \underline{d\ell} \tag{3.17}$$

with

$$Q_{d\hat{x}} = (A^T P_{d\ell} A)^{-1}, \quad \underline{\hat{v}} = A\underline{d\hat{x}} - \underline{d\ell} \ ,$$

and

$$\hat{\sigma}_o^2 = \frac{\underline{\hat{v}}^T P_{d\ell} \underline{\hat{v}}}{\nu} \ , \quad \nu = n_{d\ell} - d - n_{dx}$$

This has been presented as the solution using explicit minimal constraints. The same considerations would be given as for a network adjustment - pseudo-observation differences of zero, stations with $\underline{dx}_c = 0$ (section 3.1.1.1). Also, the same alternate methods, e.g. inner constraints, could be used to obtain the displacement components. After the above solution, the $\underline{dx}$ and Q_{dx} would be fully dimensioned with additional rows and columns of zeros as there were constant coordinates in the solution for coordinates. So, for all of the common stations,

$$\underline{dx} = \begin{bmatrix} \underline{d\hat{x}} \\ \underline{dx}_c \end{bmatrix} \quad \text{with} \quad Q_{dx} = \begin{bmatrix} Q_{d\hat{x}} & 0 \\ 0 & 0 \end{bmatrix}$$

From this, stable point analysis or the weighted projection could be performed as for the displacements from separate campaign adjustments.

3.1.3 Equivalence of the Coordinate and Observation Approaches

Earlier discussion has already referred to the existence of correlation between campaigns and it is intuitive that, under certain circumstances, the coordinate or indirect approach and the observation or direct approach would yield the same results. If these circumstances do not normally prevail, then the consequence of following the one rather than the other should be regarded. The discussion here has been taken from Vanicek and Krakiwsky (1982) to which Chen (1983) has alluded.

In order to consider equivalence, several conditions must already exist. For the two campaigns being compared, the observations have been made of the same observables and the same stations are involved, i.e. so that the configuration has not changed. All of the variances of the observations have been contained in their variance-covariance matrices, so that

$$\underline{\ell}_1 \text{ with } C_{\ell_1} = \sigma_{o1}^2 Q_1, \quad P_1 = C_{\ell_1}^{-1}$$

and

$$\underline{\ell}_2 \text{ with } C_{\ell_2} = \sigma_{o2}^2 Q_2, \quad P_2 = C_{\ell_2}^{-1}$$

Loosely speaking (when the $\underline{x}$ used in the configuration matrix A are very nearly $\hat{\underline{x}}_1$ or $\hat{\underline{x}}_2$), the adjusted coordinates are

$$\hat{\underline{x}}_1 = (A^T C_{\ell_1}^{-1} A)^{-1} A^T C_{\ell_1}^{-1} \underline{\ell}_1 \quad \text{with} \quad C_{x_1} = (A^T C_{\ell_1}^{-1} A)^{-1}$$

and

$$\hat{\underline{x}}_2 = (A^T C_{\ell_2}^{-1} A)^{-1} A^T C_{\ell_2}^{-1} \underline{\ell}_2 \quad \text{with} \quad C_{x_2} = (A^T C_{\ell_2}^{-1} A)^{-1}$$

assuming that $\hat{\sigma}_0^2 = \sigma_0^2$.

From the coordinates,

$$\underline{dx} = \underline{\hat{x}}_2 - \underline{\hat{x}}_1 \quad \text{with} \quad C_{dx} = C_{x_1} + C_{x_2} .$$

From the observations,

$$d\ell = [-1 \quad 1] \begin{bmatrix} \underline{\ell}_1 \\ \underline{\ell}_2 \end{bmatrix} = \underline{\ell}_2 - \underline{\ell}_1$$

so

$$C_{d\ell} = [-1 \quad 1] \begin{bmatrix} C_{\ell_1} & C_{\ell_1\ell_2} \\ C_{\ell_2\ell_1} & C_{\ell_2} \end{bmatrix} \begin{bmatrix} -1 \\ 1 \end{bmatrix} = C_{\ell_1} - 2C_{\ell_1\ell_2} + C_{\ell_2} ,$$

Then

$$\underline{d\hat{x}} = (A^T C_{d\ell}^{-1} A)^{-1} A^T C_{d\ell}^{-1} \underline{d\ell} \quad \text{with} \quad C_{dx} = (A^T C_{d\ell}^{-1} A)^{-1} . \tag{3.18}$$

This can be compared to

$$\underline{\hat{x}}_2 - \underline{\hat{x}}_1 = (A^T C_{\ell_2}^{-1} A)^{-1} A^T C_{\ell_2}^{-1} \underline{\ell}_2 - (A^T C_{\ell_1}^{-1} A)^{-1} A^T C_{\ell_1}^{-1} \underline{\ell}_1 \tag{3.19a}$$

with

$$C_{dx} = (A^T C_{\ell_1}^{-1} A)^{-1} + (A^T C_{\ell_2}^{-1} A)^{-1} . \tag{3.19b}$$

Equations (3.19) could not be the same as (3.18) unless, at least, $C_{\ell_1\ell_2} = 0$.

Then, $\underline{d\hat{x}} = (A^T (C_{\ell_1} + C_{\ell_2})^{-1} A)^{-1} A^T (C_{\ell_1} + C_{\ell_2})^{-1} \underline{d\ell}$

with

$$C_{dx} = (A^T (C_{\ell_1} + C_{\ell_2})^{-1} A)^{-1} .$$

Again, they could not be the same if $C_{\ell_1} \neq C_{\ell_2}$ unless $C_{\ell_2} = kC_{\ell_1}$.

Then,

$$\underline{d\hat{x}} = (A^T \frac{1}{1+k} C_{\ell_1}^{-1} A)^{-1} A^T \frac{1}{1+k} C_{\ell_1}^{-1} \underline{d\ell} = (A^T C_{\ell_1}^{-1} A)^{-1} A^T C_{\ell_1}^{-1} \underline{d\ell}$$

with

$$C_{dx} = (1+k)(A^T C_{\ell_1}^{-1} A)^{-1} .$$

If $k = 1$, then both the $\underline{d\hat{x}}$ and the C_{dx} would be equivalent. If $k \neq 1$ and $k > 0$, then the $\underline{d\hat{x}}$ would still be the same, but the C_{dx} would differ in scale.

The consequence of assuming $C_{\ell_1\ell_2} = 0$ may be seen from the following. Now, with $C_{\ell_1\ell_2} \neq 0$ and with $C_{\ell_1} = C_{\ell_2} = C_\ell = \text{diag}\,(\sigma^2_{\ell_1}, \sigma^2_{\ell_2}, \ldots, \sigma^2_{\ell_h}, \ldots)$, assuming a statistical dependence only between the same observables in the two campaigns creates

$$\begin{aligned} C_{\ell_1\ell_2} &= \text{diag}\,(\sigma_{12_{\ell_1}}, \sigma_{12_{\ell_2}}, \ldots, \sigma_{12_{\ell_n}}, \ldots) \\ &= \text{diag}\,(\rho_1\sigma^2_{\ell_1}, \rho_2\sigma^2_{\ell_2}, \ldots, \rho_h\sigma^2_{\ell_h}, \ldots) \\ &= \text{diag}\,(\rho_1, \rho_2, \ldots, \rho_h, \ldots)\, C_\ell . \end{aligned}$$

This makes

$$\begin{aligned} C_{d\ell} &= C_\ell - 2C_{\ell_1\ell_2} + C_\ell = 2C_\ell - 2C_{\ell_1\ell_2} = 2(C_\ell - C_{\ell_1\ell_2}) \\ &= 2(C_\ell - \text{diag}(\rho_1, \rho_2, \ldots, \rho_h, \ldots)C_\ell) \\ &= 2(I - \text{diag}\,(\rho_1, \rho_2, \ldots, \rho_h, \ldots))C_\ell \end{aligned}$$

If a mean value, ρ, is taken for the correlation coefficient, then

$$C_{d\ell} \doteq 2(1-\rho)C_\ell$$

so,

$$C_{d\ell}^{-1} \doteq \frac{1}{2(1-\rho)} C_\ell^{-1}$$

As in the case of $C_{\ell_2} = kC_{\ell_1}$, this would result in the same $\underline{dx}$, but the C_{dx} would be smaller by $1-\rho$, i.e. when $\rho > 0$, inferring positive statistical dependence. In almost unrealistically simple terms, the direct solution would have an advantage due to the positive dependence that is likely to occur. This had been the justification in Lazzarini's (1974) discussion, that the $\underline{d\ell}$ becomes free of the systematic error that plagues both the campaigns.

The decision of which is the more appropriate should be made with regard for the circumstances. There is benefit from the separate adjustments by their providing an assessment of the observations and their allowing for configuration and observables to be peculiar to each campaign. Even then, the subset of common observables could still be used for the direct estimation, at the sacrifice of some information. Nonetheless, all of this is only for an indication of the trend. The ultimate estimation of the model parameters utilizes all of the available observations in any configuration.

3.2 Trend Analysis Through Several Campaigns

As might be expected from this separate classification, time is being taken into account explicitly, either as the rate of change of the observables or of some quantity derived from the campaign comparisons, either analytically or graphically.

If there had not been the opportunity to create discrete campaigns of measurement or to undertake estimation of displacements, then this may be more than the indication of trend, but also a means of creating rates from which the parameters of the deformation model may be estimated. From the comparisons, the rates have been implied since each comparison has its associated time interval. By regarding each series of comparisons, higher order variations, such as acceleration, may be recognized.

3.2.1 Using a Series of Observations

An obvious procedure for a visual indication would be the plotting of values of an observable against time, with the ensurance that the observations have been corrected against contamination by effects extraneous to the phenomenon of interest (e.g. temperature correction to extensometers, meteorological and calibration corrections to electromagnetic distance measuring instruments, instrument eccentricities, directions reduced to angles).

The examination and utilization of the plot of values of an observable, ℓ_i against time t_i, is also a deformation analysis - a subset of the more global analysis of concern. Hence, the same steps may be

followed in the analysis of trend. The data may appear to be behaving with some pattern. Especially if that pattern is to be quantified and used in subsequent analysis, that appearance must be described and assessed. Thus, there must be a model proposed with propagation of the errors in the data through the estimation of the parameters of that model.

In the context of repeated observables within a network, the frequency of measurement or the intervals between measurements and the number of measurements will constrict the complexity of the trend model. Such discrete data can rarely have a trend that could be realized as being more than linear or the simplicity of using rates in the subsequent analysis balances any advantage in more intricate modelling. However, especially in the case of continuously recording instruments, such as creepmeters, strainmeters, or tiltmeters, variations due to influences beyond those of interest (e.g. tidal, meteorological, hydrological) would have to be removed (Goulty et al., 1979; Harrison, 1976; Schulz et al., 1983).

With the assumption that the data are usable and that it is the rate of change of the observable that is desired, then a least squares fitting of a rate to the data may be obtained.

Each observation ℓ_i of the set of values for the observable has the same variance σ_ℓ^2 and has occurred at a time t_i which is considered as relatively errorless, i.e. $\sigma_t^2 << \sigma_\ell^2$ and would have no effect on the variance of the rate. The rate of change of the observable, $d\dot{\ell}$, is the slope of a straight line fitting through the k-membered set of ℓ_i. The model may be given with an observation equation

$$\ell_i + v_i = \ell_1 + d\dot{\ell}(t_i - t_1) \tag{3.18}$$

with the unknowns being

$d\dot{\ell}$ the desired rate

ℓ_1 an estimate of the value of the first observation, enhanced by removing the rate from each subsequent measurement.

With σ_ℓ^2 being the same for each ℓ_i, the covariance matrix for the observations is

$$C_\ell = \sigma_\ell^2 I, \quad \text{so} \quad P = \sigma_\ell^{-2} I$$

The parameters may be estimated by

$$\begin{bmatrix} \ell_1 \\ d\dot{\ell} \end{bmatrix} = (A^T A)^{-1} A^T \underline{\ell} \quad \text{with} \quad A = \left[\frac{\partial \underline{v}}{\partial \ell_1, d\dot{\ell}}\right] = \begin{bmatrix} 1 & 1 & \cdots \\ t_1 - t_1 & t_2 - t_1 & \end{bmatrix}^T$$

so

$$A^T A = \begin{bmatrix} 1 & 1 & & 1 \\ \Delta t_1 & \Delta t_2 & \cdots & \Delta t_k \end{bmatrix} \begin{bmatrix} 1 & \Delta t_1 \\ 1 & \Delta t_2 \\ & \cdot \\ & \cdot \\ & \cdot \\ 1 & \Delta t_k \end{bmatrix} = \begin{bmatrix} \sum_{i=1}^{k} 1 & \sum_{i=1}^{k} \Delta t_i \\ \sum_{i=1}^{k} \Delta t_i & \sum_{i=1}^{k} \Delta t_i^2 \end{bmatrix}$$

$$(A^T A)^{-1} = \frac{1}{k \sum_{i=1}^{k} \Delta t_i^2 - \left(\sum_{i=1}^{k} \Delta t_i\right)^2} \begin{bmatrix} \sum_{i=1}^{k} \Delta t_i^2 & -\sum_{i=1}^{k} \Delta t_i \\ -\sum_{i=1}^{k} \Delta t_i & k \end{bmatrix}$$

and

$$A^T \underline{\ell} = \begin{bmatrix} 1 & 1 & & 1 \\ \Delta t_1 & \Delta t_2 & \cdots & \Delta t_k \end{bmatrix} \begin{bmatrix} \ell_1 \\ \ell_2 \\ \cdot \\ \cdot \\ \ell_k \end{bmatrix} = \begin{bmatrix} \sum_{i=1}^{k} \ell_i \\ \sum_{i=1}^{k} \Delta t_i \ell_i \end{bmatrix}$$

so

$$\hat{d\ell} = \frac{1}{k\sum_{i=1}^{k}\Delta t_i^2 - \left(\sum_{i=1}^{k}\Delta t_i\right)^2}\left[-\sum_{i=1}^{k}\Delta t_i \sum_{i=1}^{k}\ell_i + k\sum_{i=1}^{k}\Delta t_i \ell_i\right] \tag{3.19}$$

with

$$\sigma^2_{d\dot{\ell}} = \sigma^2_{\ell}\frac{k}{k\sum_{i=1}^{k}\Delta t_i^2 - \left(\sum_{i=1}^{k}\Delta t_i\right)^2} \tag{3.20}$$

The dependence by the accuracy of the rate on the frequency or number of remeasurements and the time interval may be shown by considering that the intervals between measurements have been the same, $\Delta t_i = \Delta t$. This simplifies the variance of $d\dot{\ell}$ to be

$$\sigma^2_{d\dot{\ell}} = \frac{k}{k^2-1}\cdot\frac{\sigma^2_{\ell}}{\Delta t^2}$$

which shows how the variance is enhanced by the number of measurements and degraded by the shortness of the interval (figures 3.1 and 3.2). The number of remeasurements becomes the decided influence since it is not likely that observations would be made more frequently than every several months in network situations. Any tolerance would depend on the nature of the phenomena. If the activity is suspected of having some pattern in time, then the resolution of that behaviour would dictate the frequency of acquisition. This would have been taken into account during the design of the monitoring scheme. In the analysis of historical data, caution must be exercised against trying to obtain unavailable information from the data. But this would be reflected in the assessment of the trend model.

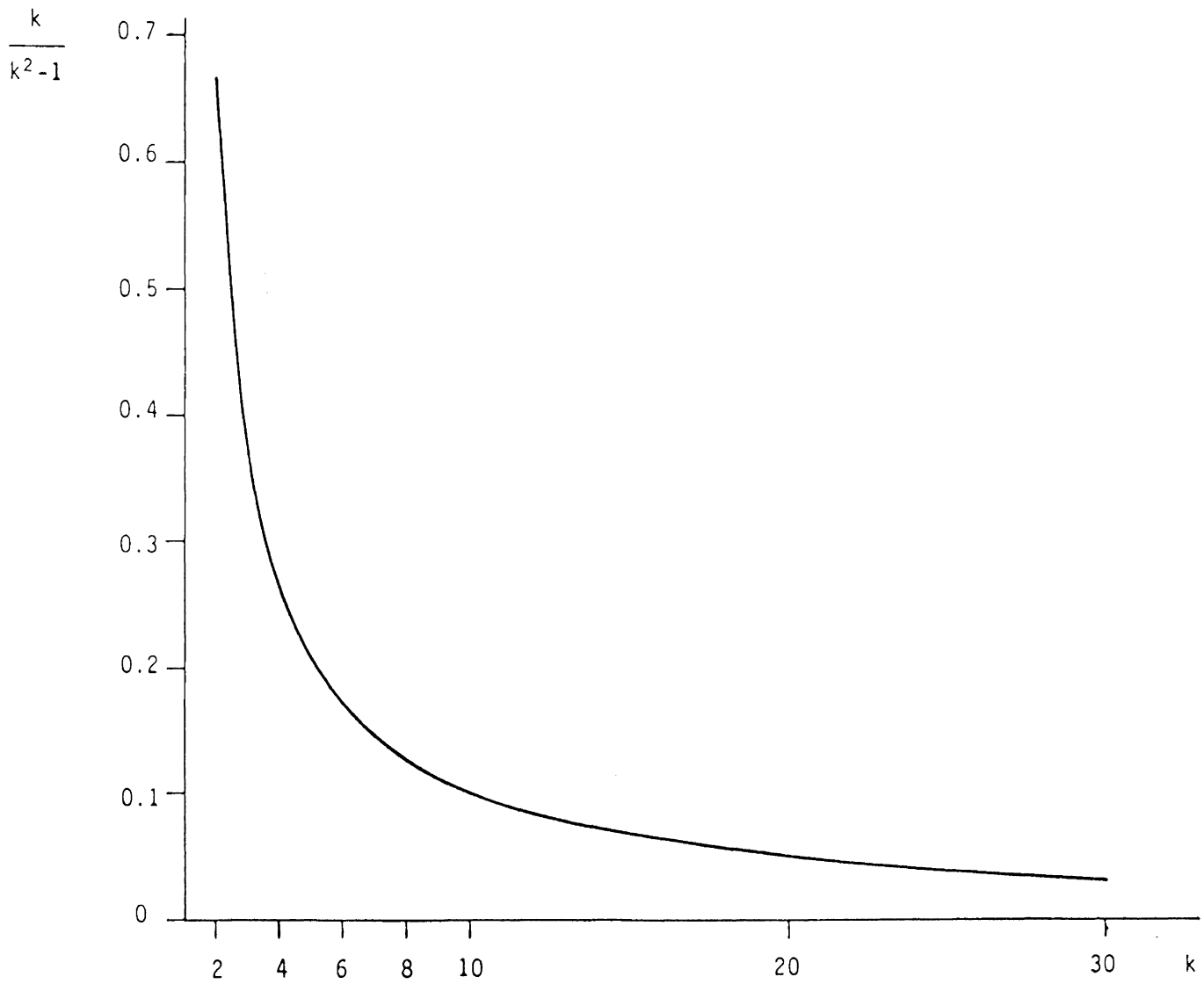

Figure 3.1 Factor of Reduction by Increased Number of Repetitions

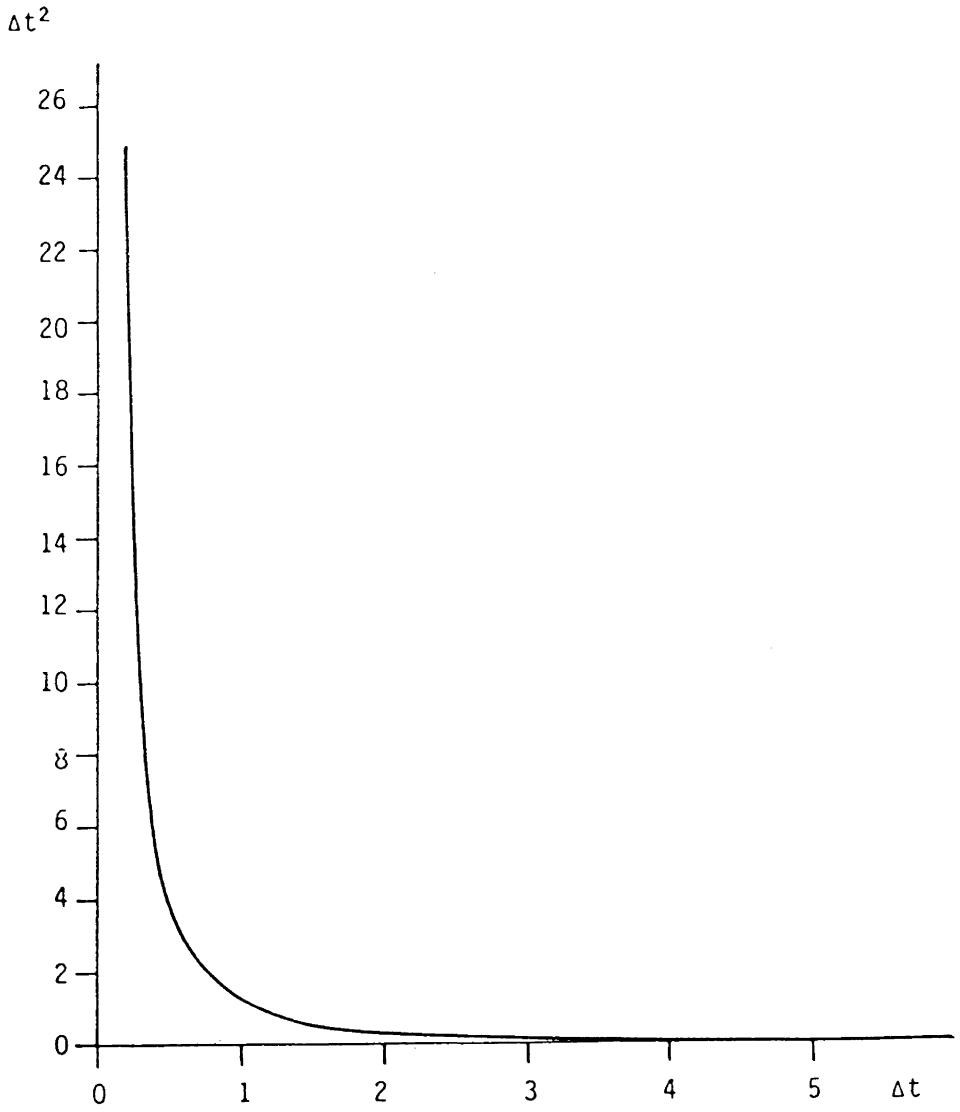

Figure 3.2 Factor of Degradation by Decreased Time Interval

Confidence in the estimates for the trend and in their variance allows their use as data in the major analysis. For instance, the rates of change of the observables, $\underline{d\dot{\ell}}$, can be used in the estimation of displacement velocities, $\underline{d\dot{x}}$, or of deformation rates, $\dot{E}$ (section 4.1), in the same manner as the $\underline{d\ell}$ were used.

An example of such treatment with spatial distances is given in figures 3.3 and 3.4. These data are from the observations of the Hollister network discussed in section 6.2. The lines of both distances cross an active fault at angles of 39^{o} and 48^{o} so that movement along the fault line would cause contraction or shortening of the two distances Coincident with a seismic event at 1979.6, the two plottings shifted toward increased contraction. Earlier reaction to other seismic events are noticeable, but are within the band of error of measurement. Taking the change in rate to have occurred consequent to the 1979.6 event results in the comparison of two rates - one from 1971 to 1979, the other from 1971 to 1982. The former is the preseismic rate, which, when advanced to the most recent measurement in 1982, is markedly offset from the rate taken overall. Without regard for the a posteriori estimate of the variance, the variances of the overall rates have been enhanced by the additional data. However, the appropriateness of the models is revealed when the a posteriori estimate is considered (table 3.1).

With assessment at the 0.95 level of confidence, only model Shore 79 is acceptable, but Sargent 79 is marginally unacceptable. Both the longer term models were grossly unacceptable even though the scaled estimates of the standard deviations for the two rates seem reasonable. These model failures would indicate anomalous reaction to the event of

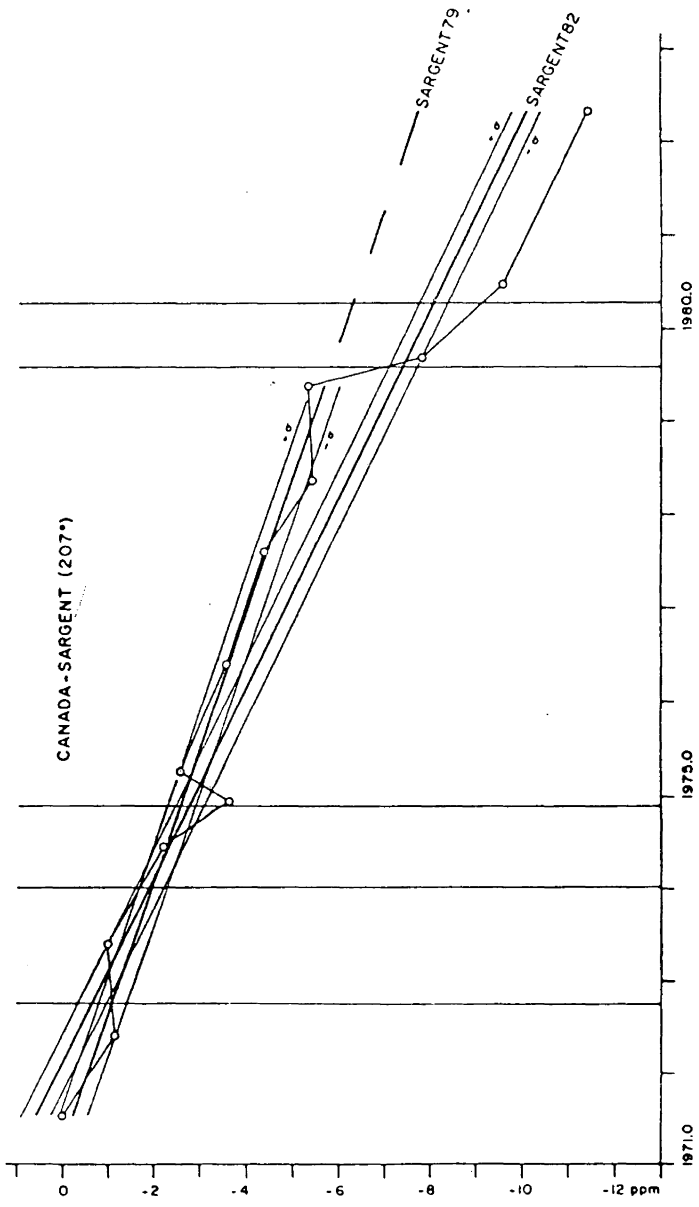

Figure 3.3 Example of Plotting Observable Values versus Time

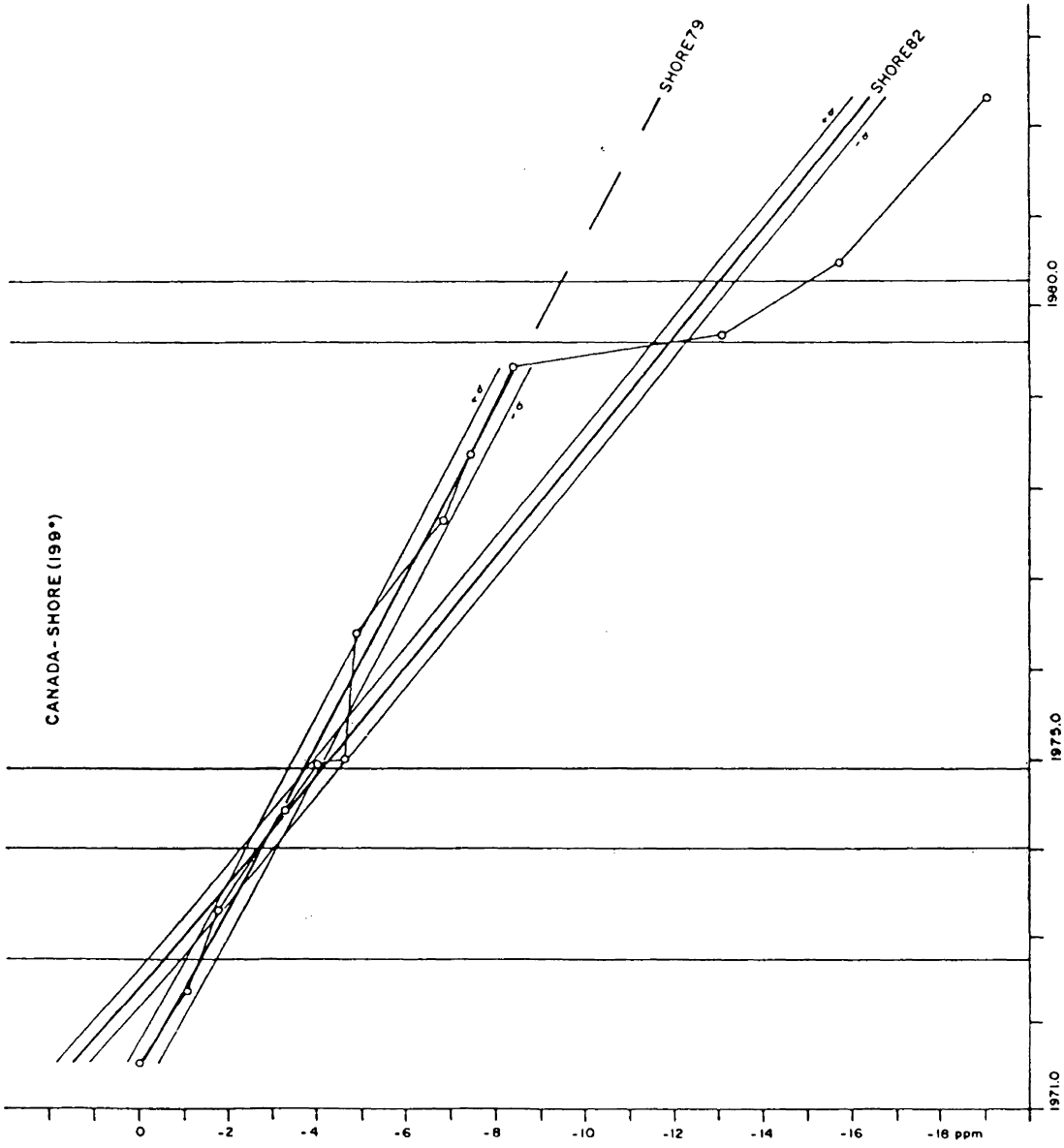

Figure 3.4 Example of Plotting Observable Values versus Time

$\dot{d\ell}$	$\sqrt{q_{d\ell}}$	lower bound χ^2	$\hat{\sigma}_o^2$ $\sigma_o^2=1$	upper bound χ^2	$\sqrt{\hat{\sigma}^2_{d\ell}}$	model
mmy^{-1} (ppmy^{-1})	mmy^{-1} (ppmy^{-1})	0.95		0.95	mmy^{-1} (ppmy^{-1})	
-10.0	±0.5	0.27	2.8588	2.19	±0.9	Sargent 79*
(-0.70)	(±0.04)				(±0.06)	1971-1979
-14.2	±0.4	0.35	12.4065	1.99	±1.3	Sargent 82
(-0.99)	(±0.03)				(±0.09)	1971-1982
-10.6	±0.5	0.27	0.9213	2.19	±0.4	Shore 79**
(-1.07)	(±0.05)				(±0.05)	1971-1979
-16.5	±0.3	0.35	27.5156	1.99	±1.6	Shore 82
(-1.66)	(±0.03)				(±0.16)	1971-1982

Distances Canada to Sargent 14299.3074 m ± 0.0041 m (±0.29 ppm) 1971.54

Canada to Shore 9957.1201 m ± 0.0036 m (±0.36 ppm) 1971.52

*compare U.S.G.S. 1971-1978 -10.9 ± 1.0 mmy^{-1}

** " " " -11.0 ± 0.6 (Savage et al., 1979)

Table 3.1. Comparison of Linear Fitting Models (figure 3.3, 3.4)

1979.6 and thus without any suspicion of a discontinuity, a network wide 1971 to 1982 analysis could possibly smooth out the influence of this event.

The caution to be exercised is having regard for the global test on the appropriateness of the model. The 1971-1978 rates were given with standard deviations but without any indication of their global fitting (Savage et al., 1979). As exaggerated in the 1971-1982 rates, this inability should signal that the attempted trend has not fit the data - for several possible reasons (section 3.1.1.3). One of these, in this case, is that the model should be redesigned to recognize the temporal discontinuity or to use a curve of higher order (e.g. acceleration). This concern is even more acute when the trend, for instance rates, is to be used later in the estimation of the parameters of a model.

These observation change rates circumvent the necessity for reducing the observations to a computational surface or creating campaigns and yet all of them can be used in the estimation of the deformation trend in contrast with using only the common observables in the observation differences method. It is possible to extend this form of linear regression to analyse the feasibility of fitting higher order curves to the data if they could be used in the subsequent analysis or at least to indicate how well a trend might be described in the model. However, it is possible that fitting a straight line or some other simple curve could be averaging short term behaviour that might be revealed by inter-campaign considerations or it could be modelling long term noise or a systematic behaviour of the instrumentation (e.g. aging of electronic components). Certainly, any analysis would not be undertaken with just the data alone, but other extrageodetic information would be taken into account.

3.2.2 Using a Series of Campaign Comparisons

From the campaign comparisons, temporal trend may be revealed by a similar plotting of parameters (e.g. u, v, w; ε_x, ε_y, ε_{xy}) against time, provided they were all obtained using the same system of station coordinates. This would ensure that all of the u_i or ε_i (section 4.1) were in the same sense since they would all relate to the same x, y system. A display of the accumulated displacement vectors could also be made, but a further requirement would be that they each are referred to the same datum or choice of minimal constraints. Other displays could be made of derived quantities such as ε_{max}, ε_{min}, or maximum shear and its orientation (section 4.1). Depending on the type of analysis, these could be converted to rates by dividing by the appropriate time intervals. Plotting of rates against time would then reveal any trend or acceleration that may not have been so obvious from a plot of the quantity against time. Any trend at all would be regarded against the error in its determination.

4. MODEL SELECTION AND ESTIMATION

The description of a deformation phenomenon is given by a mathematical model which relates how some point or collection of points will change, possibly over some interval of time. Both the description and the modelling are facilitated if the points can be identified in some system of coordinates, especially if several sources of spatial information are available. Under the assumption that the system can be recovered for each campaign and analysis or that the changes in the system can also be modelled (Reilly, 1981, 1982; Snay et al., 1983), the changes between campaigns result in a displacement vector for each point. These vectors describe a displacement field which in turn is described by some deformation model. Hence the sampling at the network stations is used to estimate the properties of the whole body through the modelling.

Eventually, once some trend has been indicated by a display of the discrete displacements, the modelling is derived directly from the changes in observables. These observables can be geometric relationships between or among stations of the network or they can be the adjusted coordinates. The functional relationship between each observable and the parameters of the deformation model can be expressed through an observation equation.

Some suggestions are given for possible models, both spatial and temporal. To go beyond the displacement field, observation equations are given for relating the observable changes to the deformation model. Next

the means for estimating the parameters and for assessing the models, as provided by the generalized method, are presented. Following these are some cautionary remarks regarding the inclusion of some parameters and the determinability of others.

4.1 Modelling

Several other sections refer to a general form of deformation model $B\underline{c}$. Its parameters, the elements of the vector $\underline{c}$, are estimated from the displacement field of a discrete number of points. This model is then used to generate some description of the deformation in graphical or analytical form. Depending on the choice of model, the parameters may be interpreted in some mechanical or physical sense. Here some suggestions for spatial, and later temporal, modelling are presented and their interpretation developed. A spatial model may be extended to rates merely by dividing by the time interval involved. For higher order models in time, e.g. acceleration, and for a simultaneous modelling of several campaigns, the model must be explicit in time as well as in space.

In the x, y, z space with typical point P having been displaced as shown in figure 4.2, the displacement field may be described as any function of the point coordinates within practical limits. Since most functions may be expressed as polynomials in x, y, z through series expansions, then, in somewhat general terms, the displacement field can be described by a polynomial function to some desired order. The practical limitation on the highest order will arise in space from the number and distribution of points and in time from the number and frequency of campaigns. Due to the nature of the observables, there may be some terms, especially having a mechanical sense, that are indeterminable. This is revealed somewhat in the section on observation equations (section 4.2) and is presented further under cautionary remarks (section 4.4).

The deformation model and hence the displacement field, $\underline{dx} = B\underline{c}$, may be expressed as

$$\underline{dx} = \begin{bmatrix} \cdot \\ \cdot \\ \cdot \\ u \\ v \\ w \\ \cdot \\ \cdot \\ \cdot \end{bmatrix} = B\underline{c}$$

in which

$$\begin{aligned} u &= a_0 + a_1x + a_2y + a_3z + a_4xy + a_5xz + a_6yz + a_7x^2 + a_8y^2 + a_9z^2 + \ldots \\ v &= b_0 + b_1x + b_2y + b_3z + b_4xy + b_5xz + b_6yz + b_7x^2 + b_8y^2 + b_9z^2 + \ldots \\ w &= c_0 + c_1x + c_2y + c_3z + c_4xy + c_5xz + c_6yz + c_7x^2 + c_8y^2 + c_9z^2 + \ldots \end{aligned} \tag{4.1}$$

A compact but no less general illustration may be given by considering only the terms that are linear in x, y, z. Thus, if

$$u = a_0 + a_1x + a_2y + a_3z$$

$$v = b_0 + b_1x + b_2y + b_3z$$

$$w = c_0 + c_1x + c_2y + c_3z$$

then the unknown parameters are

$$\underline{c} = [a_0\ a_1\ a_2\ a_3\ b_0\ b_1\ b_2\ b_3\ c_0\ c_1\ c_2\ c_3]^T$$

so that the model is

$$B\underline{c} = \begin{bmatrix} \vdots & & & & & & & & & & & \\ 1 & x & y & z & 0 & 0 & 0 & 0 & 0 & 0 & 0 & 0 \\ 0 & 0 & 0 & 0 & 1 & x & y & z & 0 & 0 & 0 & 0 \\ 0 & 0 & 0 & 0 & 0 & 0 & 0 & 0 & 1 & x & y & z \\ \vdots & & & & & & & & & & & \end{bmatrix} \begin{bmatrix} a_0 \\ a_1 \\ a_2 \\ a_3 \\ b_0 \\ b_1 \\ b_2 \\ b_3 \\ c_0 \\ c_1 \\ c_2 \\ c_3 \end{bmatrix} \qquad (4.2)$$

These three rows recur with appropriate x, y, z for each point having displacement components to be used in the estimation of the parameters. After the estimation, $B\hat{\underline{c}}$ is used in the estimation of residuals $\underline{\hat{v}}_{dx} = B\hat{\underline{c}} - \underline{dx}$. Another similar matrix B, but with x, y, z for other points, is used to generate the displacement vectors at modelling points to further illustrate or describe the deformation. If the parameters have had certain mechanical relevance, then there may also be additional characteristics derived from the estimated parameters.

One form of mechanically describing a deformation is through the infinitesimal non-translational deformation tensor for a single continuum, i.e. a deformation field in which there is no discontinuity and the same mechanical properties apply throughout. This tensor is defined as

$$E = \begin{bmatrix} \frac{\partial u}{\partial x} & \frac{\partial u}{\partial y} & \frac{\partial u}{\partial z} \\ \frac{\partial v}{\partial x} & \frac{\partial v}{\partial y} & \frac{\partial v}{\partial z} \\ \frac{\partial w}{\partial x} & \frac{\partial w}{\partial y} & \frac{\partial w}{\partial z} \end{bmatrix} = \begin{bmatrix} e_{xx} & e_{xy} & e_{xz} \\ e_{yx} & e_{yy} & e_{yz} \\ e_{zx} & e_{zy} & e_{zz} \end{bmatrix} = \left[\frac{\partial}{\partial x} B\underline{c} \quad \frac{\partial}{\partial y} B\underline{c} \quad \frac{\partial}{\partial z} B\underline{c}\right]$$

(Chen, 1983).

This tensor may be decomposed into symmetric and antisymmetric component matrices through

$$E = \frac{1}{2}(E+E^T) + \frac{1}{2}(E-E^T) = (\varepsilon_{ij}) + (\omega_{ij});\ i, j = x, y, z\ .$$

The elements of the strain tensor are obtained by

$$\varepsilon_{ij} = \frac{1}{2}(e_{ij} + e_{ji})$$

and those of rotation by

$$\omega_{ij} = \frac{1}{2}(e_{ij} - e_{ji})$$

So,

$$e_{ij} = \varepsilon_{ij}+\omega_{ij},\quad e_{ji} = \varepsilon_{ij}-\omega_{ij}\ ,$$

and

$$e_{ij} = \varepsilon_{ij} \quad \text{when } i = j.$$

Thus the elements of the tensor may be given mechanical meaning as

$$E = \begin{bmatrix} \varepsilon_{xx} & \varepsilon_{xy}+\omega_{xy} & \varepsilon_{xz}+\omega_{xz} \\ \varepsilon_{xy}-\omega_{xy} & \varepsilon_{yy} & \varepsilon_{yz}+\omega_{yz} \\ \varepsilon_{xz}-\omega_{xz} & \varepsilon_{yz}-\omega_{yz} & \varepsilon_{zz} \end{bmatrix}$$

$$= \begin{bmatrix} \varepsilon_{xx} & \varepsilon_{xy} & \varepsilon_{xz} \\ \varepsilon_{xy} & \varepsilon_{yy} & \varepsilon_{yz} \\ \varepsilon_{xz} & \varepsilon_{yz} & \varepsilon_{zz} \end{bmatrix} + \begin{bmatrix} 0 & \omega_{xy} & \omega_{xz} \\ -\omega_{xy} & 0 & \omega_{yz} \\ -\omega_{xz} & -\omega_{yz} & 0 \end{bmatrix}$$

where, for example, ε_{xx} is extension in the x direction, ε_{xy} is a shearing strain, and ω_{xy} is a rotation about the z-axis. More details may be obtained from Chen (1983), Jaeger (1969), or Sokolnikoff (1956).

If applied to a horizontal network, the tensor reduces to

$$E = \begin{bmatrix} e_{xx} & e_{xy} \\ e_{yx} & e_{yy} \end{bmatrix} = \begin{bmatrix} \varepsilon_x & \varepsilon_{xy}+\omega_{xy} \\ \varepsilon_{xy}-\omega_{xy} & \varepsilon_y \end{bmatrix} = \begin{bmatrix} \varepsilon_x & \varepsilon_{xy} \\ \varepsilon_{xy} & \varepsilon_y \end{bmatrix} + \begin{bmatrix} 0 & \omega_{xy} \\ -\omega_{xy} & 0 \end{bmatrix}$$

from which several quantities are derived.

Several direct algebraic combinations of some of the elements of E result in the terms

$$\Delta = \varepsilon_x+\varepsilon_y \tag{4.3}$$

$$\gamma_1 = \varepsilon_x-\varepsilon_y \tag{4.4}$$

$$\gamma_2 = 2\varepsilon_{xy} \tag{4.5}$$

The Δ is the dilatation (Prescott et al., 1979) or the change in area per unit area. One half of this has been termed the "mean radial dilatation" by Bibby (1976). The γ_1 is the pure shear (Chen, 1983) and γ_2 is the simple shear or engineering shear strain. Each shear is a measure of the angular change in right angles whose initial sides having azimuths of 45^o for γ_1 and 90^o for γ_2 (as in the x, y system of figure 4.1). When combined in the Pythagorean sense, they create the total shear

$$\gamma = (\gamma_1^2+\gamma_2^2)^{1/2} \tag{4.6}$$

which has an azimuth of α_γ, such that $\tan 2\alpha_\gamma = \frac{\gamma_1}{\gamma_2}$, which is described as the direction of maximum right lateral shear strain. That is, γ becomes the magnitude of the maximum angular change of the right angle having an initial side at an azimuth of α_γ. Since a pure triangulation network cannot resolve any linear changes, these derived properties are discussed

often in that context.

Further derivation yields expressions for the algebraically maximal and minimal principal strains through a diagonalization of the strain tensor. The maximum has a value

$$\varepsilon_{max} = \frac{1}{2}(\Delta+\gamma) = \frac{\varepsilon_x+\varepsilon_y}{2} + \frac{1}{2}((\varepsilon_x-\varepsilon_y)^2+4\varepsilon_{xy}^2)^{1/2} \tag{4.7}$$

and, at right angles to it, the minimum

$$\varepsilon_{min} = \frac{1}{2}(\Delta-\gamma) = \frac{\varepsilon_x+\varepsilon_y}{2} - \frac{1}{2}((\varepsilon_x-\varepsilon_y)^2+4\varepsilon_{xy}^2)^{1/2} \tag{4.8}$$

with the azimuth of ε_{max} at α_{max} such that

$$\tan 2\alpha_{max} = \frac{\gamma_2}{-\gamma_1}$$

which, as a consequence, is $\pi/4$ or 45^0 less than α_γ (Prescott et al., 1979).

This is the same diagonalization as is commonly done to obtain the squares of the major and minor semi-axes of the confidence ellipses in geodetic surveying. Here, of course, there is a slight difference since the principal strains could have negative values. Often the representation is the same but showing only the magnitude of the axes of the "strain ellipse" (Tissot's indicatrix Vanicek and Krakiwsky 1982) with, for example, arrows outward for plus (expansion) or inward for minus (contraction). (see also Thapa (1980), Schneider (1982)).

Using the linear polynomial model of equation 4.1, the relative displacement between P and Q becomes

$$(B_Q-B_P)\underline{c} = \begin{bmatrix} 0 & \Delta x & \Delta y & \Delta z & 0 & 0 & 0 & 0 & 0 & 0 & 0 & 0 \\ 0 & 0 & 0 & 0 & 0 & \Delta x & \Delta y & \Delta z & 0 & 0 & 0 & 0 \\ 0 & 0 & 0 & 0 & 0 & 0 & 0 & 0 & 0 & \Delta x & \Delta y & \Delta z \end{bmatrix} \underline{c}$$

which would be a submatrix of the whole model $B\underline{c}$. The zeros that result in the columns for a_o, b_o, c_o illustrate that the relative position change of P and Q does not involve the rigid body translation by a_o, b_o, c_o in the x, y, z directions of the whole configuration or block to which P and Q belong, i.e. they have moved together through the translation $[a_o, b_o, c_o]^T$.

This is in harmony with considering the model through the use of the tensor E, which is non-translational. Taking the partial derivatives of u, v, w of the linear polynomials for the model of equation 4.1 with respect to x, y, z create the elements of E as

$$E = \begin{bmatrix} a_1 & a_2 & a_3 \\ b_1 & b_2 & b_3 \\ c_1 & c_2 & c_3 \end{bmatrix}$$

Because these elements are not functions of x, y, z, then a homogeneous strain field is being described by this form of the tensor E.

To illustrate how the model fits into an observation equation, the remeasurement of the spatial distance from P to Q is given (section 4.2),

$$\begin{aligned} s_t + v_t &= s_{t_o} + \underline{r}^T (B_Q - B_P)\underline{c} \\ &= s_{t_o} + [\sin\beta\sin\alpha \quad \sin\beta\cos\alpha \quad \cos\beta] (B_Q - B_P)\underline{c} \\ &= s_{t_o} + [\tfrac{\Delta x}{s} \quad \tfrac{\Delta y}{s} \quad \tfrac{\Delta z}{s}] (B_Q - B_P)\underline{c} \\ &= s_{t_o} + \tfrac{\Delta x}{s}(u_Q - u_P) + \tfrac{\Delta y}{s}(v_Q - v_P) + \tfrac{\Delta z}{s}(w_Q - w_P) \\ &= s_{t_o} + \tfrac{\Delta x}{s}(\Delta x a_1 + \Delta y a_2 + \Delta z a_3) + \tfrac{\Delta y}{s}(\Delta x b_1 + \Delta y b_2 + \Delta z b_3) \\ &\quad + \tfrac{\Delta z}{s}(\Delta x c_1 + \Delta y c_2 + \Delta z c_3) \end{aligned}$$

If the network were in the homogeneous strain field described above, then the observation equation becomes

$$s_t + v_t = s_{t_o} + s\,\underline{r}^T E \underline{r}$$

$$= s_{t_o} + \underline{r}^T \begin{bmatrix} a_1 & a_2 & a3 \\ b_1 & b_2 & b_3 \\ c_1 & c_2 & c_3 \end{bmatrix} \begin{bmatrix} \Delta x \\ \Delta y \\ \Delta z \end{bmatrix}$$

$$= s_{t_o} + \left[\frac{\Delta x}{s} \quad \frac{\Delta y}{s} \quad \frac{\Delta z}{s}\right] \begin{bmatrix} \Delta x a_1 + \Delta y a_2 + \Delta z a_3 \\ \Delta x b_1 + \Delta y b_2 + \Delta z b_3 \\ \Delta x c_1 + \Delta y c_2 + \Delta z c_3 \end{bmatrix}$$

$$= s_{t_o} + \frac{\Delta x}{s}(\Delta x a_1 + \Delta y a_2 + \Delta z a_3) + \frac{\Delta y}{s}(\Delta x b_1 + \Delta y b_2 + \Delta z b_3)$$

$$+ \frac{\Delta z}{s}(\Delta x c_1 + \Delta y c_2 + \Delta z c_3)$$

In this example, the general model and the strain tensor are the same deformation model since the deformation tensor is merely another way of stating the model and yet has mechanical meaning.

The pattern of displacements might exhibit minima or maxima in a small section of the configuration. This might be modelled by second or higher order polynomials. The deformation might be regarded as the change in the shape of a surface from when it connected all of the points in their original positions to when it connected them together in their more recent positions. The deformation surface is created by making all

of the vectors of displacements emanate from a plane, if it would seem that the displacements are not behaving in reaction to the various heights (i.e. their z-coordinates). The surface is then defined by the more recent ends of the vectors. This is what could be considered in a horizontal network.

Using second order polynomials, the displacement components are given in equations 4.1. These make the deformation model

$$B\underline{c} = \begin{bmatrix} \vdots & & & & & & & & & & & & & & \\ y^2 & z^2 & 0 & 0 & 0 & 0 & 0 & 0 & 0 & 0 & 0 & 0 & 0 & 0 & \\ \ldots 0 & 0 & 1 & x & y & z & xy & xz & yz & x^2 & y^2 & z^2 & 0 & 0 & \ldots \\ 0 & 0 & 0 & 0 & 0 & 0 & 0 & 0 & 0 & 0 & 0 & 0 & 1 & x & \\ \vdots & & & & & & & & & & & & & & \end{bmatrix} \begin{bmatrix} \vdots \\ a_8 \\ a_9 \\ b_1 \\ b_2 \\ b_3 \\ b_4 \\ b_5 \\ b_6 \\ b_7 \\ b_8 \\ b_9 \\ c_1 \\ c_2 \\ \vdots \end{bmatrix}$$

so that the relative displacement becomes

$$(B_Q-B_P)\underline{c} = \begin{bmatrix} y_Q^2-y_P^2 & z_Q^2-z_P^2 & 0 & 0 & 0 & 0 & 0 & \\ \cdots\ 0 & 0 & 0 & \Delta x & \Delta y & \Delta z & x_Q y_Q - x_P y_P & \cdots \\ 0 & 0 & 0 & 0 & 0 & 0 & 0 & \end{bmatrix} \underline{c}$$

From the complexity that develops even at second order, it can be appreciated that the simplest possible model is more likely applicable due to the usual sparsity of stations. The deformation tensor now becomes

$$E = \begin{bmatrix} a_1+2a_4x+a_7y+a_8z & a_2+2a_5y+a_7x+a_9z & a_3+2a_6z+a_8x+a_9y \\ b_1+2b_4x+b_7y+b_8z & b_2+2b_5y+b_7x+b_9z & b_3+2b_6z+b_8x+b_9y \\ c_1+2c_4x+c_7y+c_8z & c_2+2c_5y+c_7x+c_9z & c_3+2c_6z+c_8x+c_9y \end{bmatrix}$$

and has elements whose values are position dependent. The strain field is no longer homogeneous.

Discontinuities or zone or group boundaries may be introduced to part off groups of stations for which the behaviour might be similar. As illustrated and discussed in Chrzanowski et al. (1983) for a horizontal network, the deforming of two blocks may be modelled. With the identification of figure 4.1, several models may be considered.

1. Rigid body translation of block B vs block A:

   a) $u_A = 0 \quad u_B = a_o$ figure 4.1a)

      $v_A = 0 \quad v_B = b_o$

   The constraining azimuth is not between two deformable points.

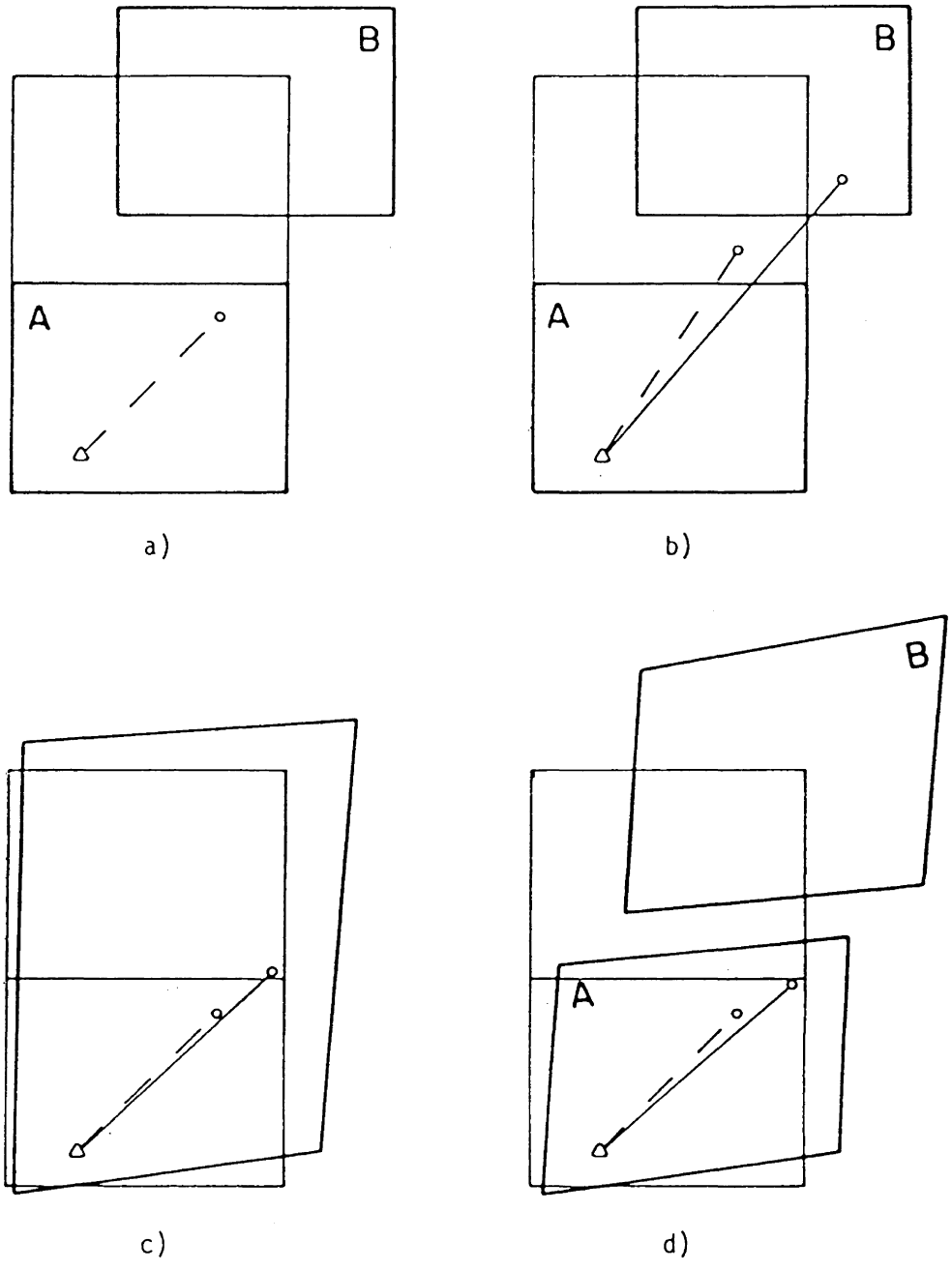

Figure 4.1 Examples of Two Block Modelling

b) $u_A = 0-\omega y \qquad u_B = a_o-\omega y$ figure 4.1b)

$v_A = 0+\omega x \qquad v_B = b_o+\omega x$

The constraining azimuth connects two stations between which deformation has occurred.

2. Homogeneous strain over all of block A and block B together:

$u_A = \varepsilon_x x+\varepsilon_{xy} y-\omega y \quad u_B = \varepsilon_x x+\varepsilon_{xy} y-\omega y$ figure 4.1c)

$v_A = \varepsilon_{xy} x+\varepsilon_y y+\omega x \quad v_B = \varepsilon_{xy} x+\varepsilon_y y+\omega x$

3. Homogeneous strain in block A and differently in block B and recognizing the discontinuity between blocks:

$u_A = \varepsilon_{xA} x+\varepsilon_{xyA} y-\omega y \quad u_B = \varepsilon_{xB} x+\varepsilon_{xyB} y-\omega y$ figure 4.1d)

$v_A = \varepsilon_{xyA} x+\varepsilon_{yA} y+\omega x \quad v_B = \varepsilon_{xyB} x+\varepsilon_{yB} y+\omega x$

The inclusion of the rotation parameter ω depends on the nature of the constraints imposed in obtaining the displacement field. Further discussion on its influence is given in section 4.4.

As may have been noticed in model 1 (figure 4.1a)), there could be as few as only one station or point in block B. Hence, this model could be used for a reference network by containing all of the reference stations in block A and by containing a single object point or, if feasible, a group of them in a separate block for each. The residuals for the u, v of block A would reveal any incongruities to the assumption that its stations are serving as a stable reference among themselves.

4.2 Observation Equations

To be truly rigorous, especially when concerned with deformation of the earth's crust, even the coordinate system must be considered in a kinematic sense since it is a local vector of gravity to which the observations are referred. This local reference would change in both magnitude and direction in reaction to the redistribution of mass about the station. This is most dramatically obvious in areas of intense seismic activity - tectonic plate movement; in areas of gross resource exploitation - subsidence due to mining or petroleum extraction; or about hydro-electric or other reservoirs when drastic changes in water levels and hence capacity are made. This has been considered by Reilly (1981, 1982) using tensor calculus. Unfortunately, the necessary information is very sparsely available. Often the networks are of very limited extent with apertures of only several kilometres. Hence, the geodetic implications will not be considered here in favour of presenting the manner in which the observation equations may be formed.

Considering a regular three-dimensional Cartesian system leads to the typical situation of two stations involved in an observation being made at station P to or in the direction of station Q, as illustrated in figure 4.2. Each of the stations would have a unique position vector from the origin of the x, y, z system. Here the concern is with the relative positions of P and Q as defined by the observations and with the effect that their movement has on a repeated observable and with how this effect is considered in the modelling of the deformation through the observation equations. The relative position from P to Q may be described by the vector

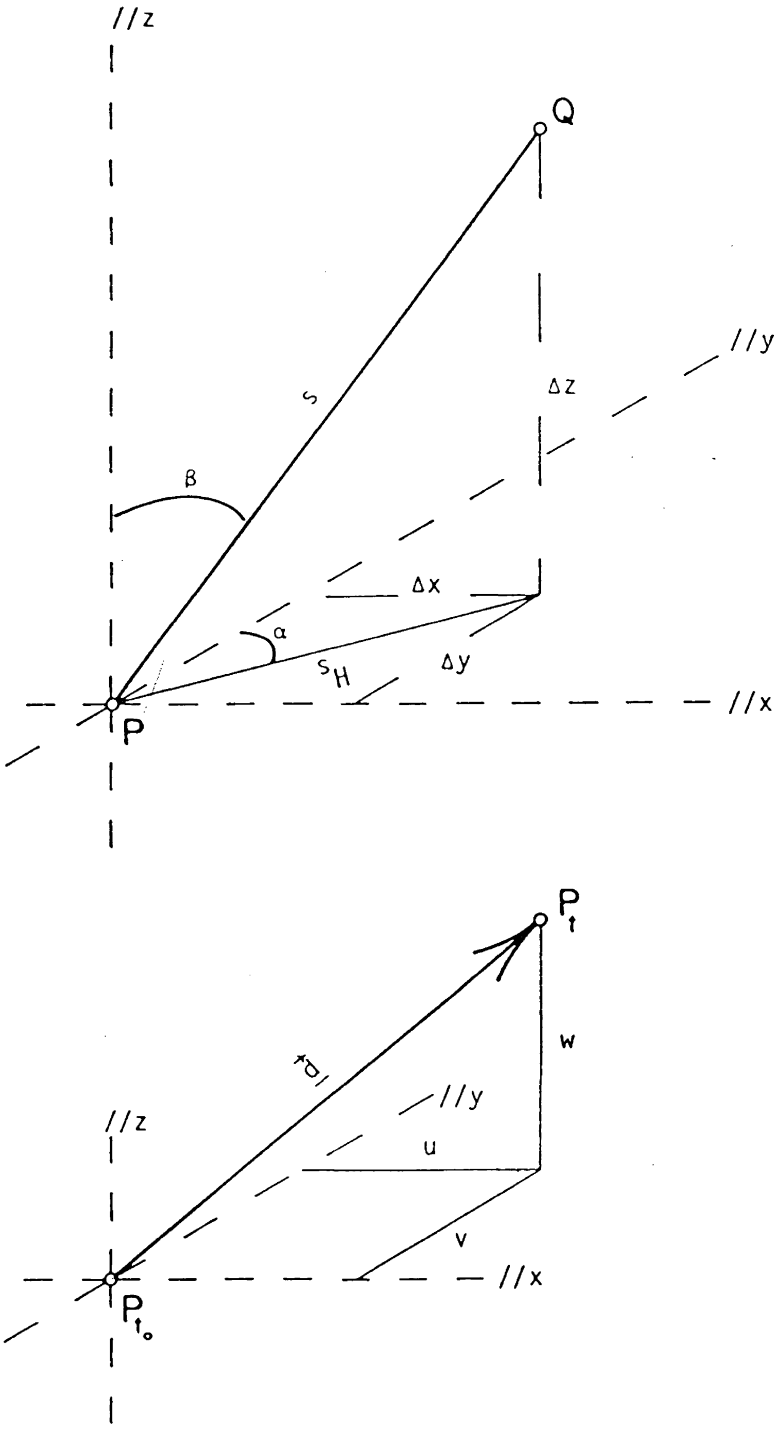

Figure 4.2 Coordinate System and Conventions

$$\vec{PQ} = \begin{bmatrix} \Delta x \\ \Delta y \\ \Delta z \end{bmatrix} = s \begin{bmatrix} \sin\beta \sin\alpha \\ \sin\beta \cos\alpha \\ \cos\beta \end{bmatrix} = s\underline{r} \tag{4.9}$$

with the spatial distance

$$s = \sqrt{s^2} \; ; \quad s^2 = \Delta x^2 + \Delta y^2 + \Delta z^2 \; . \tag{4.10}$$

In the x, y plane, the horizontal distance is

$$s_H = s \sin\beta = \sqrt{s_H^2}; \quad s_H^2 = \Delta x^2 + \Delta y^2 \tag{4.11}$$

with an azimuth, α, such that

$$\tan\alpha = \frac{\sin\alpha}{\cos\alpha} = \frac{\Delta x / s_H}{\Delta y / s_H} = \frac{\Delta x}{\Delta y} \tag{4.12}$$

And, conversely, the relative position from Q to P is

$$\vec{QP} = -\vec{PQ} = -s\underline{r} \tag{4.13}$$

If a point, typically P, had changed position from some location as P_{t_o} at time t_o to another P_t at time t, then it has been displaced through a vector having components, u, v, w, parallel to the x, y, z axes respectively. These components can be functions of space and of time, so that a displacement field for all the points of the network can be represented by

$$\underline{dx} = \begin{bmatrix} \cdot \\ \cdot \\ \cdot \\ u_p(x_p, y_p, z_p;\ t-t_o) \\ v_p(x_p, y_p, z_p;\ t-t_o) \\ w_p(x_p, y_p, z_p;\ t-t_o) \\ \cdot \\ \cdot \\ \cdot \end{bmatrix} = B_{x,y,z;\ t-t_o}\underline{c} \tag{4.14}$$

which has the deformation model $B\underline{c}$ having the parameters of the model in the vector $\underline{c}$ and the functional relationships between the u, v, w components and the elements of $\underline{c}$ expressed through the elements of B which are thus functions of x, y, z and $t - t_o$.

Following from the discussions of chapter 3, a repeated observable may be related to the displacement field and, further, to the deformation model. A campaign repeated at time t may be compared to the values at time t_o by

$$\underline{\ell}_t + \underline{v}_t = \underline{\ell}_{t_o} + AB\underline{c} \ . \tag{4.15}$$

From this, a single observable may be extracted. There is the one row of the design matrix A which has 3p columns, all elements of which would be zero except for those corresponding to x_P, y_P, z_P; x_Q, y_Q, z_Q. Correspondingly, there are the six rows of the design matrix B for u_P, v_P, w_P; u_Q, v_Q, w_Q which have non-zero elements wherever an element of the $\underline{c}$ vector affects the displacement component. Hence,

$$\ell_t + v_t = \ell_{t_o} + A_\ell B_{PQ}\underline{c} \tag{4.16}$$

Because the movement of either or both points is possible, the relative displacement $(\underline{d}_Q - \underline{d}_P)$ is considered. This may be reflected by a rearrangement of equation (4.16), i.e.

$$\ell_t + v_t = \ell_{t_o} + A_P(B_Q - B_P)\underline{c} \tag{4.17}$$

in which $A_P = [\frac{\partial}{\partial \ell}\ s\underline{r}]^T$ with $\ell = s, \alpha, \beta$ depending on the type of observable.

In section 4.1, discussion of modelling considered a deformation tensor, E which as a special case is the homogeneous strain field. Here it can be regarded as being a specific form of $B\underline{c}$ for which the whole of the network of stations may be considered as a single continuum, i.e. with no discontinuities. The relative displacement $(B_Q-B_P)\underline{c}$ is then brought about by the effect of this strain field, specifically along the line joining P to Q so that

$$(B_Q-B_P)\underline{c} = E\underline{r} \qquad (4.18)$$

Thus the elements of the tensor E are the parameters being sought and become the elements of $\underline{c}$ with appropriate elements in B.

The discussion that follows deals with the observables:

1. coordinates;
2. coordinate differences (levelling, pendula displacements, alignment);
3. azimuths and horizontal angles;
4. distances and strain;
5. zenith angles and tilts.

It has been assumed that some reasonable measure of the variance and correlation of these observables is available so that appropriate relative weighting can be made during the estimation of the model parameters.

4.2.1 Coordinates

If the point P were to change its location from P_{t_o} to P_t, then the magnitude of its position vector in the x, y, z system would change as well. The x, y, z system of t_o is recoverable at t if at least three other suitably located stations of the configuration can be considered as "stable" among themselves over the interval $t\text{-}t_o$. Then, the two position vectors can be considered as observables and compared through

$$\underline{\ell}_{P_t} + \underline{v}_t = \underline{\ell}_{P_{t_o}} + B_p \underline{c} \tag{4.19}$$

with

$$\underline{\ell}_{P_t} = \begin{bmatrix} x_p \\ y_p \\ z_p \end{bmatrix}_t, \qquad \underline{\ell}_{P_{t_o}} = \begin{bmatrix} x_p \\ y_p \\ z_p \end{bmatrix}_{t_o}$$

which can degenerate to a pair or single component. These coordinates, along with their variances and covariances, could have been transferred from another system, such as from photogrammetric measurements, into the x, y, z system.

4.2.2 Coordinate Differences

These may be observed simply, as in levelling; in pairs, as in pendula; or in less obvious combinations, as in alignment.

For a levelling run between points P and Q, the observable has been Δz_{PQ} which has changed over the time period $t\text{-}t_o$ according to the relative vertical movement of P and Q.

$$\ell_t + v_t = \ell_{t_o} + (B_{Q_w} - B_{P_w})\frac{c}{} \qquad (4.20)$$

with

$$\ell_t = \Delta z_{PQ_t} \quad \text{and} \quad \ell_{t_o} = \Delta z_{PQ_{t_o}}$$

For a suspended pendulum, the upper end of the line is "fixed" and the lower station or stations have displacement relative to the line suspended from the fixed end. So, the scale readings reveal the change in the station relative to the suspending point. For an inverted pendulum, the conditions are reversed. The stations are displaced relative to the "fixed" bottom of the line. With the appropriate z-coordinate values, the difference between suspended and inverted pendula is by sign convention. In either case, the x, y values are considered constant along the plumbline - with suitable corrections for physical aberrations of the line having been applied. The scale readings can be considered to be made in a horizontal plane (i.e. parallel to the x,y plane) $z = z_p$ with the fixed point at $z = z_Q$. If the y' scale is oriented at an angle of θ through which a clockwise rotation would bring it parallel to the y coordinate axis and likewise, the x' scale as shown in figure 4.3.

The $\delta x'$ and $\delta y'$ are the scale reading differences for the time interval $t-t_o$. When multiplied by the factor k, they are in the same units as the x, y coordinate system. The points P_{t_o} and P_t are the positions of the plumb-line at t_o and t respectively relative to the scale x', y'. The displacement of P with respect to Q the "fixed" end of the plumbline is $-\delta x'$ and $-\delta y'$. But the relative displacement of Q w.r.t. P is δx, δy, positive in the sense as given above in the figure.

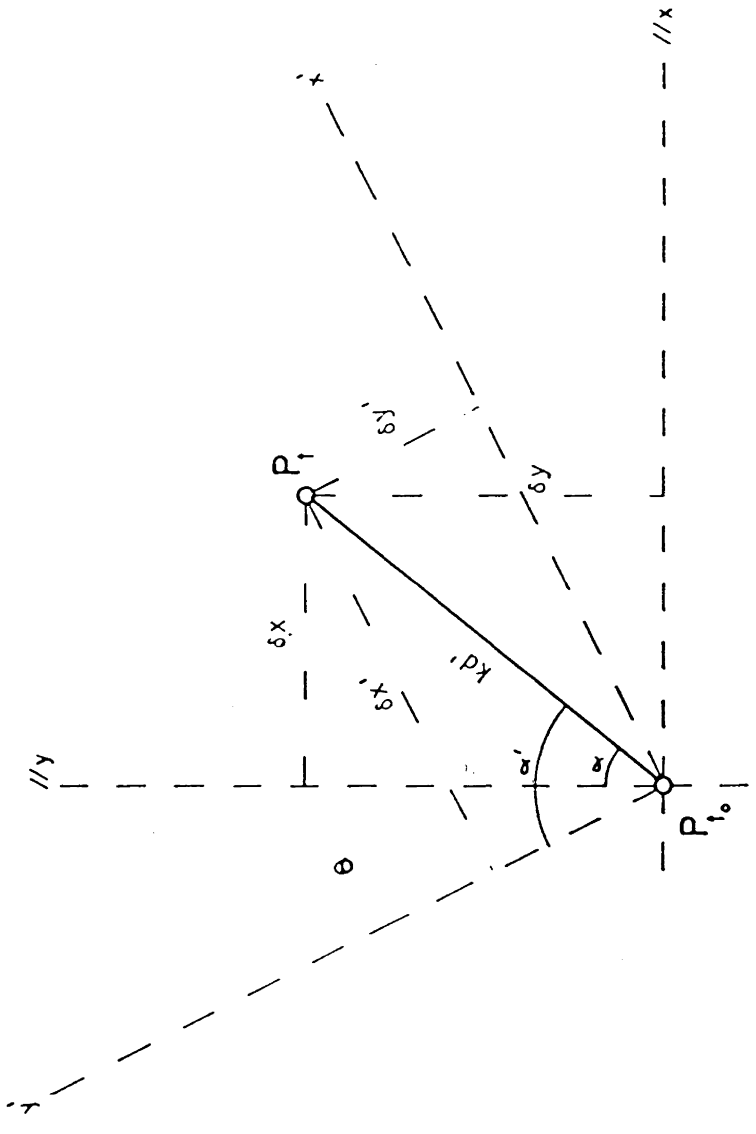

Figure 4.3 Pendulum Displacements

$$d' = [(\delta x')^2 + (\delta y')^2]^{1/2}; \quad \alpha' = \arctan \frac{\delta x'}{\delta y'}, \quad \alpha = \alpha' - \theta$$

$$\delta x = kd' \sin \alpha, \quad \delta y = kd' \cos \alpha$$

If the scale readings at t_o were not zero, then the observables at t and t_o are related by

$$\ell_{x_t} - \delta x_t = \ell_{x_{t_o}}; \quad \ell_{y_t} - \delta y_t = \ell_{y_{t_o}}$$

so, the observation equations become

$$\ell_{x_t} + v_t = \ell_{x_{t_o}} + (B_{\underset{u}{Q}} - B_{\underset{u}{P}})\underline{c}$$

$$\ell_{y_t} + v_t = \ell_{y_{t_o}} + (B_{\underset{v}{Q}} - B_{\underset{v}{P}})\underline{c} \qquad (4.21)$$

in which

$$B_{\underset{u,v}{Q}} = B(x_Q, y_Q, z_Q; t-t_o); \quad B_{\underset{u,v}{P}} = B(x_Q, y_Q, z_Q; t-t_o)$$

Horizontal alignment, figure 4.4, is similar to the displacement of the pendulum; however, here it is likely that only the one component, the y' has been remeasured. Hence only the displacement of Q' laterally relative to the line PQ can be resolved. However, the position of the line PQ may also have changed because of the movement of P and Q.

First, considering the axes to coincide, i.e. that $\theta = 0$, leads to a direct measurement of $\delta y_{Q'}$,

$$\delta y_{Q'_{t-t_o}} = y_t - y_{t_o} = \ell_t - \ell_{t_o}$$

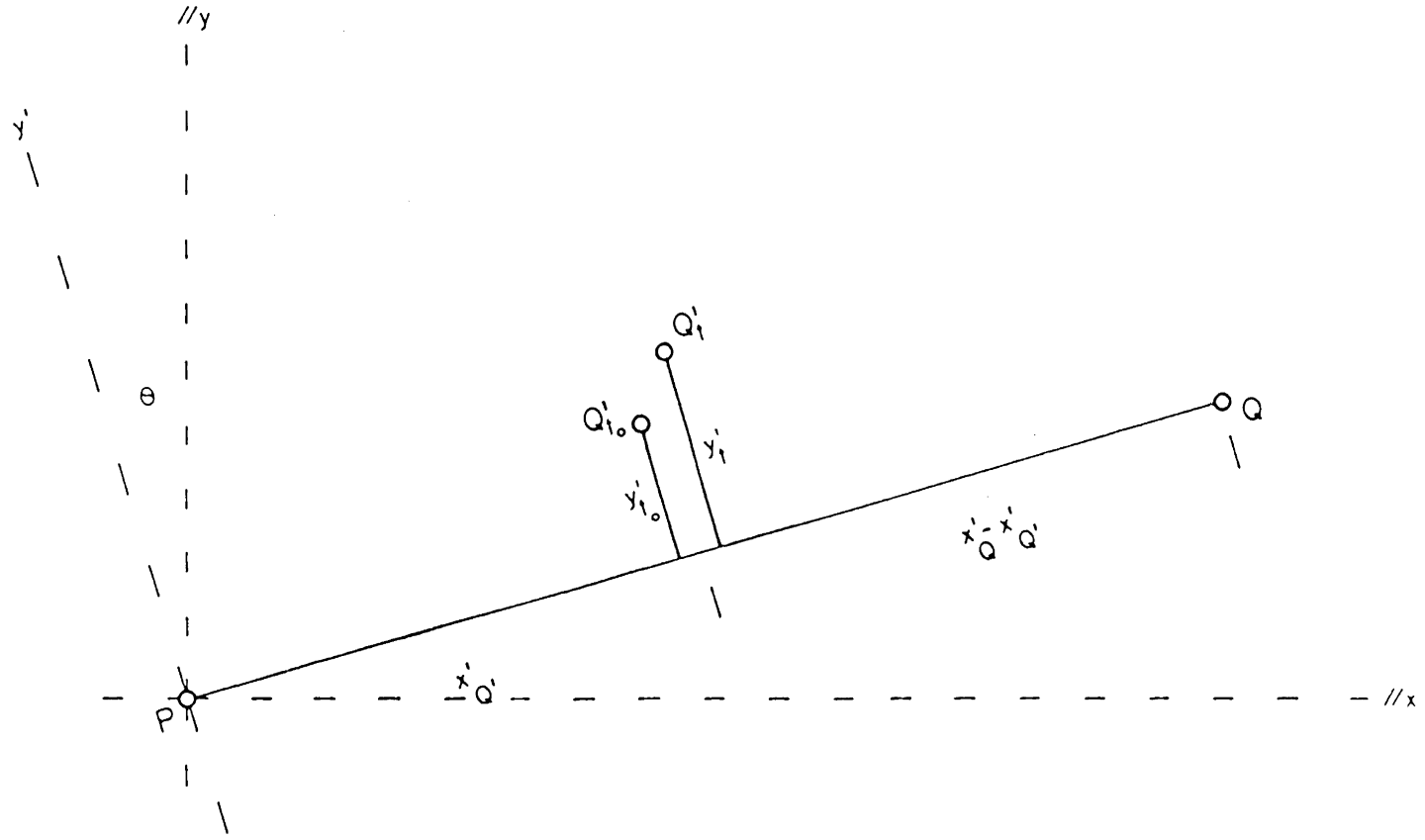

Figure 4.4 Alignment

so, incorporating the movement of P and Q which in this case is only the component, v, which would cause lateral movement of the line PQ, results in the observation equation:

$$\ell_t + v_t = \ell_{t_o} + \{B_{Q'_v} - (\frac{x'_Q - x'_{Q'}}{x'_Q})B_{Q_v} - \frac{x'_{Q'}}{x'_Q} B_{P_v}\}\underline{c} \qquad (4.22)$$

If the line PQ is at some other orientation, i.e. θ, then both the u and v components of the movement of P and Q will affect the position of the reference line at the foot of its perpendicular to Q'. The azimuth of the line PQ is α, so the direction of the displacement affecting the y' measurement is α-90°. Hence, the components of displacement can be applied to be along the perpendicular to Q', i.e. the azimuth α-90°. So,

$$\ell_t + v_t = \ell_{t_o} + [\sin\alpha \ \cos\alpha] \begin{bmatrix} B_{Q'_u} - (\frac{x'_Q - x'_{Q'}}{x'_Q})B_{Q_u} - \frac{x'_{Q'}}{x'_Q} B_{P_u} \\ B_{Q'_v} - (\frac{x'_Q - x'_{Q'}}{x'_Q})B_{Q_v} - \frac{x'_{Q'}}{x'_Q} B_{P_v} \end{bmatrix} \underline{c}$$

$$= \ell_{t_o} + [\sin\alpha \ \cos\alpha] \frac{1}{x'_Q} \begin{bmatrix} x'_Q B_{Q'_u} + (x'_{Q'} - x'_Q) B_{Q_u} - x'_{Q'} B_{P_u} \\ x'_Q B_{Q_v} + (x'_{Q'} - x'_Q) B_{P_v} - x'_{Q'} B_{P_v} \end{bmatrix} \underline{c}$$

$$= \ell_{t_o} + [\sin\alpha \ \cos\alpha] \begin{bmatrix} B_{Q'_u} & B_{Q_u} & B_{P_u} \\ B_{Q'_v} & B_{Q_v} & B_{P_v} \end{bmatrix} \frac{1}{x'_Q} \begin{bmatrix} x'_Q \\ x'_{Q'} - x'_Q \\ -x'_{Q'} \end{bmatrix} \underline{c} \qquad (4.23)$$

Vertical alignment would be a combination of the above, but in some vertical plane passing through the zenith at P, and levelling. The slope of the line would now be θ with only the vertical, w, component that could be resolved. Hence,

$$\ell_t+v_t = \ell_{t_o} + [B_{Q'w} \quad B_{Qw} \quad B_{Pw}] \frac{1}{x'_Q} \begin{bmatrix} x'_Q \\ x'_{Q'}-x'_Q \\ -x'_{Q'} \end{bmatrix} \underline{c} \qquad (4.24)$$

4.2.3 Azimuths and Horizontal Angles

Following the general form of observation equation,

$$\alpha_t+v_t = \alpha_{t_o}+A_\alpha(B_Q-B_P)\underline{c}$$

and from the definition of the azimuth,

$$\alpha = \arctan \frac{\Delta x}{\Delta y}$$

within which are the coordinates x_P, y_P; x_Q, y_Q. So, the partial derivatives for the configuration matrix A may be expressed as

$$\frac{\partial \alpha}{\partial x} = \ldots = \frac{\Delta y}{\Delta y^2+\Delta x^2} = \frac{\Delta y}{s_H^2} = \frac{\cos \alpha}{s_H}$$

$$\frac{\partial \alpha}{\partial y} = \ldots = \frac{-\Delta x}{\Delta y^2+\Delta x^2} = \frac{-\Delta x}{s_H^2} = \frac{-\sin \alpha}{s_H}$$

$$\frac{\partial d}{\partial z} = 0$$

which would infer that only the horizontal components of the deformation model affect the observation of azimuth. The equation may be more explicit as

$$\alpha_t+v_t = \alpha_{t_o} + \frac{1}{s_H}[\cos\alpha \;\; -\sin\alpha \;\; 0]\,(B_Q-B_P)\underline{c} \tag{4.25}$$

In this and in the following expressions, the columns for the unaffected stations have been left out of the row of the A matrix.

In a homogeneous strain field, this becomes

$$\alpha_t+v_t = \alpha_{t_o}+A_\alpha \underline{Er}$$

in which only the x, y components are involved.

A horizontal angle can be defined as the difference between two azimuths. With a second azimuth from P to R, the observation of the angle $\ell_t = \alpha_R-\alpha_Q$ becomes

$$\ell_t+v_t = \ell_{t_o} - \frac{1}{s_{H_Q}}[\cos\alpha_Q \;\; -\sin\alpha_Q \;\; 0]\,(B_Q-B_P)\underline{c}$$

$$+ \frac{1}{s_{H_R}}[\cos\alpha_R \;\; -\sin\alpha_Q \;\; 0]\,(B_R-B_P)\underline{c}$$

$$= \ell_{t_o} - A_{\alpha_Q}\,(B_Q-B_P)\underline{c} + A_{\alpha_R}\,(B_R-B_P)\underline{c} \tag{4.26}$$

which, in a homogeneous strain field, becomes

$$\ell_t+v_t = \ell_{t_o} - A_{\alpha_Q}\underline{Er}_{PQ} + A_{\alpha_R}\underline{Er}_{PR} \tag{4.27}$$

Because the two azimuths, α_Q and α_R, have not been measured, there is a loss of orientation and the ω_{xy} cannot be resolved. Consequently, if a pseudo-observation of azimuth is used to remove the datum

defect in the creation of the displacement field, then the ω_{xy} must be included as a nuisance parameter in the deformation model to ensure the independence of the other parameters from the arbitrary selection of a datum (Chrzanowski et al., 1983; Chen, 1983). This would also apply to pure trilateration or triangulation, wherever the pseudo-azimuth had been applied over a deformable zone. Further discussion is given in section 4.4.

4.2.4 Distances and Strain

Following the general form, the observation of a spatial distance at the subsequent campaign can be compared through

$$s_t + v_t = s_{t_o} + A_s(B_Q - B_P)\underline{c}$$

The observable has been defined, so that

$$s = (\Delta x^2 + \Delta y^2 + \Delta z^2)^{1/2}$$

for which

$$\frac{\partial s}{\partial x} = \ldots = \frac{\Delta x}{s} = \frac{s \sin\beta \sin\alpha}{s} = \sin\beta \sin\alpha$$

$$\frac{\partial s}{\partial y} = \ldots = \frac{\Delta y}{s} = \frac{s \sin\beta \cos\alpha}{s} = \sin\beta \cos\alpha$$

$$\frac{\partial s}{\partial z} = \ldots = \frac{\Delta z}{s} = \frac{s \cos\beta}{s} = \cos\beta$$

So, more explicitly,

$$s_t+v_t = s_{t_o} + [\sin\beta \sin\alpha \quad \sin\beta \cos\alpha \quad \cos\beta](B_Q-B_P)\underline{c}$$

$$= s_{t_o} + \underline{r}^T (B_Q-B_P)\underline{c} \tag{4.28}$$

The measurement of strain along the line PQ is defined as $\frac{s_t-s_{t_o}}{s_{t_o}} = \frac{\Delta s}{s}$. So, the measurement of strain, as by a gauge, at P in the direction of Q makes the separation of Q from P, i.e. s, differentially small. Thus, as an observable, strain becomes

$$\ell_t+v_t = \ell_{t_o} + \underline{r}^T E \underline{r} = \ell_{t_o} + A_s^T E A_s \tag{4.29}$$

in which the $\underline{r}^T E \underline{r}$ represents the strain that has accumulated over the time interval $t-t_o$ to cause the reading of the strain meter to change from ℓ_{t_o} to ℓ_t.

4.2.5 Zenith Angles and Tilt

From the general form, the observations of a zenith angle may be compared by

$$\beta_t+v_t = \beta_{t_o} + A_\beta (B_Q-B_P)\underline{c}$$

From the definition of zenith angle,

$$\beta = \arctan \frac{(\Delta x^2+\Delta y^2)^{1/2}}{\Delta z}$$

so that the design matrix has partial derivatives

$$\frac{\partial\beta}{\partial x} = \ldots = \frac{\Delta x \Delta z}{s^2 s_H} = \ldots = \frac{\cos\beta \sin\alpha}{s}$$

$$\frac{\partial\beta}{\partial y} = \ldots = \frac{\Delta y \Delta z}{s^2 s_H} = \ldots = \frac{\cos\beta \cos\alpha}{s}$$

$$\frac{\partial\beta}{\partial z} = \ldots = \frac{-s_H}{s^2} = \ldots = \frac{-\sin\beta}{s}$$

These make an explicit form

$$\beta_{t+v_t} = \beta_{t_o} + \frac{1}{s}\left[\cos\beta \sin\alpha \quad \cos\beta \cos\alpha \quad -\sin\beta\right](B_Q - B_P)\underline{c}$$

$$= \beta_{t_o} + \left[\frac{\partial}{\partial\beta}\underline{r}\right]^T (B_Q - B_P)\underline{c} \tag{4.30}$$

The measurement of tilt may be considered as that of the zenith angle at P in the direction of Q which is only differentially distant from P. This type of measurement cannot resolve any ω_{xy} nor any horizontal strain. Hence only the z-component of deformation can be considered. Thus the tilt observable may be expressed by

$$\ell_{t+v_t} = \ell_{t_o} + A_\beta \left[\frac{\partial}{\partial x,y} B_w \underline{c}\right]$$

$$= \ell_{t_o} + \left[\sin\alpha \quad \cos\alpha \quad 0\right]\begin{bmatrix} \frac{\partial}{\partial x} B_w\underline{c} \\ \frac{\partial}{\partial y} B_w\underline{c} \\ \frac{\partial}{\partial z} B_w\underline{c} \end{bmatrix} \tag{4.31}$$

In a homogeneous strain field, this becomes

$$\ell_{t+v_t} = \ell_{t_o} + A_\beta E\underline{r}$$

$$= \ell_{t_o} + \left[\sin\alpha \cos\alpha\right]\underline{\phi} \tag{4.32}$$

in which

$$\underline{\phi} = \begin{bmatrix} -e_{zx} \\ -e_{zy} \end{bmatrix} = \begin{bmatrix} -(\varepsilon_{xz}-\omega_{xz}) \\ -(\varepsilon_{yz}-\omega_{yz}) \end{bmatrix}$$

for a horizontal tiltmeter, or

$$\underline{\phi} = \begin{bmatrix} e_{xz} \\ e_{yz} \end{bmatrix} = \begin{bmatrix} \varepsilon_{xz}+\omega_{xz} \\ \varepsilon_{yz}+\omega_{yz} \end{bmatrix}$$

for a vertical (borehole) tiltmeter (Reilly, 1981).

4.3 Model Estimation and Assessment

As an end in itself, or as a more elaborate indication of the trend, the deformation model may be considered for only two campaigns of measurement. Discussion of campaign pair modelling is likely to be more often applicable and may be readily extended to the simultaneous modelling described in chapter 5 since it is really a special case of multiple-campaigns.

The form of the observation equations of section 4.2 and the estimation of the elements of $\underline{c}$, the parameters, are based on the hypothesis (Chrzanowski et al., 1983):

$$H_o: \quad E\{\underline{\ell}_t\} = E\{\underline{\ell}_{t_o}\} + A_{t_o} B\underline{c} = \underline{\xi} + A_{t_o} B\underline{c}$$

versus

$$H_A: E\{\underline{\ell}_t\} \neq \underline{\xi} + A_{t_o} B\underline{c}$$

The matrix B is as the design matrix B of earlier sections. The elements of the $\underline{\ell}_t$ and $\underline{\ell}_{t_o}$ may be coordinates. If they were all coordinates, then $\underline{dx} = \underline{\ell}_t - \underline{\ell}_{t_o}$ and the matrix A would be an identity matrix.

From this, the mathematical model, as used for the observation equations, may be stated as

$$\underline{\ell}_{t_o} + \underline{v}_{t_o} = \underline{\xi}$$

$$\underline{\ell}_t + \underline{v}_t = \underline{\xi} + AB\underline{c}$$

For only a pair of campaigns, these two may be combined as

$$\underline{d\ell} + \underline{v} = AB\underline{c}$$

with

$$C_{d\ell} = \sigma_o^2 Q_{d\ell} = \sigma_{o_{t_o}}^2 Q_{t_o} + \sigma_{o_t}^2 Q_t$$

If the two campaigns had been adjusted using the same minimal constraints, then

$$\underline{d\ell} = \underline{dx} = \underline{\hat{x}}_t - \underline{\hat{x}}_{t_o}$$

with

$$C_{d\ell} = \sigma_o^2 Q_{dx} = \sigma_o^2 (Q_{x_{t_o}} + Q_{x_t}) \quad \text{and} \quad \sigma_o^2 = \frac{\nu_{t_o} \hat{\sigma}_{o_{t_o}}^2 + \nu_t \hat{\sigma}_{o_t}^2}{\nu}$$

and

$$\nu = \nu_{t_o} + \nu_t$$

The parameters are estimated by

$$\underline{\hat{c}} = ((AB)^T Q_{d\ell}^{-1} (AB))^{-1} (AB)^T Q_{d\ell}^{-1} \underline{d\ell} \tag{4.33}$$

with

$$\hat{C}_c = \hat{\sigma}_o Q_c = \hat{\sigma}_o^2 ((AB)^T Q_{d\ell}^{-1} (AB))^{-1}$$

and

$$\underline{\hat{v}} = AB\underline{\hat{c}} - \underline{d\ell} \quad \text{so} \quad \hat{\sigma}_o^2 = \frac{\underline{v}^T Q_{d\ell}^{-1} \underline{v}}{\nu_c \sigma_o^2}$$

with $\nu_c = n_\ell - d - u$

The degrees of freedom in the estimation of $\hat{\sigma}_o^2$, ν_c, is the number of observations ($n_\ell = 3p$ if three dimensional displacements) minus the defect of the network and minus the number of parameters. The global appropriateness of the model may be assessed from the hypotheses

$$H_o: \hat{\sigma}_o^2 = \sigma_o^2 \text{ versus } H_A: \hat{\sigma}_o^2 \neq \sigma_o^2$$

using the statistic

$$T^2 = \frac{\hat{\sigma}_o^2}{\sigma_o^2} \leq F(\nu_c, \nu; \alpha) \tag{4.34}$$

Individual parameters or groups of parameters may be assessed through

$$T^2 = \frac{\underline{c}_i^T Q^{-1} \underline{c}_i}{u_i \hat{\sigma}_o^2} = F(u_i, \nu_c; \alpha) \tag{4.35}$$

from which α may be obtained. The groupings are such that $\underline{c}_i \in \underline{c}$, $u_i = 1, 2, 3, \ldots, u$ with Q extracted from Q_c.

4.4 Cautionary Remarks

Just as there are precautions in the position determination of conventional geodetic surveying, the creation of a model for deformation must have regard for the determinability of parameters and for ensuring that the parameters have been suitably chosen to result in an unbiased solution.

Whether the value of a parameter will be adequately determined may be realized from the type of repeated observables and from the forms of the observation equations involved. This aspect has been discussed by Reilly (1981) and is repeated here.

Being horizontal angular measurement, pure triangulation can resolve only the components of shearing strain, ε_{xy} and $(\varepsilon_y - \varepsilon_x)$ in which the two components cannot be separated. In addition, horizontal distances would separate ε_x and ε_y. The height differences of a levelling network enable determining $(\varepsilon_{xz} - \omega_{xz})$ and $(\varepsilon_{yz} - \omega_{yz})$, the terms of which could be separated through using also borehole tiltmeters by adding $(\varepsilon_{xz} + \omega_{xz})$ and $(\varepsilon_{yz} + \omega_{yz})$. The use of a borehole or vertical extensometer or strainmeter would resolve the ε_z extension which could also come out of an appropriately configured levelling network, since

$$\frac{\Delta z_{i+1} - \Delta z_i}{\Delta z_i} = \varepsilon_z \quad .$$

Even when the network has been intentionally three dimensional, the relative heights of the stations affect the determinability. As the deformation field is applied to the line of observation, the orientation of the line reflects its ability to resolve components of the deformation model. As the relative heights become less, the observation line approaches

the horizontal, β nears 90°, and cos β becomes very small. The consequence is a degradation in accuracy and, in the limit, in the determinability as given above.

This is very much apparent when mechanical properties are being considered. The danger arises especially in the use of polynomials and the gradual removal of insignificant parameters to obtain the least complicated model. The most common mistake is to remove or to consider as zero the rigid body rotation component ω_{xy} in a horizontal network when there has been no opportunity for external orientation through an azimuth observable. The nature of the constraining pseudo-azimuth imposed may require the inclusion of ω_{xy}, either implicitly or explicitly, as a nuisance parameter (Chrzanowski et al., 1983). As either or both of the stations involved, say P and Q as in figure 4.1, are situated in a zone in which $\underline{dx} \neq 0$, then the possible relative movement is confined to occur along the line having the azimuth α so that $\tan \alpha = \frac{u_Q - u_P}{v_Q - v_P}$. This creates a functional relationship between the coefficients of the expressions for $(u_Q - u_P)$ and $(v_Q - v_P)$. For example, if

$$u = \varepsilon_x x + \varepsilon_{xy} y - \omega y$$

$$v = \varepsilon_{xy} x + \varepsilon_y y + \omega x$$

then

$$\tan \alpha = \frac{\varepsilon_x \Delta x + \varepsilon_{xy} \Delta y - \omega \Delta y}{\varepsilon_{xy} \Delta x + \varepsilon_y \Delta y + \omega \Delta x}$$

so that

$$\omega = \frac{1}{2} (\varepsilon_x - \varepsilon_y) \sin 2\alpha + \varepsilon_{xy} \cos 2\alpha$$

and any variation associated with changes in the minimal constraints is absorbed by a change in the value of ω. This renders the values of the other parameters invariant.

The inclusion of ω when the parameters are estimated using displacements must also be ensured. The displacements and their attendant covariance matrix are datum dependent if estimated using minimal constraints. This dependency is removed with the inclusion of ω (Chrzanowski and Chen, 1981; Chrzanowski et al., 1983; Chen, 1983). In the use of polynomials to describe the u, v, the existence of the terms such as $(\varepsilon_{xy}-\omega)\Delta y$ and $(\varepsilon_{xy}+\omega)\Delta x$ simultaneously is not so explicit and care must be exercised to ensure their inclusion (Chrzanowski and Chen, 1981).

The effect of this rotation parameter may be illustrated by simulating the horizontal rigid body movement of one block against another (figure 4.1b). For simplicity, station P has been taken as the origin of the x, y coordinate system and also as the fixed station of the network (figure 4.5). Station P is situated in the reference block A for which

$$H_o: \underline{dx} = 0$$

However, the constraining azimuth, α_{PQ}, extends beyond block A to some point Q in block B for which

$$H_o: \underline{dx} \neq 0.$$

If the actual or simulated movement of block B is

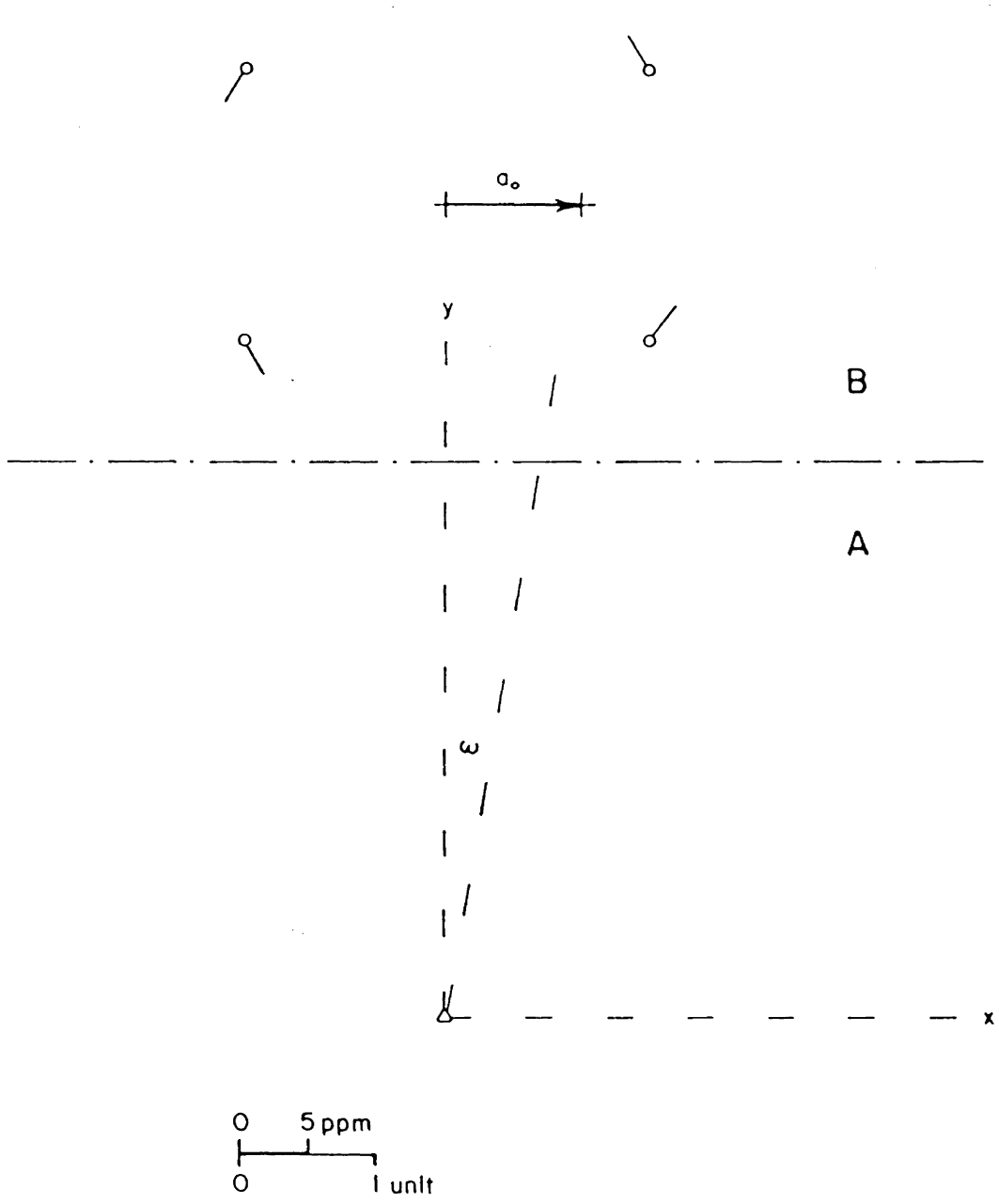

Figure 4.5 Example of the Effect of the Rotation Parameter

$$\underline{dx}_B = \begin{bmatrix} 1 \times 10^{-5} \\ 0.000 \end{bmatrix}$$

then the movement of Q, within or as a part of block B, is $\underline{dx}_B$ which creates a rotation of the azimuth α_{PQ} by $\omega = \frac{10^{-5}}{6} = 1.67 \times 10^{-6}$ radian = 0.3". The effect of this has been superimposed on the displacement vectors at the four stations of block B, one of which could be Q. This results in a set of displacement components that are used as the observations, i.e.

$$\underline{\ell} = \underline{dx} = [-1.67 \quad -2.5 \quad 1.67 \quad -2.5 \quad 1.67 \quad 2.5 \quad -1.67 \quad 2.5]^T \times 10^{-6}$$

If each is regarded as having the same accuracy and no correlation with the others, then P = I which further simplifies the illustration.

If the deformation of block B is given the model

$$u_B = a_o$$

$$v_B = b_o$$

then for the four points of block B, the deformation model becomes

$$B\underline{c} = \begin{bmatrix} 1 & 0 & 1 & 0 & 1 & 0 & 1 & 0 \\ 0 & 1 & 0 & 1 & 0 & 1 & 0 & 1 \end{bmatrix}^T \begin{bmatrix} a_o \\ b_o \end{bmatrix}$$

so

$$\hat{\underline{c}} = (B^T B)^{-1} B^T \underline{dx}$$

$$= \begin{bmatrix} 4 & 0 \\ 0 & 4 \end{bmatrix}^{-1} \begin{bmatrix} 0 \\ 0 \end{bmatrix} = \begin{bmatrix} 0 \\ 0 \end{bmatrix}$$

with

$$Q_c = \begin{bmatrix} 0.25 & 0 \\ 0 & 0.25 \end{bmatrix}$$

However, when the model is given as

$$u_B = a_o - \omega y$$

$$v_B = b_o + \omega x$$

then the deformation model becomes

$$B\underline{c} = \begin{bmatrix} 1 & 0 & 1 & 0 & 1 & 0 & 1 & 0 \\ 0 & 1 & 0 & 1 & 0 & 1 & 0 & 1 \\ -y_a & x_a & -y_b & x_b & -y_c & x_c & -y_d & x_d \end{bmatrix}^T \begin{bmatrix} a_o \\ b_o \\ \omega \end{bmatrix}$$

making

$$\underline{\hat{c}} = (B^TB)^{-1}B^T\underline{dx}$$

$$= \begin{bmatrix} 4 & 0 & -\Sigma y \\ 0 & 4 & \Sigma x \\ -\Sigma y & \Sigma x & \Sigma(x^2+y^2) \end{bmatrix}^{-1} \begin{bmatrix} 0 \\ 0 \\ \Sigma(-yu + xv) \end{bmatrix}$$

$$= \begin{bmatrix} 4 & 0 & -24 \\ 0 & 4 & 0 \\ -24 & 0 & 157 \end{bmatrix}^{-1} \begin{bmatrix} 0 \\ 0 \\ 21.68 \times 10^{-6} \end{bmatrix}$$

$$= \begin{bmatrix} 1.0006 \times 10^{-5} \\ 0 \\ 1.67 \times 10^{-6} \end{bmatrix}$$

with

$$Q_c = \begin{bmatrix} 3.02 & 0 & 0.46 \\ 0 & 0.25 & 0 \\ 0.46 & 0 & 0.08 \end{bmatrix}$$

which would be realistic if σ_0^2 were given as 1×10^{-6} or smaller.

In the repeated measurement of distances, there is always the danger of misinterpreting changes in the characteristics of the measuring system as being changes in the line lengths. The system is comprised of the instrument itself (electronic or mechanical), the ancillary measuring of temperatures and pressure, and the reduction procedures. Rigorous and frequent calibration and attention to measurement procedures (e.g. Rueger, 1980) can alleviate this concern and render the measurements comparable.

As inferred by Reilly (1981), the integration of these several types of observables and further, to extraterrestrial connections, such as through astronomical azimuths, latitude, and longitude, very long baseline interferometry (VLBI), or Global Positioning System (GPS), would certainly enhance the monitoring of any large scale deformation such as tectonic plate movement, especially by overcoming the problem of datum defect.

5. MODEL ESTIMATION OVER SEVERAL CAMPAIGNS SIMULTANEOUSLY

From the successive campaign comparisons, it may appear that a model with only subtle variation might apply through several or all of the campaigns. Or, it may appear that some function of time could fit through the campaigns. For these, the campaigns involved could be used together to simultaneously estimate all of the parameters. It would be a matter of necessity in doing so if the observations had been made over time so that they could not be practically grouped as campaigns. Nonetheless, the observations would be grouped as much as possible and indexed according to some instant of time. In all cases, in order to accommodate the identification of the different varieties of model, whether as space or time, with the observations that they would affect, both the campaigns and the model would recognize some function of time (e.g. discrete values for the campaigns, functions from first instant for the models).

For a total of k campaigns, there is an assortment of observations, typically $\underline{\ell}_i'$, with a suitably ascribed cofactor matrix, Q_i (so that $P_i = \sigma_o^{-2} Q_i^{-1}$ with σ_o^2 the same for each of the k campaigns), and index of time, t_i. These vectors are redimensioned so that each campaign contains all possible observables in the same order but non-zero weights occur only when the real observations have been made. Now, each $\underline{\ell}_i$ and its P_i have the same dimension, n_ξ, but may be populated by some false

observations with corresponding zero weight.

The estimation of the parameters is based on the expectation that

$$H_o: E\{\underline{\ell}_i\} = E\{\underline{\ell}_1\} + A_iB_i\underline{c} = \underline{\xi} + A_iB_i\underline{c}$$

versus

$$H_A: E\{\underline{\ell}_i\} \neq \underline{\xi} + A_iB_i\underline{c} \ .$$

With the P_i and the unknown parameters being $\underline{\xi}$ and $\underline{c}$, this is undertaken in the usual least squares sense, i.e. minimizing $\underline{v}^T P \underline{v}$. The system of equations may be given more explicitly as

$$\begin{bmatrix} \underline{\ell}_1 \\ \underline{\ell}_2 \\ \vdots \\ \underline{\ell}_i \\ \vdots \\ \underline{\ell}_k \end{bmatrix} + \begin{bmatrix} \underline{v}_1 \\ \underline{v}_2 \\ \vdots \\ \underline{v}_i \\ \vdots \\ \underline{v}_k \end{bmatrix} = \begin{bmatrix} I & 0 \\ I & A_2B_2 \\ \vdots & \\ I & A_iB_i \\ \vdots & \\ I & A_kB_k \end{bmatrix} \begin{bmatrix} \underline{\xi} \\ \underline{c} \end{bmatrix} \qquad (5.1)$$

with the diagonal weight hypermatrix $P = \text{diag}\,(P_1, P_2, \ldots, P_i, \ldots, P_k)$ in which some of the P_i may be singular due to the zero weighting for false observations.

The system of normal equations is formed as

$$\begin{bmatrix} \sum_{i=1}^{k} P_i & \sum_{i=2}^{k} P_iA_iB_i \\ \sum_{i=2}^{k} B_i^TA_i^TP_i & \sum_{i=2}^{k} B_i^TA_i^TP_iA_iB_i \end{bmatrix} \begin{bmatrix} \underline{\xi} \\ \underline{c} \end{bmatrix} = \begin{bmatrix} \sum_{i=1}^{k} P_i\underline{\ell}_i \\ \sum_{i=2}^{k} B_i^TA_i^TP_i\underline{\ell}_i \end{bmatrix} \qquad (5.2)$$

i.e.

$$\begin{bmatrix} N_{11} & N_{12} \\ N_{21} & N_{22} \end{bmatrix} \begin{bmatrix} \underline{\xi} \\ \underline{c} \end{bmatrix} = \begin{bmatrix} \underline{u}_1 \\ \underline{u}_2 \end{bmatrix} \tag{5.3}$$

After the elimination of the nuisance parameter $\underline{\xi}$, the desired parameters are estimated by

$$\hat{\underline{c}} = [N_{22} - N_{21}N_{11}^{-1}N_{12}]^{-1} [\underline{u}_2 - N_{21}N_{11}^{-1}\underline{u}_1] \tag{5.4}$$

with $Q_c = [N_{22} - N_{21}N_{11}^{-1}N_{12}]^{-1}$.

The estimation of the residuals requires the estimates for the elements of the $\underline{\xi}$ vector, so

$$\hat{\underline{\xi}} = N_{11}^{-1}[\underline{u}_1 - N_{21}\hat{\underline{c}}] \tag{5.5}$$

Thus, for each campaign

$$\underline{v}_i = \underline{\ell}_i - [I \quad A_iB_i] \begin{bmatrix} \hat{\underline{\xi}} \\ \hat{\underline{c}} \end{bmatrix} = \underline{\ell}_i - \hat{\underline{\xi}} - A_iB_i\hat{\underline{c}} \tag{5.6}$$

which contribute to a grand quadratic form through

$$\Delta R = \sum_{i=1}^{k} \hat{\underline{v}}_i^T P_i \hat{\underline{v}}_i$$

With this, the variance factor is estimated by

$$\hat{\sigma}_{oc}^2 = \frac{\Delta R}{\nu_c} \tag{5.7}$$

with $\nu_c = \text{rank}(P) - \dim(\underline{\xi}) - \dim(\underline{c}) - d$ in which $\text{rank}(P) = \sum_{i=1}^{k} n_{\underline{\ell}_i}$, the total number of real observations; $\dim(\underline{\xi}) + \dim(\underline{c})$ is the total number of unknown parameters; d is the defect which would be zero if P were of full rank which would be the case if all of the elements of the

$\underline{\ell}_i'$ were real observations. This would likely be the case so that N_{11}^{-1} is regular. Also as a consequence, the global test on the appropriateness of the overall modelling uses the statistic, as in the usual form of adjustment, from H_o: $\hat{\sigma}_{oc}^2 = \sigma_o^2$ versus H_A: $\hat{\sigma}_{oc}^2 \neq \sigma_o^2$,

$$T^2 = \frac{\hat{\sigma}_{oc}^2}{\sigma_o^2} = \frac{\Delta R}{\nu_c \sigma_o^2} \leq F(\nu_c, \nu_o; \alpha)$$

for which ν_o is likely ∞ (infinity) with σ_o^2 considered as known and as being unity, consequent of the $\underline{\ell}_i'$ being all real observations.

The individual parameters or groupings of them or values derived from them may be assigned $(1-\alpha)$ levels using the same manner as in section 4.3 with the appropriate degrees of freedom and scaling of variances.

Several aspects of this solution warrant attention. If the $\underline{\ell}_i'$ are inhabited purely by real observations, then there is no need for imposing pseudo-observations to remove datum or configuration defects. Hence, the parameters are truly unbiased without requiring the inclusion of the ω nuisance parameter. An unrepeated observation, if included as one of the possible observables, is of no consequence since it is balanced by an element of the $\underline{\xi}$ vector which has as many elements as the number of possible observables. The elements of both design matrices are functions of x, y, and possibly z, not of the unknown parameters. Thus the solution is direct, with no iteration. Also, the sense of the parameters is dictated by the values of these elements. Hence, the approximate coordinates of the stations should be reasonable to reflect the configuration and its desired orientation in some system of coordinates.

6. EXAMPLES OF THE IMPLEMENTATION

The criteria for a generalized method, as given in chapter 1, have been met by Chen (1983). This may be revealed by the examples that he has given and also by those given in several of the references (Chrzanowski and Secord, 1983a, b; Chrzanowski et al., 1982b, c, 1983a, b). Further illustration by two examples in more detail is given here. The first, Lohmuehle, is a reference network of small aperture in which pure triangulation has been available for four campaigns with varying intervals between them. The second, Hollister, is a relative network of pure trilateration with fairly large aperture and many regularly annual campaigns, often with configuration defects.

The two following discussions are given to illustrate the applicability of the generalized approach. The analysis of structural behaviour or of tectonic activity is not within the realm of this thesis.

6.1 Lohmuehle Reference Network

Just after the construction of the Lohmuehle Dam in 1961, a network of six concrete pillars was established with the situation and configuration shown in figure 6.1. In addition to the stations of the network, there were three rows of object points on the downstream face of the structure at elevations of 211 m, 219 m, and 227 m, the highest of which is near the crest of the dam. By 1978, there had been eleven campaigns of pure triangulation but the data from only four was distributed to the FIG ad hoc committee centres (table 6.1). The observables of a typical campaign are shown in figure 6.2. The intersections at only the highest row of object points were included in the data.

The actual data were the means from several sets of directions at each station. Originally, the only indication of likely variances was the number of sets contributing to each mean. However, after its analysis of all of the campaigns, the group that was providing the data suggested the weighting of 1.0 and 2.5, in correlation with the weather, with an observation of unit weight having a standard deviation of 0.240 mgon. This was ascribed to each observation through the campaign, regardless of the number of sets. For the 2.5 weighting, the standard deviation became $0.240 \text{ mgon}/(2.5)^{1/2}$ which is 0.152 mgon. Each campaign was adjusted in a mapping plane defined by the set of approximate coordinates provided with the data, under the constraints of fixing two stations. The estimated variance factors were compatible with the a priori value of unity and no campaign required the rejection of any outlier. Hence, the data and the suggested standard deviations were considered acceptable for further analysis.

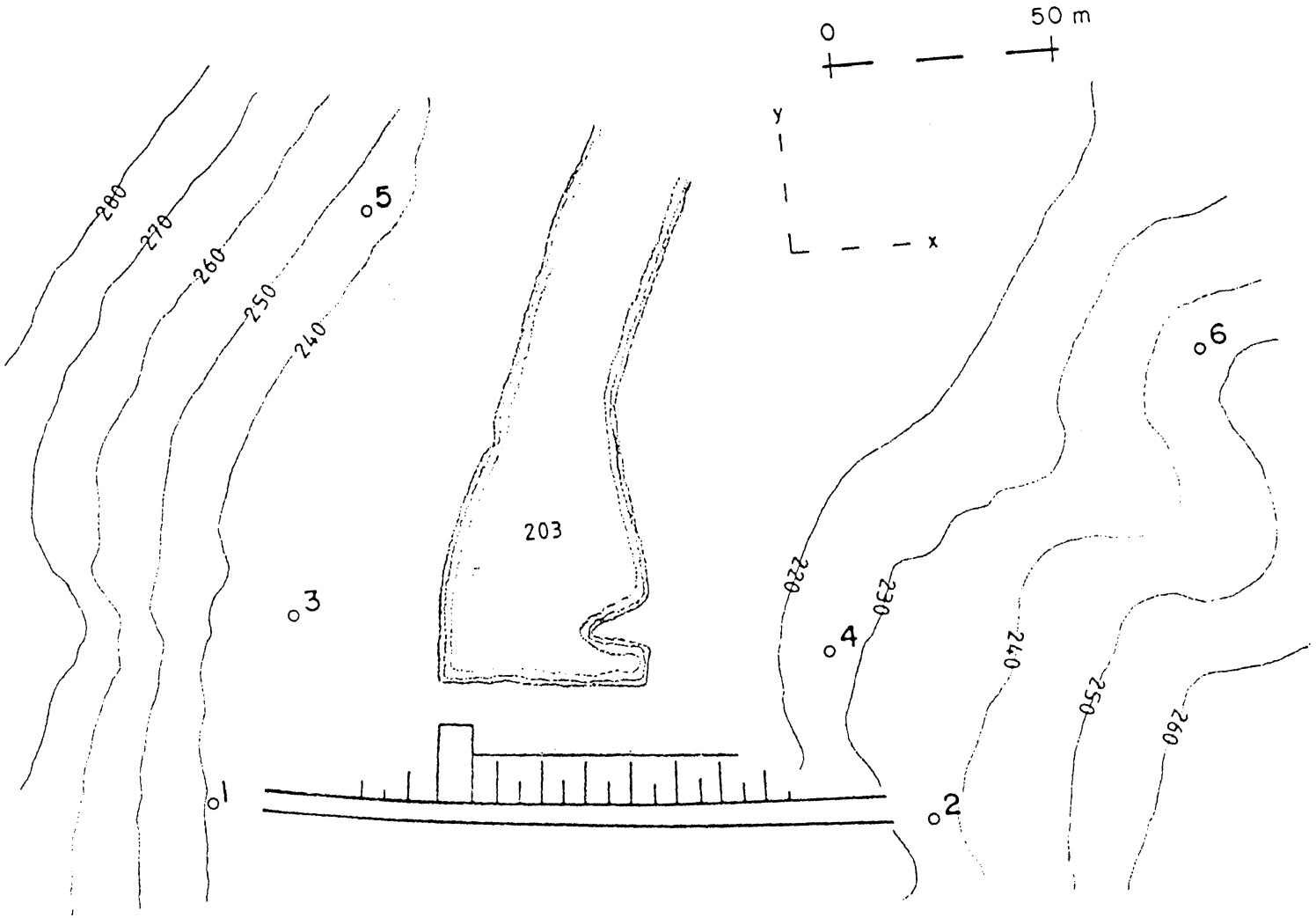

Figure 6.1 Lohmuehle Reference Network: Situation

Epoch	Year/Month	Interval	Observables *	Weight	Standard Deviation	ν	$\hat{\sigma}_0^2$ **
1	1962 06		50 directions	2.5	0.49"	15	1.1428
		7 months					
2	1963 01		47 directions	1.0	0.78"	13	0.9389
		63 months					
3	1968 04		53 directions	2.5	0.49"	18	0.9628
		127 months					
4	1978 11		54 directions	1.0	0.78"	17	0.9169

* observables include rays forming unique intersections at the ten object points

** all $\hat{\sigma}_0^2$ were found to be compatible with the $\sigma_0^2 = 1$ at 0.95.

No observation was considered as an outlier.

Table 6.1. Lohmuehle Reference Network: Campaigns

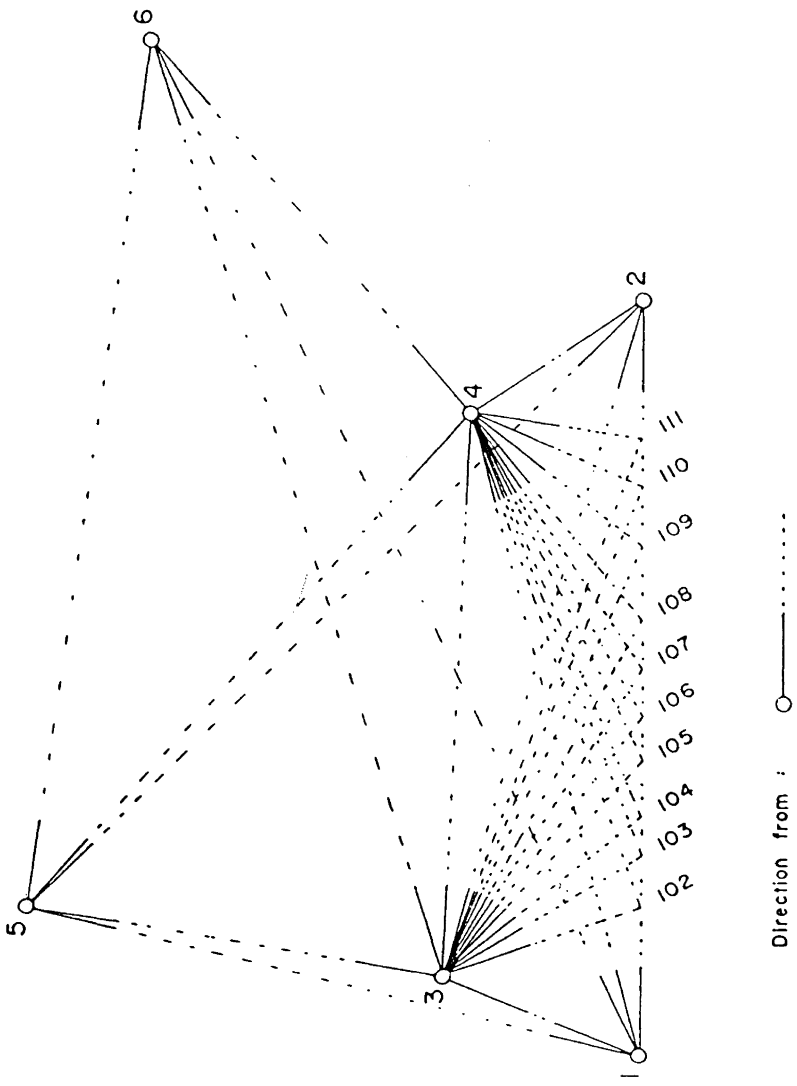

Figure 6.2 Lohmuehle Reference Network: Campaign 1962 06 (epoch 1) Observables

Although the choice was somewhat arbitrary for the initial stages of analysis, each campaign was adjusted under the same constraints stations 5 and 6, so that the scale of the network was created by the distance that is the inverse from the x, y coordinates of these two stations. Similarly, the orientation was created by the azimuth between them. However, since this was done by considering the x, y coordinates of stations 5 and 6 as being known ($\sigma^2 = 0$) then no pseudo-observations were necessary.

Since the network of six stations was intended to serve as the reference to which the behaviour of the dam could be described, the object points were considered as moving and only the six pillar stations were considered as the network. Also with such an intention, it would be desirable if the six stations could be considered as stable among themselves in order to create this reference. Thus the network was subjected to stable point analysis to determine whether any of the stations would have to be regarded as being unstable, at least for the interval between each pair of campaigns. With four campaigns, there are six possible pairings: 1 to 2, 1 to 3, 1 to 4, 2 to 3, 2 to 4, and 3 to 4; however, for the comparison with the other groups of the FIG ad hoc Committee, only the first four and last intervals were investigated.

Having only four campaigns and the nature of the phenomena did not warrant any sort of simultaneous modelling. The model - single point movement against or referred to the block containing all the stable points - was established a priori. The only real testing or trend to be investigated was whether any of the six stations would have to be segregated from the block as moving single points.

For illustration, the first comparison, 1962 06 to 1963 01, will be given in detail and the results from all five, in summary.

From each of the sets of adjusted campaign results ($\hat{\underline{x}}_i$; C_{x_i}; ν_i; $\hat{\sigma}^2_{oi}$), the coordinates and respective elements of the variance-covariance matrix were extracted for the network stations. Augmented to these were the values of the fixed coordinates for stations 5 and 6 that had acted as the minimal constraints and four rows and columns of zeros to the matrix to account for their variance and covariance. From each of $\underline{x}_i$, the derived observations were generated and from the C_{x_i}, the variances and covariances were propagated - yielding $\underline{\ell}^D_i$, $C^D_{\ell_i}$. For each comparison, it was merely the taking of the appropriate differences for whatever pair of campaigns were involved.

For the first pairing, 1962 06 to 1963 01 or epoch 1 to epoch 2, the observables corresponding to the observation differences whose standardized form exceeded the critical values (given in parentheses at the head of each column) were tabulated for 0.90, 0.95 and 0.99 (table 6.2). A distance observable was at the station under "AT", from the same station under "FR" and to the second station under "TO". An angle observable was made at the station under "AT", from the second station under "FR", and in a clockwise arc to the third station under "TO". The procedure of generating $\underline{\ell}^D_i$ had been done using other pairs of stations as constraints in the adjustments, e.g. 3 and 5; 1 and 2, with identical results.

OBSERVATIONS FAILING THE ONE DIMENSIONAL F-TEST

AT 0.90 (1.70)			AT 0.95 (2.05)			AT 0.99 (2.76)		
AT	FR	TO	AT	FR	TO	AT	FR	TO
1	1	4	1	1	4	1	1	4
1	3	6	1	3	6			
1	6	4	1	6	4	1	6	4
1	4	2	1	4	2			
2	2	3						
2	2	4	2	2	4	2	2	4
2	5	4	2	5	4	2	5	4
2	4	6	2	4	6	2	4	6
3	3	4	3	3	4	3	3	4
4	4	5	4	4	5	4	4	5
4	4	6						
4	6	2	4	6	2	4	6	2
4	2	1	4	2	1	4	2	1
4	1	3	4	1	3	4	1	3
4	3	5	4	3	5	4	3	5
5	6	4	5	6	4	5	6	4
5	4	2	5	4	2	5	4	2
6	2	4	6	2	4	6	2	4
6	4	1	6	4	1	6	4	1
6	3	5	6	3	5			

Table 6.2. Lohmuehle Reference Network: 1962 06 to 1963 01 (Epoch 1 to Epoch 2) Stable Point Analysis.

The stable point analysis for this pair (epoch 1 to epoch 2) was done through the following steps (referring to table 6.2).

1. Frequencies of involvement in failures at 0.90.

Station	1	2	3	4	5	6
Angles	6	7	4	12	5	8
Distances	1	2	2	5	1	1
Both	7	9	6	17	6	9

2. From these frequencies, station 4 would be highly suspect. In the observables failing at 0.95, all of those in which station 4 was involved were "removed" from the list. This left the following observables failing at 0.95, still unexplained.

AT	FR	TO
1	3	6
6	3	5

3. These could be explained by station 6. Station 2 had the same overall (angle plus distance) frequency but station 6 had one more angle failure which would be more indicative in triangulation. Besides, station 2 was not involved in any failures other than those with station 4 and would not explain the two remaining anyway.

4. Consequently, station 4 and station 6 were segregated from the network with each having its own single point movement as each of the object points had been allowed to do.

Thus the single point displacements were obtained using a model having one block for reference and several, one for each point, having rigid

body movement. So, for stations 1, 2, 3 and 5, the reference block:

$$(x_2-x_1)_i + v_i = 0 \quad i = 1, 2, 3, 5$$

$$(y_2-y_1)_i + v_i = 0 \quad i = 1, 2, 3,5.$$

While, for the others:

$$(x_2-x_1)_i + v_i = u_i \quad \text{for } i = 4, 6, 102, 103, \ldots, 111$$

$$(y_2-y_1)_i + v_i = v_i \quad \text{for } i = 4, 6, 102, 103, \ldots, 111.$$

The v_i of the left side of these equations is the residual, while the v_i on the right side is the displacement component in the y-direction. The resultant parameters are shown graphically as displacement vectors against their respective error ellipses at 0.95 in figure 6.5.

Intuition would have selected stations 5 and 6 to be used in the constraints since they are situated most distant from the structure. However, an obvious bias had been introduced by such a choice. This is revealed in a comparison of figures 6.3, 6.4, and 6.5. The pattern of the displacements in the latter two figures, after the weighted projection and from the modelling respectively, are practically identical. The trend has been readily indicated by applying the projection without pursuit of stable points (actually unstable stations). As shown in section 3.1.1.1 and 6.2, the same projection results regardless of the choice of minimal constraints and so, the indication has not been biased. So, if only the movement of the structure were desired, then this would be revealed through the projection.

The results of the modelling for the other intervals are given in table 6.3 and are shown in figure 6.6. These show how a long term trend can be masked when considering only the shorter intervals. In the comparison of successive campaigns, stations 1, 2 and 3 had remained stable through each of the intervals, but station 3 had been slowly moving

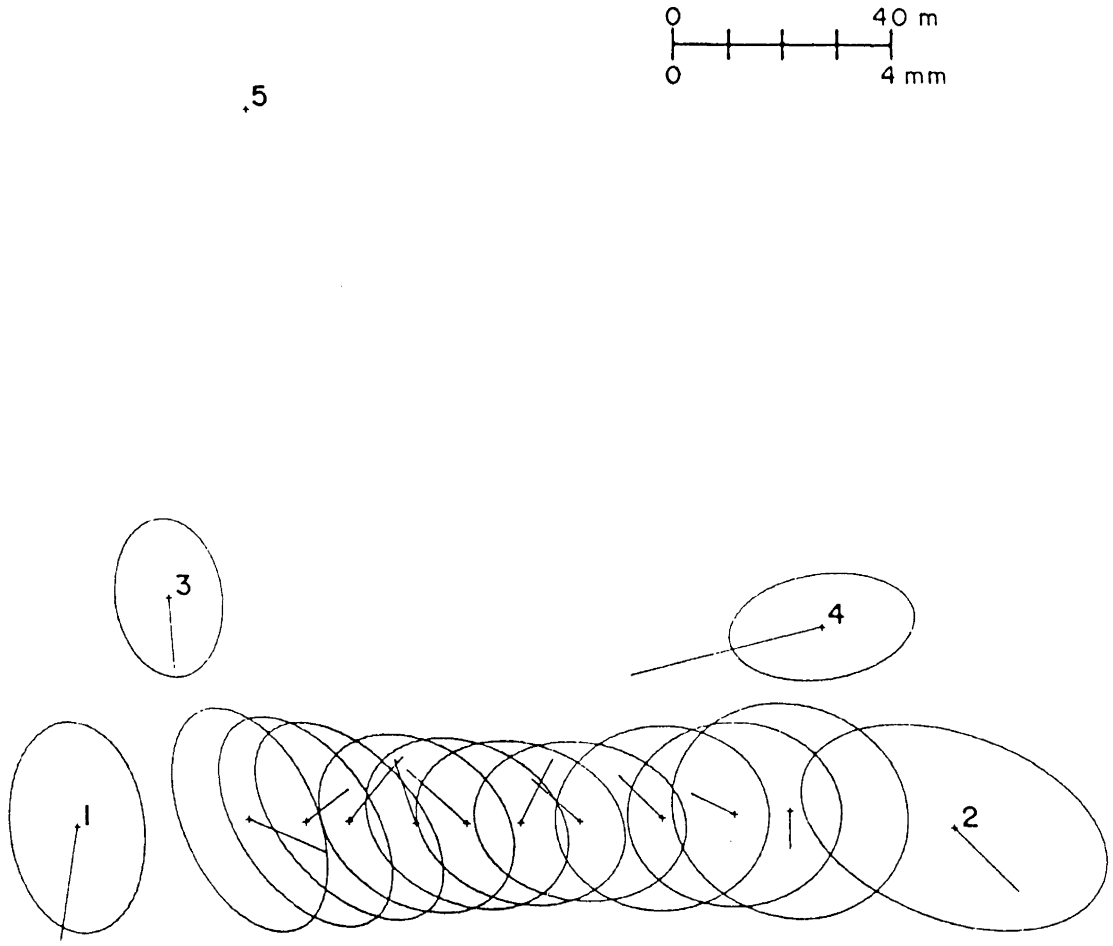

Figure 6.3 Lohmuehle Reference Network: Displacements and Confidence Regions at $\alpha = 0.05$ from Minimal Constraints 1962 06 to 1963 01 (epoch 1 to epoch 2)

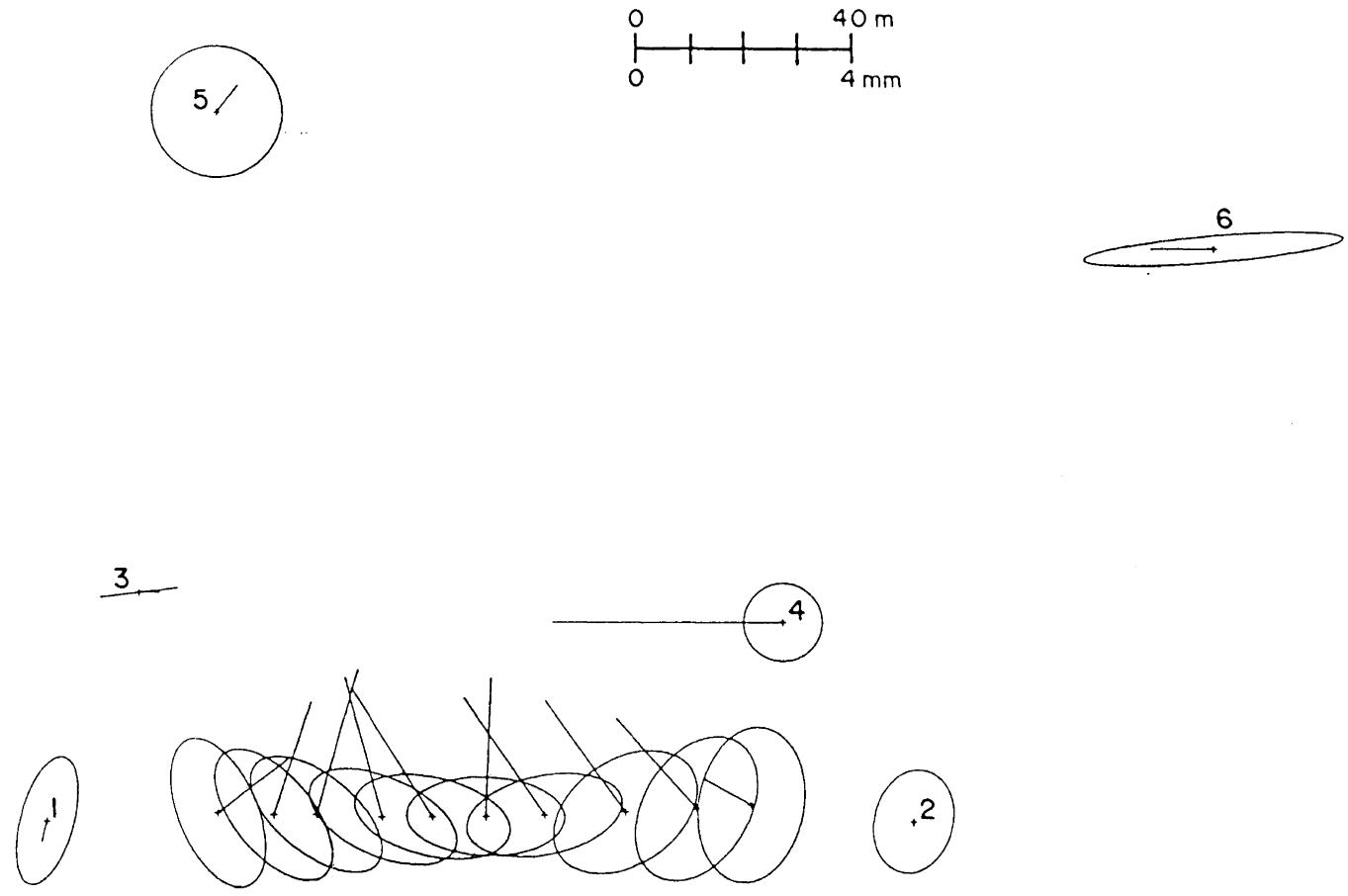

Figure 6.4 Lohmuehle Reference Network: Displacements and Confidence Regions at $\alpha = 0.05$ after Weighted Projection of Station Displacements 1962 06 to 1963 01

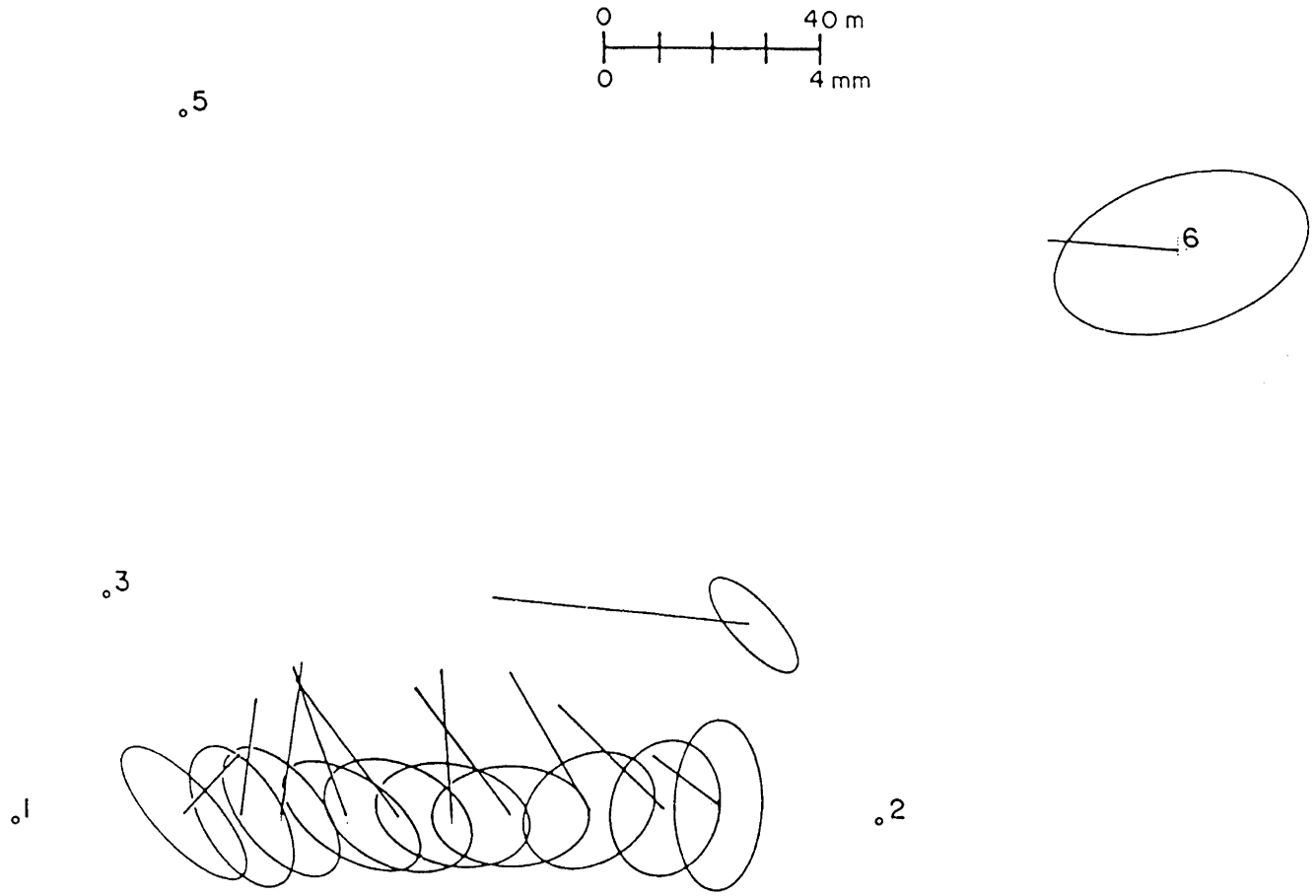

Figure 6.5 Lohmuehle Reference Network: Displacements and Confidence Regions at $\alpha = 0.05$
Derived from Model of Single Point Movement 1962 06 to 1963 01 (epoch 1 to epoch 2)

Comparison	1 to 2		2 to 3		3 to 4		1 to 4		1 to 3		
Station	7 months		63 months		127 months		197 months		70 months		
	u (dx)	v (dy)	u (dx)	v (dy)	u (dx)	v (dy)	u (dx)	v (dy)	u (dx)	v (dy)	
	[mm]		[mm]		[mm]		[mm]		[mm]		
1	--	--	--	--	--	--	--	--	--	--	
2	--	--	--	--	--	--	-1.1	-1.3	--	--	
3	--	--	--	--	--	--	1.5	0.3	0.7	0.2	
4	-4.8	0.5	-11.6	3.8	-8.6	3.0	-25.0	5.6	-16.4	4.3	
5	--	--	--	--	-2.0	0.6	--	--	--	--	
6	-2.5	0.2	--	--	1.2	2.2	--	--	-2.4	0.2	
global test on model*	1.0838		1.7628		0.7436		0.7604		1.1883		T^2_{model}
	2.714		2.409		3.267		3.295		3.285		$F(28\text{-}n_u, \nu, 0.05)$*

* includes displacements of each of the ten object points

Table 6.3. Lohmuehle Reference Network: Components of total station displacements significant at $\alpha \geq 0.05$ from modelling

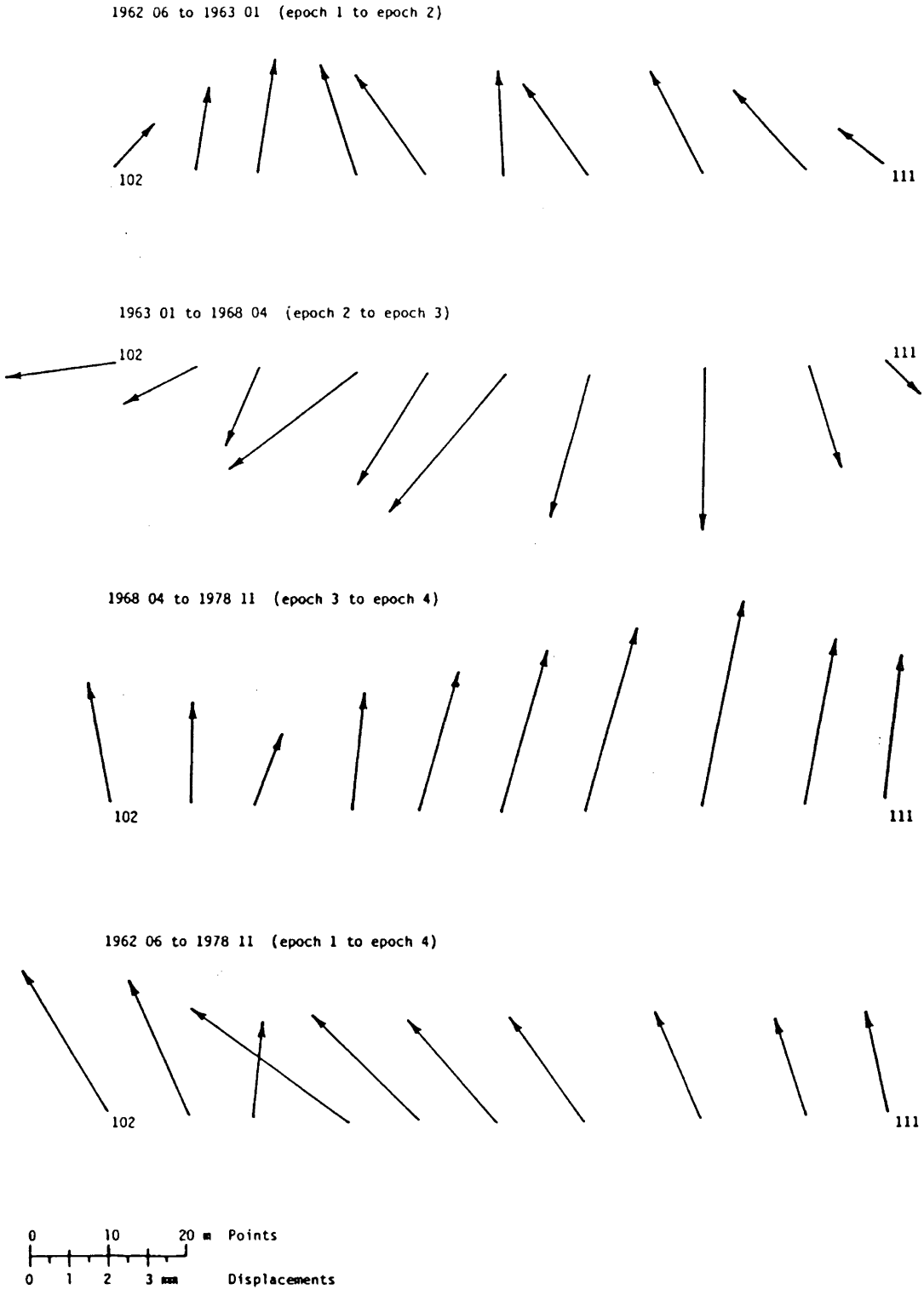

Figure 6.6 Lohmuehle Reference Network: Object Point Displacements

to the northeast (downslope) and its accumulating movement was shown when comparing the fourth with the first campaign (197 months) and half as much from the first to the third (70 months). Similarly, station 2 had moved significantly (also downslope) only over the period of 197 months, but not in the 70 month or 127 month period separately. Apart from the obvious downslope movement of station 4, the other station movement is small. Yet, because of the observation scheme (use of only triangulation (Kern DKM3 precision theodolite) and forced centering on concrete pillars for the reference stations and the lengths of sight (34.7 m to 241.8 m)), these were detected. This was important since the movement of the structure, at least at the crest of the dam, was only by several millimetres. Hence, the analysis has been able to create a reasonable reference against which the behaviour of the dam could be described. Because the data was distributed in an edited form, its form (number and timing of campaigns) was not entirely suited for properly indicating the response of the dam, especially when no other information such as water levels, temperatures of concrete, water, and air, or even the rays to the other object points, was given.

6.2 Hollister Relative Network

This example has many of the inconsistencies or difficulties that are likely to be associated with deformation surveys. There have been many campaigns of remeasurement with a variable number of observations and often with changes in configuration (stations involved) and with configuration defects. The heights of the stations were not known well enough to allow reasonable reduction to a computational surface. Hence, individual campaign adjustments were not possible. Nonetheless, most of the data could be used in campaign comparisons for trend and all of the data, in the full modelling.

The Hollister network is part of an array of stations along the Pacific coast of the United States and has 27 stations, some of which form part of the U.S. Coast and Geodetic Survey primary triangulation control network (now National Geodetic Survey). Remeasured practically annually by the U.S. Geological Survey (e.g. Savage et al., 1979), this grouping of stations has been named for the municipality about which they are located (figure 6.7). Hollister is at the junction of several plate boundaries and in an area that is very active seismically (e.g. table 6.4). The Pacific plate, southwest of the San Andreas fault, is known to be gradually moving northward against the North American plate, east of the Calaveras fault, with the Humboldt plate wedged between them (Anderson, 1971; Herd, 1979; Savage et al., 1979). As a consequence, the plate boundaries are rather diffuse and the region of the network is riddled with fault traces (figure 6.7; Jennings and Stand, 1958; Rogers, 1966). Nonetheless, three blocks or zones are commonly outlined by the San Andreas and Calaveras faults (figure 6.8).

	M_L	Date	Year	Symbol *
San Juan Bautista	4.9	1972 10 03	1972.7568	SJB
Gilroy	4.4	1974 01 10	1974.0274	G
Hollister	5.1	1974 11 28	1974.9096	H
Coyote Lake	5.9	1979 08 06	1979.5973	C
(Savage et al. 1981)	4.8	1980 04 13	1980.2842	S

* symbol identifying location of epicentre shown in figure 6.8.

Table 6.4. Hollister Relative Network: Notable Seismic Events
(Savage et al., 1979; King et al., 1981; Savage et al., 1981)

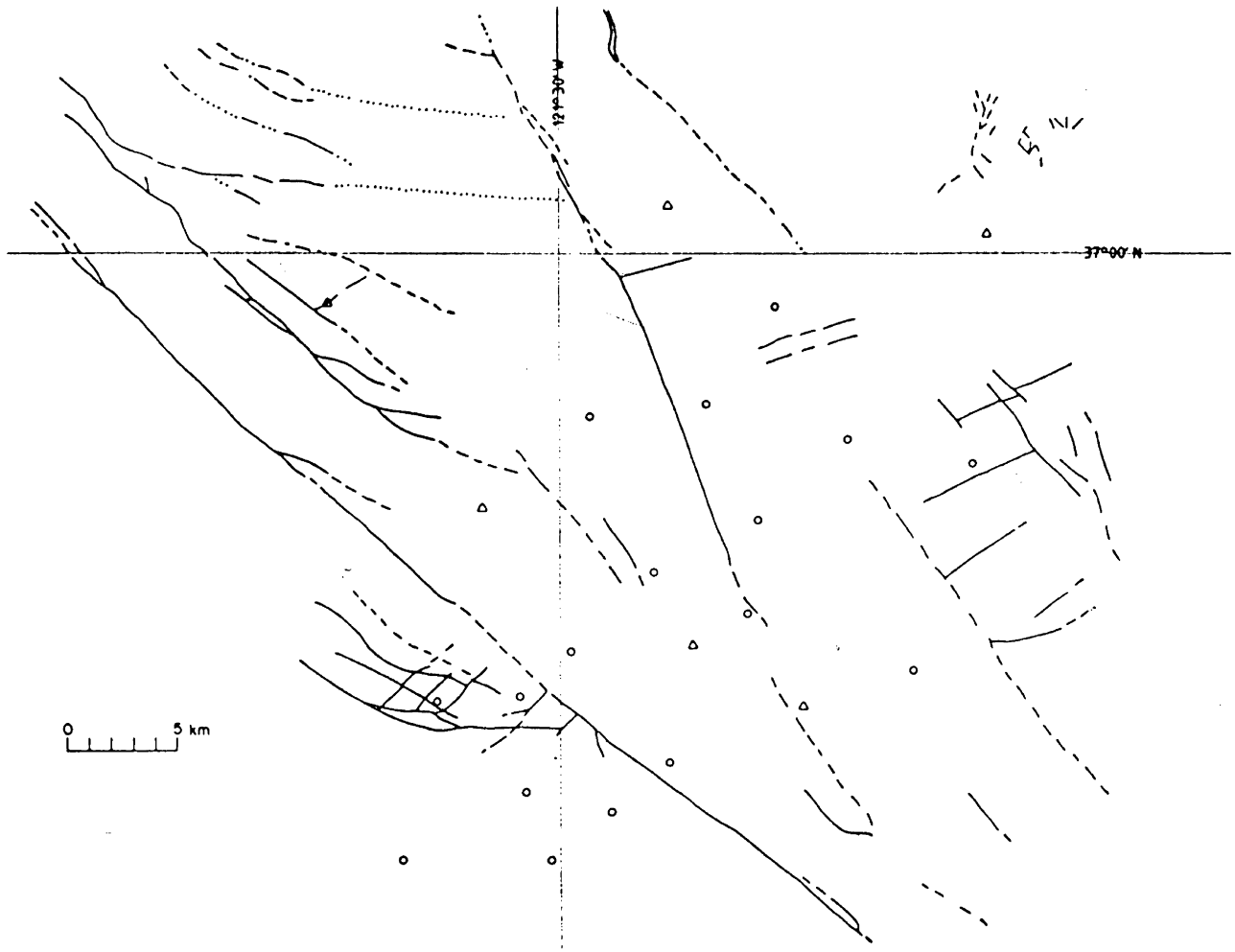

Figure 6.7 Hollister Relative Network: Situation and Fault Traces (Jennings & Strand 1958; Rogers 1966). Approximate traces are broken. Concealled traces are dotted.

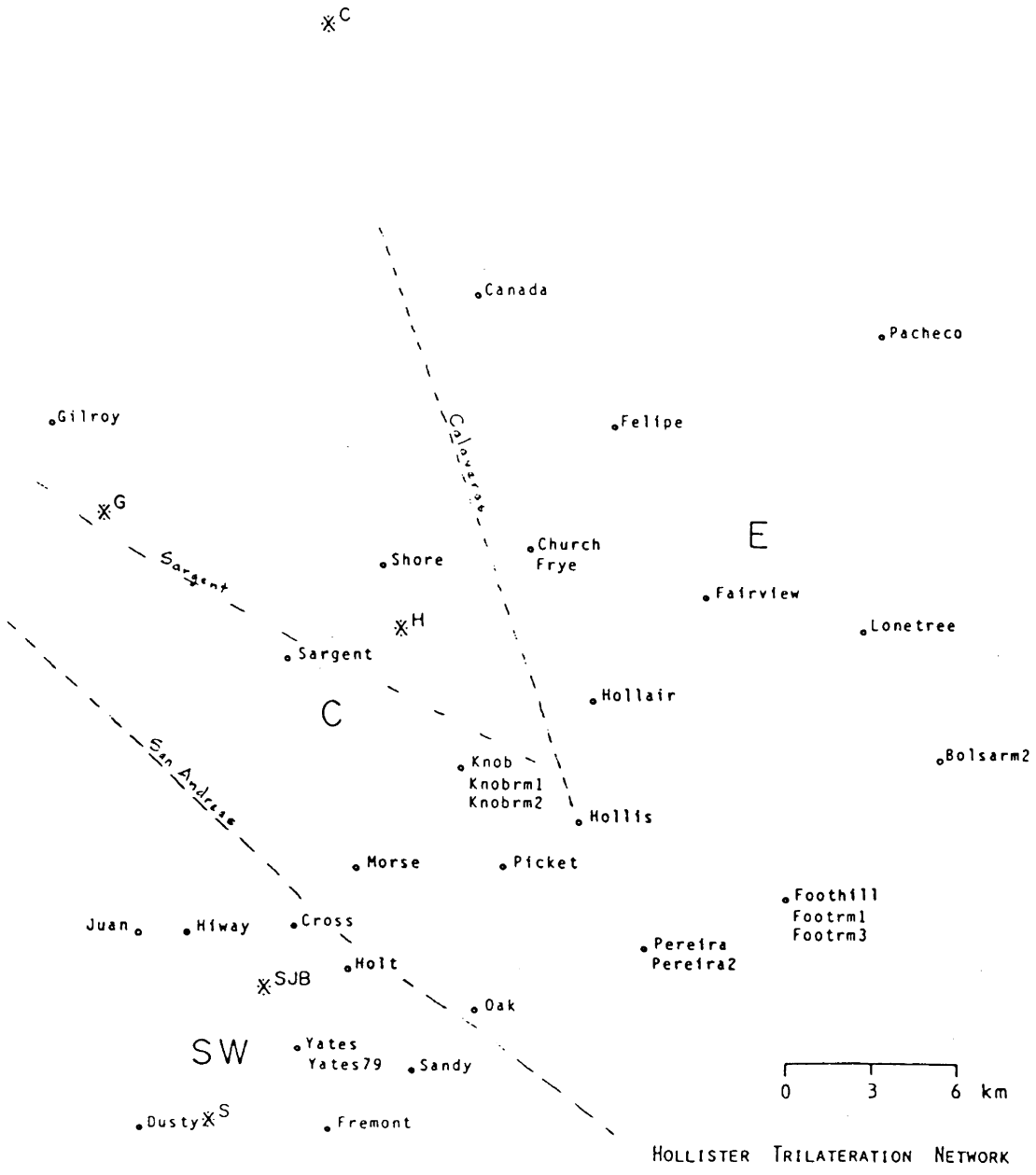

Figure 6.8 Hollister Relative Network: Possible Stations and Blocks

Through the interval from 1970 to 1982, several of the stations have been replaced (e.g. Pereira by Pereira2 in 1976; Yates by Yates79),, some have been abandoned in favour of nearby reference marks (e.g. Knob by Knobrm1 and Knobrm2; Foothill by Footrm1 and Footrm3), and others have been involved only occasionally (e.g. Juan) or only recently (e.g. Frye, Bolsarm2). Often the concern was for the repeating of a distance measurement even though the distance might be hanging or totally isolated from the main network. Hence, the configuration has been neither complete nor constant throughout the twelve years.

In the data supplied by the American Geophysical Union (Savage et al., 1979), the stations were described by geographic latitude and longitude (Clarke 1866 ellipsoid) and elevations above an unspecified datum, likely mean sea level, from a variety of sources of varying reliability. The network extends from 36°45'N to 37°02'N and from 121°15'W to 121°37'W - 30 km by 31 km. These coordinates were projected onto the 3° Transverse Mercator mapping plane with central meridian at 121°30'W. Although geographic coordinates could have been used with the appropriate displacement field and observation equations (e.g. Pope, 1966; Bibby, 1973; Reilly, 1981, 1982), they would be more suited to pure triangulation. The resultant Eastings and Northings were used as x, y coordinates in the design matrices A and B after having the origin shift to one of the stations within the network. Because of the fairly large aperture and spacing between stations (1.8 km to 26.7 km) and because the movement is in the order of 0.01 my^{-1}, these could be considered as representative of the configuration over the whole twelve years.

This is a purely trilateration network. The data have provided mark to mark distances that have been already corrected for instrumental heights and calibration and for atmospheric conditions. Hence, they can be considered as spatial distances in metres. During this period from 1970 to 1982, the distances have been measured using the Spectra-Physics Geodolite Laser Distance Measuring Instrument (Savage et al., 1979). The Geodolite is 0.86 m by 0.40 m square and its 48 kg is usually mounted on a heavy tripod, such as for the Wild T3 theodolite, with an optical plummet for centering over the ground marks. Operating from 115V AC and using a He-Ne CW gas laser, the Geodolite is capable of a range to 64 km in daylight or 80 km at night with a resolution of $\pm$0.001 m or $\pm$ 1 ppm, whichever is greater, after a couple of minutes of measuring time.

For this data, the U.S. Geological Survey (Savage and Prescott, 1973) has given an estimate of the variance of a distance measurement as

$$\sigma_s^2 = a^2 + b^2 s^2$$

with

$$a = 0.003 \text{ m}, \quad b = 0.2 \text{ ppm}.$$

This extraordinary accuracy has been estimated from the reproducibility when comparing the remeasurement of a network of 30 lines in a tectonically dormant area at Hanford, Washington. The constant component, a, includes a centering error of 0.001 m at each of the instrument and reflector stations and the limit of 0.001 m in phase resolution. The proportional component, b, has been remarkably reduced by the additional elaborate sampling of atmospheric temperature and humidity along the line of sight during the measurement (mean pressure $\pm$ 0.3 mb from the stations, mean

temperature $\pm$ 0.1°C, mean water vapour pressure $\pm$ < 3 mb) and by close monitoring of the modulation frequency of the Geodolite (mandatory agreement within 0.04 ppm with a quartz oscillator before and after measurement). Following from the discussion of section 3.1.3 and as mentioned by Schneider (1982), this is a rather optimistic estimate of σ_0^2 since the correlation between the two campaigns had been neglected in the comparison.

The distribution of observations for the period including 1970 to 1982 is illustrated in figure 6.9. Against this distribution, the occurrence of notable seismic events (table 6.4) is shown. The clustering results in 31 "campaigns" some of which follow closely after an event. Of these 31, some could be grouped together as the annual campaign, but in the final estimation such grouping was not necessary since even a "campaign" of a single distance could be accommodated.

It has been reported that the station heights are known only to within 1.0 m (Chen, 1983; confer 0.3 m Schneider, 1982). This creates a configuration defect that does not allow treatment even in a horizontal adjustment since the error introduced by reducing the distances to a computational surface, e.g. a mapping plane, would amount to 0.08 m or 0.09 m for several station combinations and as much as 0.1 m (0.03 m if heights to 0.3 m) which is contaminative by more than one order of magnitude than the error in measurement. Consequently, the observation approach was followed in searching for a trend and the simultaneous estimation, for the values of the parameters.

For each successive pairing, the common observables were extracted and the vector of observation differences were obtained (e.g.

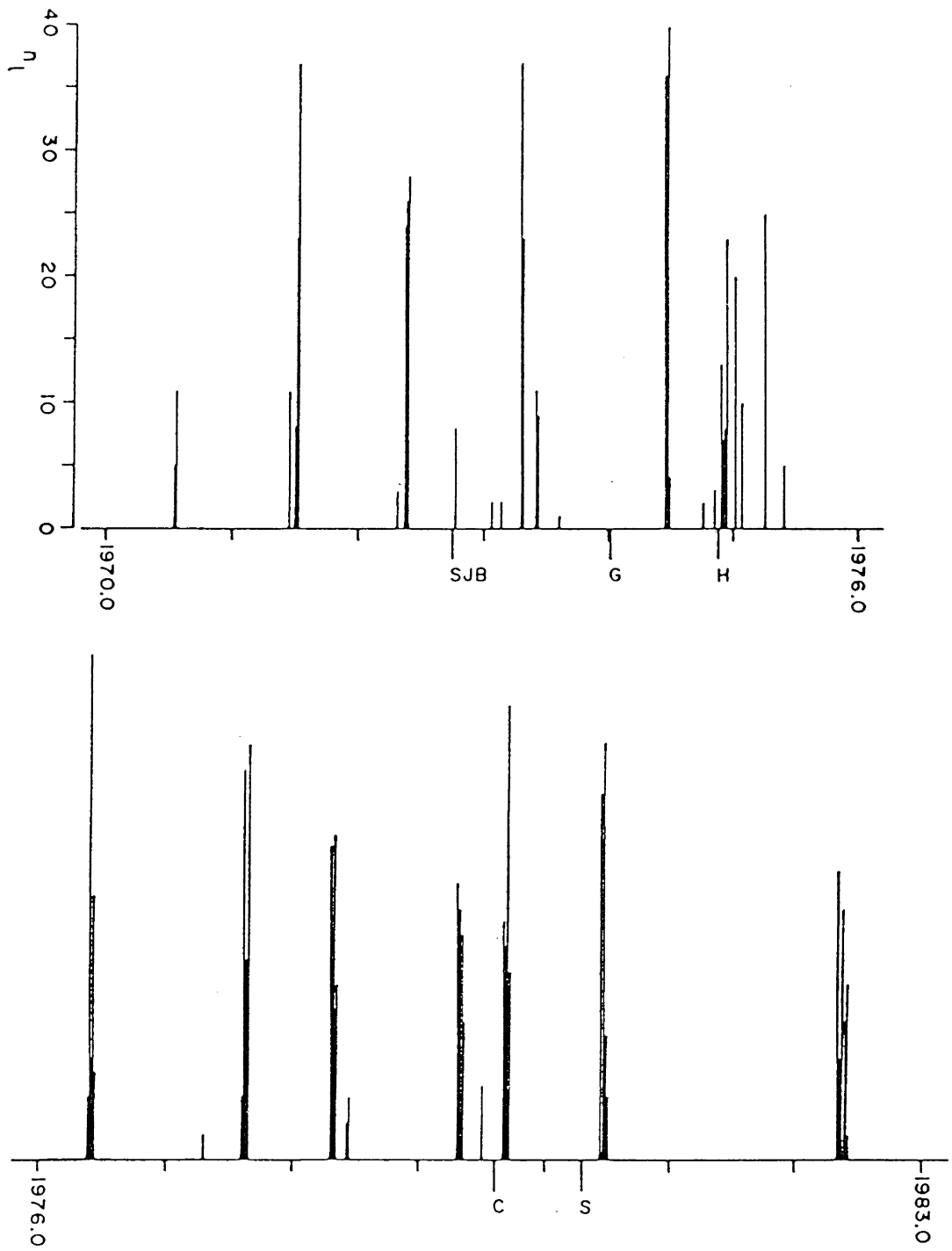

n_l: number of observations

Figure 6.9 Hollister Relative Network: Temporal Distribution of Observations 1970 to 1982

figure 6.10). With $\underline{d\ell} = \underline{\ell}_{i+1} - \underline{\ell}_i$, then $\sigma^2_{d\ell} = 2\sigma^2_{\ell_i}$ neglecting the correlation between campaigns (section 3.1.3; Schneider, 1982).

The displacement components were estimated using the observation approach through

$$\underline{d\hat{x}}_s = (A^T P_{d\ell} A)^{-1} A^T P_{d\ell} \underline{d\ell}$$

with

$$P_{d\ell} = \text{diag}\ (\sigma^2_{d\ell_1}, \sigma^2_{d\ell_2}, \ldots)$$

by constraining one station to have $\underline{dx}_c = \begin{bmatrix} u \\ v \end{bmatrix} = \begin{bmatrix} 0 \\ 0 \end{bmatrix}$ and adding one azimuth change of zero, $d\alpha = 0$, for the datum defect and an additional $d\alpha = 0$ for each hanging distance. The resulting special solution displacements were shown as vectors against their respective ellipses at 0.95 (e.g. figure 6.11, 6.12) and similarly, after the weighted projection (e.g. figure 6.13). The bias related to the choice of minimal constraints is well revealed in comparing the trends exhibited through figures 6.11 and 6.12, both of which used the same $\underline{d\ell}$ but differ only in the choice of constraints. In figure 6.11, the constraints are in the Eastern block as station Canada fixed and its azimuth to station Church also fixed. In figure 6.12, fixing station Oak and its azimuth to station Sargent placed the constraints in the Central block. Each set of $\underline{dx}$ resulted in the same weighted projection (figure 6.13). In addition to the successive weighted projections, the values of the observables were plotted against time, as in figures 3.3 and 3.4. Some showed an obvious tendency of expansion or contraction or reaction to the events. Regard for their situation (location and orientation with respect to the fault traces) aided in the interpretation of the trends exhibited after the weighted projection.

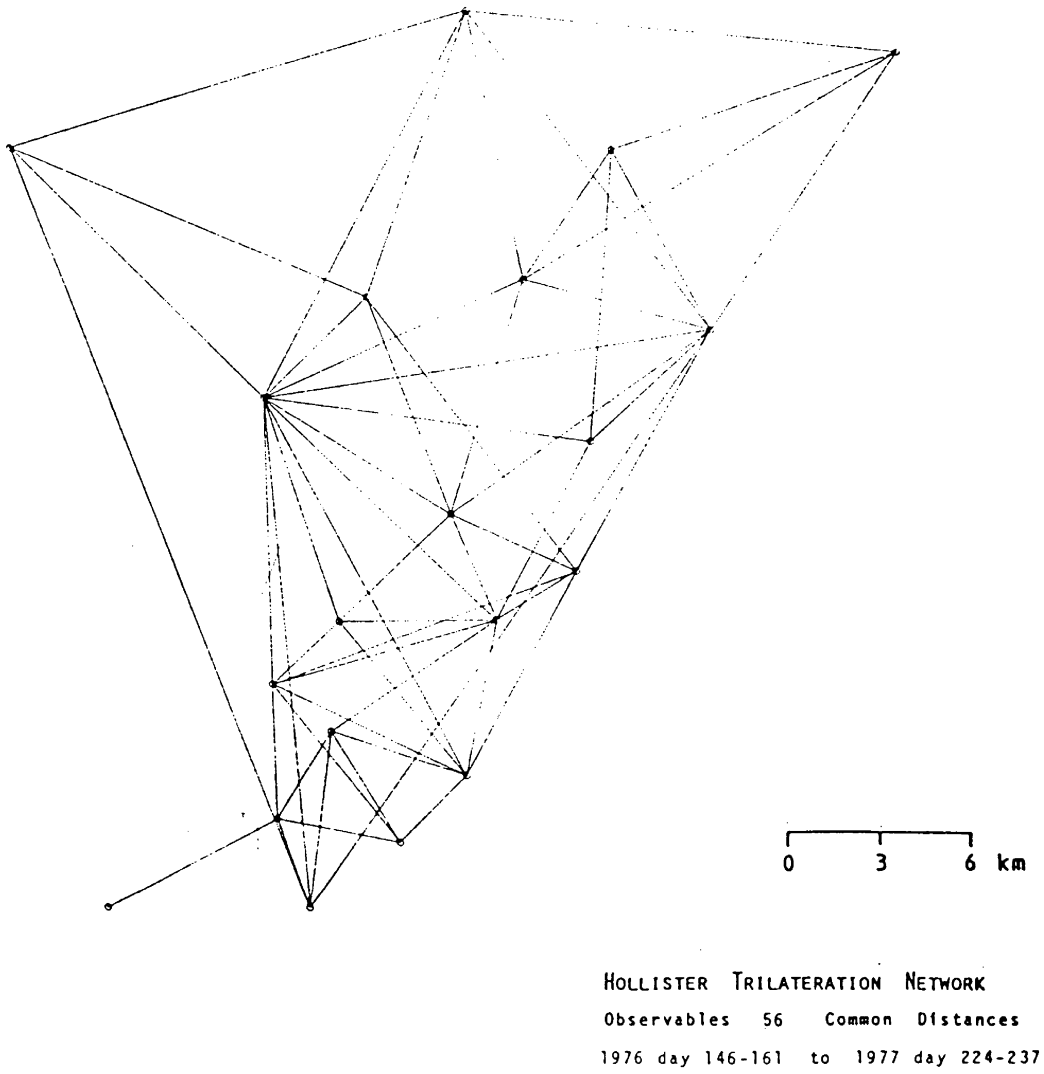

Figure 6.10 Hollister Relative Network: Common Observables 1976.42 to 1977.63

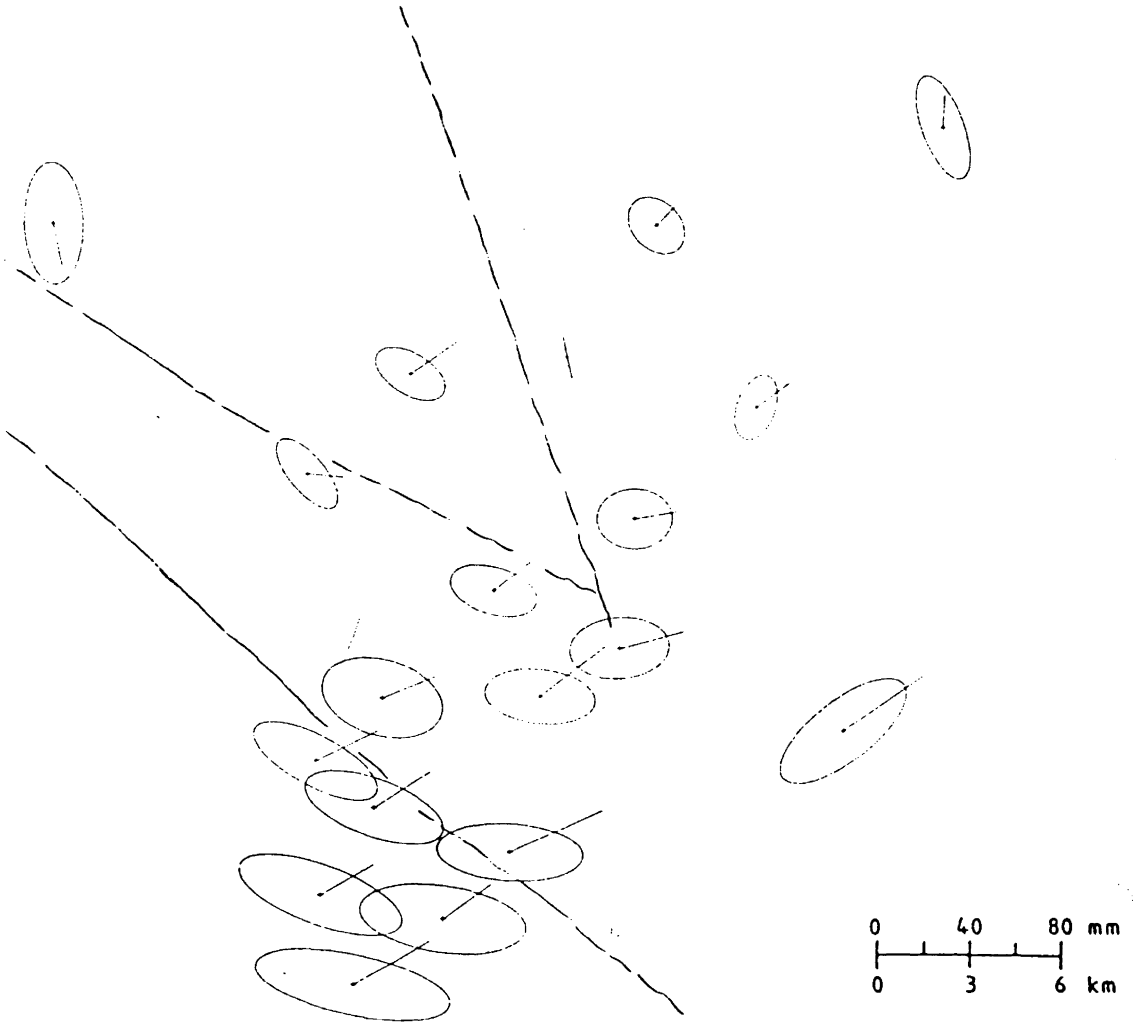

Figure 6.11 Hollister Relative Network: Displacements 1976.42 to 1977.63

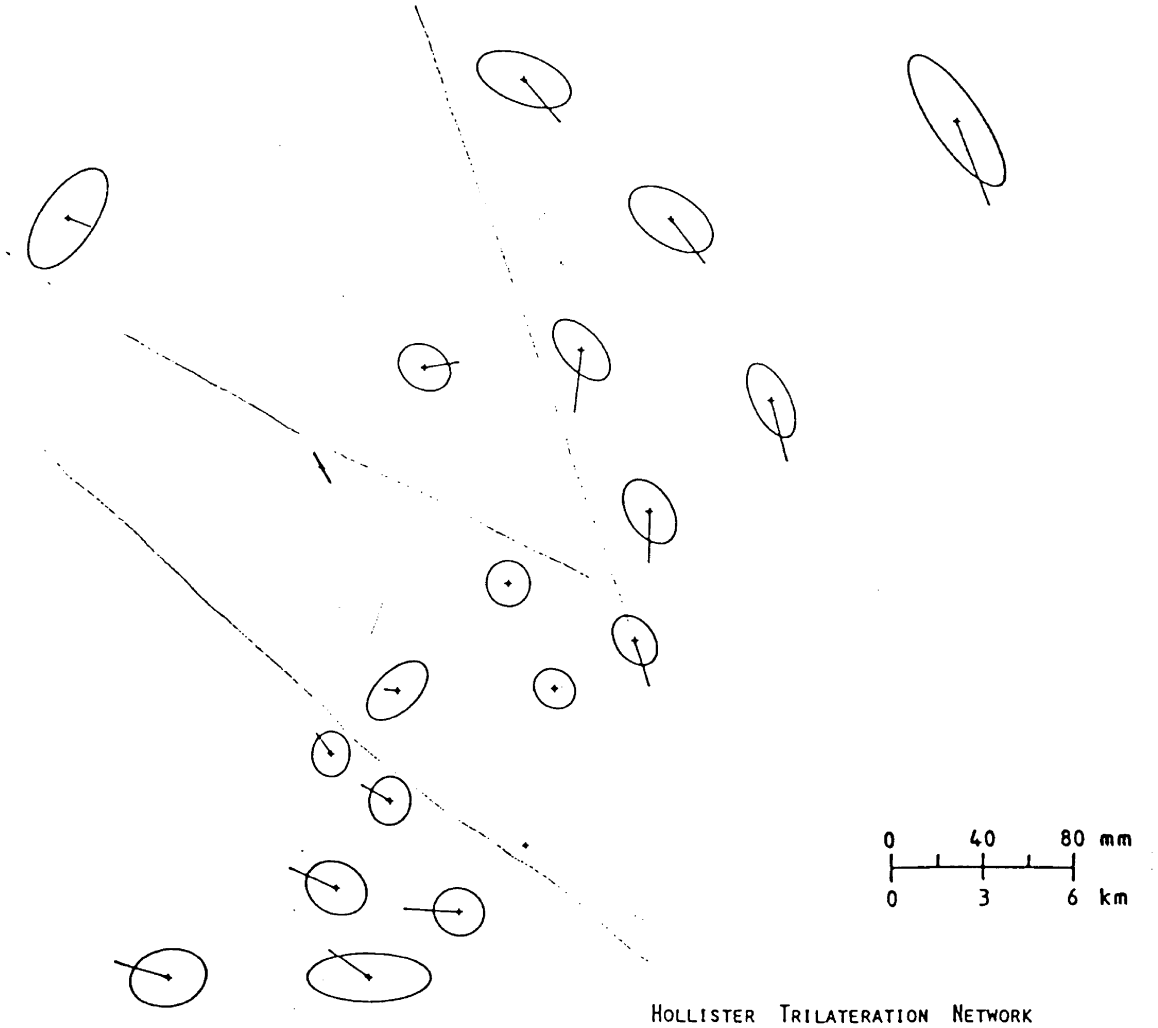

Choice 2.

Figure 6.12 Hollister Relative Network: Displacements 1976.42 to 1977.63

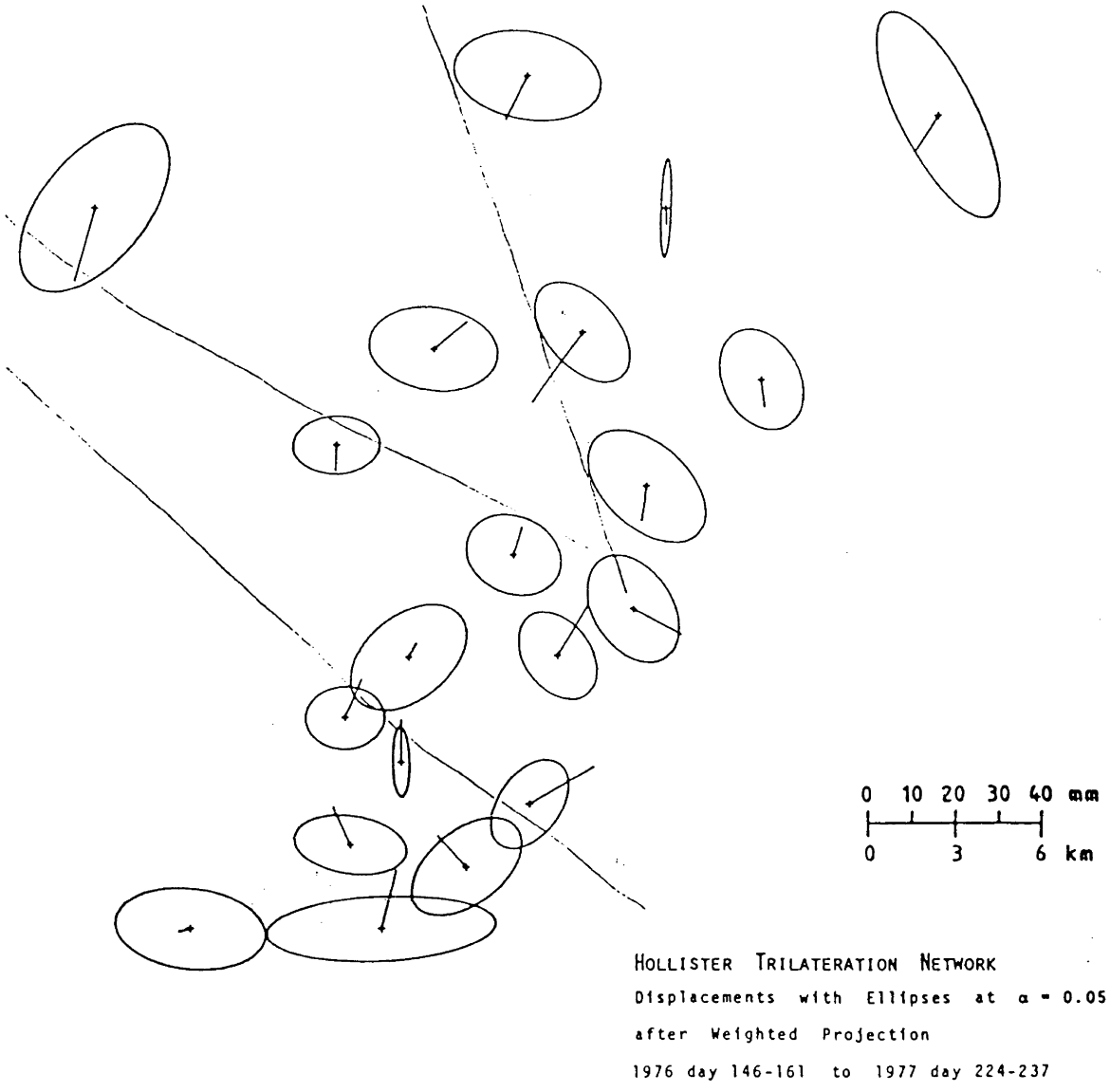

Figure 6.13 Hollister Relative Network: Displacements 1976.42 to 1977.63

Further trend was pursued by using the $\underline{d\ell}$ vectors to estimate deformation parameters for the successive intervals. For example, the maximum and minimum strain "ellipses" were depicted as shown in figure 6.16, but for peculiar zoning as mentioned below.

The conventional form of modelling in this area involved the three blocks as shown in figure 6.8. The style of deformation was simply the rigid body movement of the southwest block (SW) and central block (C) against the eastern block (E), along the San Andreas and along the Calaveras faults, regarding the Sargent fault as a dormant branch of the San Andreas. The simplicity of this model ignored the consequence of the triple junction at the convergence of the two main fault traces - the movement of the two blocks must alter the central block (C). Hence, the model would be enhanced by also allowing for homogeneous strain in each of the three blocks. The locations of stations Hollis and Pereira in the diffuse Calaveras fault zone required their exclusion from either block and each was given its own single point movement by four extra parameters, a_{oH}, b_{oH}, a_{oP}, b_{oP}, which are not mentioned below.

These are the two models with which Savage et al. (1979) deal for the interval from 1971 to 1978. They have been followed here using the simultaneous estimation for 1970 to 1979 (preseismic) and the rates are compared in table 6.5. The 9 year interval was taken since the reactions by most of the distances to the earlier events were at the same level as the noise of the observations.

Since the simultaneous estimation of parameters directly from the observations did not require any minimal constraints for its solution (chapter 5), the models for the three blocks may be considered together by respective

Relative Block Movement Only $\dot{\underline{d}} = (\dot{a}_o, \dot{b}_o)$ [mm y^{-1}]

	1971 to 1978*		1970 to 1979		1974 to 1979	
C vs. E	N19°W±9°	16.7±2.5	337°±1°	18.4 ±0.5	338°±1°	16.9±0.9
SW vs. E	29 3	29.5 1.3	328 1	31.2 0.7	330 1	28.8 1.2
SW vs. C	42 10	13.4 2.2	316	13.7	319	12.3
$\hat{\sigma}_o^2$ applied	?		3.584 = 1.89^2**		2.740 = 1.66^2**	

		Strain Separately [μstrain y^{-1}] 1971 to 1978*		Strain Simultaneously with Relative Block Movement [μstrain y^{-1}] ; [mm y^{-1}] 1970 to 1979		1974 to 1979	
$\dot{\varepsilon}_x$	E	0.16 ± 0.03		0.14 ± 0.04		0.17 ± 0.07	
$\dot{\varepsilon}_y$		-0.11	0.03	-0.02	0.04	0.00	0.07
$\dot{\varepsilon}_{xy}$		0.08	0.02	0.03	0.03	0.02	0.06
$\dot{\varepsilon}_x$	C	0.48 ± 0.05		0.39	0.05	0.70	0.10
$\dot{\varepsilon}_y$		-0.15	0.04	-0.24	0.04	-0.21	0.08
$\dot{\varepsilon}_{xy}$		0.09	0.04	0.05	0.04	0.20	0.07
$\dot{\underline{d}}$	C vs. E	--	--	345°±3	13.0±0.9	007°±3°	11.6±1.1
$\dot{\varepsilon}_x$	SW	-0.09 ± 0.06		-0.07	0.08	-0.08	0.02
$\dot{\varepsilon}_y$		-0.09	0.04	-0.05	0.06	-0.11	0.11
$\dot{\varepsilon}_{xy}$		0.02	0.04	0.02	0.06	0.10	0.12
$\dot{\underline{d}}$	SW vs. E	--	--	330°±2°	28.4±1.5	314°±2°	14.4±1.5
$\hat{\sigma}_o^2$ applied		?		3.076=1.75^2**		2.236=1.50^2**	
Along Calaveras				13.2 near Canada 16.9 near Hollis		11 near Canada 16 near Hollis	
Along San Andreas				~ 11		~ 10	

* Savage et al. (1979)

**Failed global test at 0.95

Table 6.5. Hollister Relative Network: Simple Models (blocks shown in figure 6.3).

subscripts for a station in each block as

$$\underline{\ell}_i + \underline{v}_i = \underline{\ell}_1 + A_i B_i \underline{c} \quad \text{at} \quad t_i = t_1 + \Delta t_i$$

using observation equation 4.28 with the elements of the configuration matrix, A_i, as $\frac{\Delta x}{s_H}$, $\frac{\Delta y}{s_H}$, $s_H = (\Delta x^2 + \Delta y^2)^{1/2}$ and the displacement field as shown by the matrix expression in figure 6.14, with the x, y reduced to a station in block E as the origin. Both the $\dot{a}_{oC}$, $\dot{b}_{oC}$ and the $\dot{a}_{oSW}$, $\dot{b}_{oSW}$ are with respect to block E. The relative movement of block SW with respect to block C is then $(\dot{a}_{oSW} - \dot{a}_{oC})$, $(\dot{b}_{oSW} - \dot{b}_{oC})$. The actual relative displacement rate along either fault line is dependent on the position. So, at a point (x_F, y_F) with respect to the same station in block E as origin, for example along the Calaveras fault, the relative movement rate would be $(\dot{u}_C - \dot{u}_E)$, $(\dot{v}_C - \dot{v}_E)$ with

$$\begin{bmatrix} \dot{u}_C \\ \dot{v}_C \end{bmatrix} = \begin{bmatrix} 1 & 0 & x_F & 0 & -y_F \\ 0 & 1 & 0 & y_F & x_F \end{bmatrix} \begin{bmatrix} \hat{\dot{a}}_{oC} \\ \hat{\dot{b}}_{oC} \\ \hat{\dot{\varepsilon}}_{xC} \\ \hat{\dot{\varepsilon}}_{yC} \\ \hat{\dot{\varepsilon}}_{xyC} \end{bmatrix}$$

and

$$\begin{bmatrix} \dot{u}_E \\ \dot{v}_E \end{bmatrix} = \begin{bmatrix} x_F & 0 & -y_F \\ 0 & y_F & x_F \end{bmatrix} \begin{bmatrix} \hat{\dot{\varepsilon}}_{xE} \\ \hat{\dot{\varepsilon}}_{yE} \\ \hat{\dot{\varepsilon}}_{xyE} \end{bmatrix}$$

$$
B_i \underline{c} = \begin{bmatrix}
\vdots & & & & & & & & & & & & \\
x_E \Delta t_i & 0 & -y_E \Delta t_i & 0 & 0 & 0 & 0 & 0 & 0 & 0 & 0 & 0 & 0 \\
0 & y_E \Delta t_i & x_E \Delta t_i & 0 & 0 & 0 & 0 & 0 & 0 & 0 & 0 & 0 & 0 \\
0 & 0 & 0 & \Delta t_i & 0 & x_C \Delta t_i & 0 & -y_C \Delta t_i & 0 & 0 & 0 & 0 & 0 \\
0 & 0 & 0 & 0 & \Delta t_i & 0 & y_C \Delta t_i & x_C \Delta t_i & 0 & 0 & 0 & 0 & 0 \\
0 & 0 & 0 & 0 & 0 & 0 & 0 & 0 & \Delta t_i & 0 & x_{SW} \Delta_i & 0 & -y_{SW} \Delta t_i \\
0 & 0 & 0 & 0 & 0 & 0 & 0 & 0 & 0 & \Delta t_i & 0 & y_{SW} \Delta t_i & x_{SW} \Delta t_i \\
\vdots & & & & & & & & & & & & \\
\end{bmatrix}
\begin{bmatrix}
\dot{\varepsilon}_{xE} \\
\dot{\varepsilon}_{yE} \\
\dot{\varepsilon}_{xyE} \\
\dot{a}_{oC} \\
\dot{b}_{oC} \\
\dot{\varepsilon}_{xC} \\
\dot{\varepsilon}_{yC} \\
\dot{\varepsilon}_{xyC} \\
\dot{a}_{oSW} \\
\dot{b}_{oSW} \\
\dot{\varepsilon}_{xSW} \\
\dot{\varepsilon}_{ySW} \\
\dot{\varepsilon}_{xySW}
\end{bmatrix}
$$

Figure 6.14.

Unfortunately, the global test on the appropriateness of the model was not passed at 0.95 ($\hat{\sigma}_0^2 = 3.076 = 1.754^2 \neq 1$). Its value would indicate that the scale of the P_i weight matrices might be too optimistic by 1.75 times. However, this interval (1970.565 to 1979.490) has contained several seismic events, especially that of 1974. None of the residuals would be flagged for possible rejection at 0.95 under the τ_{max}-test (in context, with $\frac{\alpha}{n_\ell}$ as the argument for the critical value (Vanicek and Krakiwsky, 1982)); however, of the 12 excessive residuals that were nearly suspect for rejection before 1974.910, 8 were negative and in block C or crossing the Calaveras fault. Also, after 1974.910, all 9 save 1 were positive and predominantly in block C or in block E or crossing the Calaveras fault.

Using the same model, but only over the interval from 1974.94 to 1979.49, reduced the estimated variance factor to $\hat{\sigma}_0^2 = 2.236 = 1.50^2$ which was still not compatible at 0.95. None of the observations deserved rejection and very few could be considered excessive.

It is possible that since the weighting did not regard the correlation between campaigns, the result, without scaling, would be too optimistic by a factor of 1.50. However, all of the testing of significance utilized the estimated scale ($\hat{\sigma}_0^2 q$ versus $\sigma_0^2 q = q$).

Apart from the slight difference in time intervals, the values in table 6.5 by Savage et al. (1979) for 1971 to 1978 and by the author for 1970 to 1979 may be compared in so far as the same modelling was done. Their estimation used the same observation equation - taking the homogeneous strain field and applying its effects onto the orientation of the line

being measured. The estimation of the strain parameters entailed taking the line length changes and converting them to strain at some time t_i by $\varepsilon_{\alpha_i} = \frac{\ell_i - \bar{\ell}}{\bar{\ell}}$ in which $\bar{\ell}$ is a reference state of the line length - the mean line length at the mean time $\bar{t}$. Thus there is a series of strains for each line, with an orientation of α. With the redundancy of more than three lines in a block, least squares estimates for ε_x, ε_y, ε_{xy} were made which are independent of the choice of a datum, as in the generalized method - their sense dictated by the definition of the azimuths in the coordinate system (Prescott et al., 1979). In their discussion of the parameters, Savage et al. (1979) gave no mention of how well the models fit the data, only comparing the parameters to their "standard deviations" which may or may not have been scaled by an estimated variance factor. Also, the trend had been perceived from a displacement rate field dependent on the choice of datum (minimal constraints as in figure 6.11) although the choice had been justified by a preconceived notion of the behaviour.

It is interesting to note that since both components of rigid body movement were considered as parameters, the direction of movement had not been specified or constrained. Nonetheless, the orientation of the resultant vectors are very close to those of the accepted strikes of the fault traces (Savage et al., 1979). However, these models regard the two faults to be open for their full extent in the region of the network.

Although the traces are not entirely continuous or always strongly defined, there is evidence, both visual and from measurements, that the upper portion of the San Andreas fault and the lower portion of

the Calaveras fault are locked at the surface while the amount of slip increases in progression away from the locked portion (Herd, 1979; Schulz et al., 1982).

All of this led to a reconsideration of the modelling. Scrutiny of the successive campaigns weighted projections, trying to accommodate the gradation of observed slip along the two fault traces, and the broader movement of the Pacific plate against the North American plate resulted in the groupings of stations as shown in figure 6.15. The block boundaries were not intended to be fault traces, although there is the Busch fault running perpendicularly northeasterly from the Sargent fault. They merely serve as a means of separating groups of points that were thought to have some similar behaviour. Many of the weighted projection depictions suggested some "flow" of points around Station Hollis and up into block E. A portion of block E was kept and redesignated as zone 1. The northwestern part of block C was mated with block SW, as zone 2, to account for the locked portion of the San Andreas. The remainder of block C was considered with the lower portion of block E, as zone 3, to account for the locked section of the Calaveras fault. Hence, the movement of the Pacific plate against the North American plate would be reflected by the movement of zone 2 with respect to zone 1.

The maximum and minimum strains for these three peculiar groupings are shown with their deviations at 0.95 against the time intervals between campaigns in figure 6.16. If the rates are considered by scaling the depictions by the inverse of the time interval, there is a very obvious anticipation of the 1974 event and reaction to the 1979

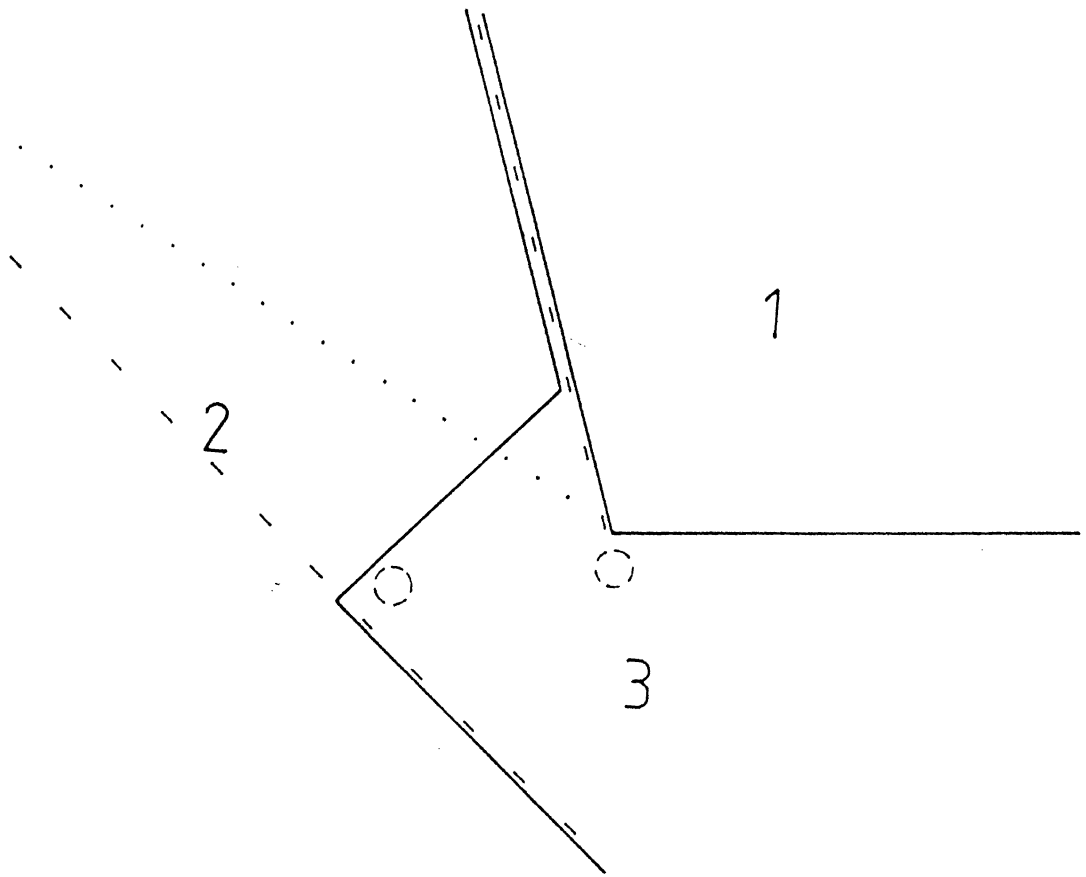

Figure 6.15 Hollister Relative Network: Peculiar Zoning

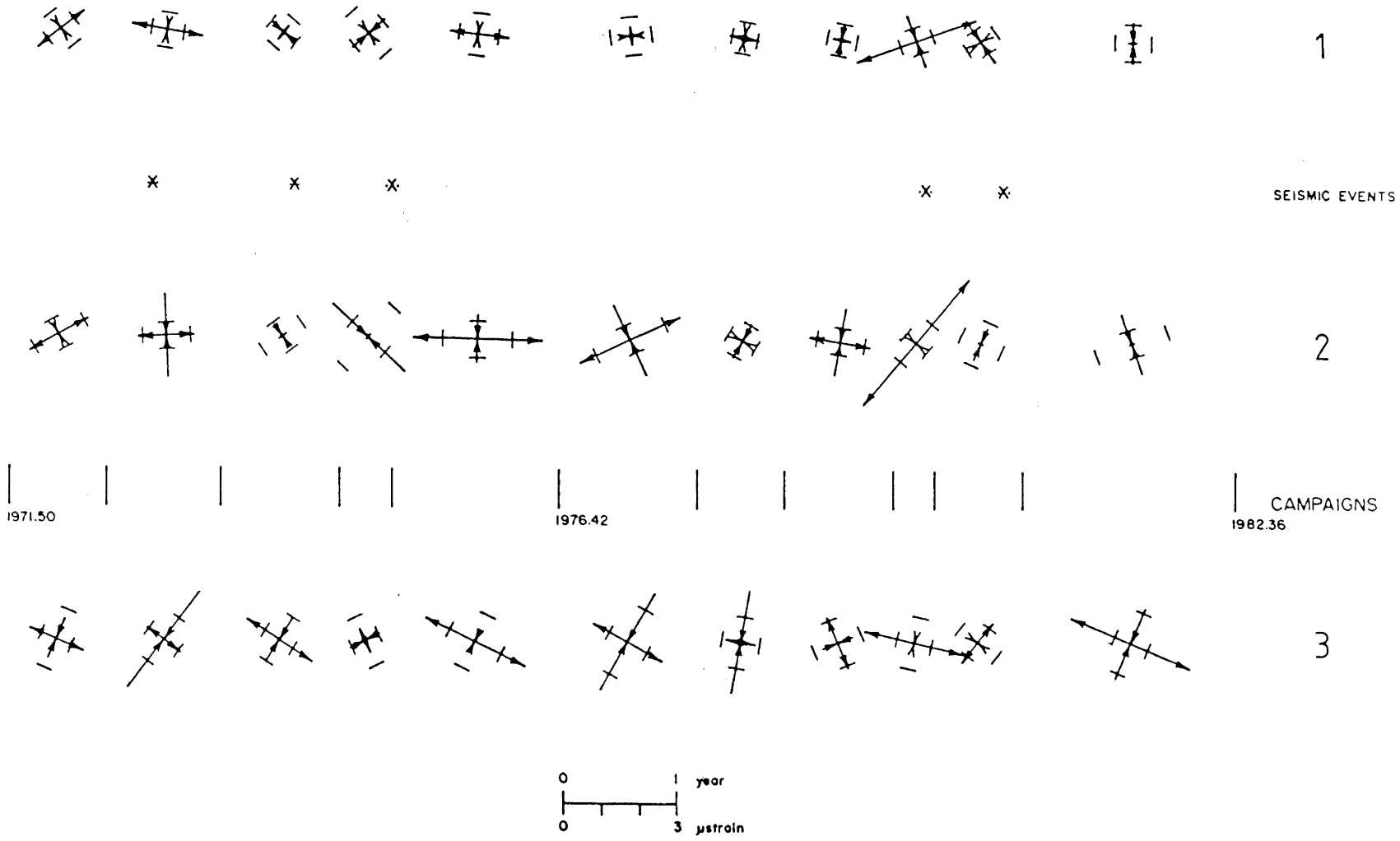

Figure 6.16 Hollister Relative Network: Maximum and Minimum Strain for Successive Time Intervals for Peculiar Zones (deviations at $\alpha = 0.05$)

event. Thus, the time intervals for modelling were defined to reflect these discontinuities by considering 1970 to 1974 preseismic, 1974 postseismic to 1979 preseismic, and 1979 postseismic to 1982.

A multitude of models (rates, accelerations, higher order polynomials in both space and time) were attempted for a variety in the simultaneous solution for the parameters. Some solutions were statistically acceptable, while others were similar to the ones above. A sampling is given in table 6.6. However, such gymnastics isolated from any dialogue with geophysicists would be neverending.

Any sort of elaborate model could be fitted to the data; however, both the number and distribution of stations limit the level of complication and the quality of fitting. Although there may be many observables,. e.g. ~120 in Hollister, and even though the degrees of freedom in statistical assessment is high, the modelling quality stems from the sampling points. Commonly, a surface describing the deformation of a horizontal network is not likely to be of an order higher than third. This is revealed in the complex crustal strain approximation by Schneider (1982) in which nearly 100 models were attempted on the Hollister data for 1970 to 1980. His final model had $(\hat{\sigma}_0^2)^{1/2} = (4.915)^{1/2}$ = 2.217 (979 observations, 826 degrees of freedom) which had been recognized as not being compatible with $\sigma_0^2 = 1$. Yet, it was this model that was the basis for his conclusions about the behaviour of the network.

Although the sample models using the generalized approach were not entirely successful, they serve to illustrate the flexibility of the generalized method and its ability to provide an assessment of its overall appropriateness and of the significance of specific

Interval	Blocks or Zones i,j,k	i						j vs. i										j										k vs. i										k										T^2 model $\frac{\hat{\sigma}_o^2}{\sigma^2} = \hat{\sigma}_o^2$
		$\dot{\epsilon}_x$		$\dot{\epsilon}_y$		$\dot{\epsilon}_{xy}$	$\ddot{\epsilon}_x$		$\ddot{\epsilon}_y$		$\ddot{\epsilon}_{xy}$		$\dot{a}_o$		$\dot{b}_o$		$\ddot{a}_o$		$\ddot{b}_o$		$\dot{\epsilon}_x$		$\dot{\epsilon}_y$		$\dot{\epsilon}_{xy}$		$\ddot{\epsilon}_x$		$\ddot{\epsilon}_y$		$\ddot{\epsilon}_{xy}$		$\dot{a}_o$		$\dot{b}_o$		$\ddot{a}_o$		$\ddot{b}_o$		$\dot{\epsilon}_x$		$\dot{\epsilon}_y$		$\dot{\epsilon}_{xy}$		$\ddot{\epsilon}_x$		$\ddot{\epsilon}_y$		$\ddot{\epsilon}_{xy}$	
1970.565 1979.490	E,C,SW							-7.1		16.9																			-16.8		26.4																			3.584
1970.565 1980.480	E,C,SW							-7.4		18.5																			-16.8		27.3																			4.778
1970.565 1982.355	E,C,SW							-6.8		18.6																			-16.0		26.8																			5.635
1970.565 1980.480	E,C,SW	0.24		-0.11		0.10		-2.8		17.9								0.44		-0.07		0.11							-15.8		29.2								74		81		30							4.064
1970.565 1982.355	E,C,SW	0.24		-0.20		0.13		-3.3		19.8								0.42		71		0.11							-15.0		29.7								54		70		14							4.516
1974.940 1979.490	E,C,SW	0.68		17		38	-0.11		16	42			94		0		90		2.7	0.88		-0.58		82		43	86		43	32		29.7		77		55		11		72		61		26		84		51	2.177
1970.565 1979.490	E,C,SW	93		0		81	57		18	73			-11.3		9.5		0.8		60	42		-0.45		93		81	79		0.03	-15.2		33.8		17		81		74		65		26		79		76		23	2.989
1970.565 1972.380	1,2,3	0.52		79		0.57							71		18.6					0.78		42		0.66					-15.9		82						0.59		-0.90		-0.58							1.005*
1971.460 1972.380	1,2,3	0.50		82		0.55							78		18.3					0.83		38		0.69					-14.9		14						93		72		94							0.943*
1974.940 1979.490	1,2,3	94		-0.16		74							26		4.8					0.55		-0.62		90					-8.1		7.2						0.40		-0.39		-0.42							2.285
1979.690 1980.480	1,2,3	67		73		85							94		29.4					44		86		19					-40.3		29.0						73		41		-1.43							1.703
1980.480 1982.355	1,2,3	21		-0.36		58							85		18.0					32		-0.37		91					-16.1		12.1						0.67		84		-0.62							1.418*
1974.940 1979.490	1,2,3	88		10		36	69		44	5			87		37		91		46	0.93		-0.48		89		77	58		75	88		41		39		22		84		73		-0.62		45		14		50	2.212
1973.315 1975.270	1,2,3	3		44		46	30		62	25			82		84		94		26	65		14		84		86	78		72	58		21		9		69		63		37		79		38		38		28	2.076
1973.315 1975.270	1,2,3	"Third Order "Polynomial"																																														1.684
1970.565 1974.900	1,2,3	"Third Order "Polynomial"																																														2.150

values of parameters are given in μstrain y^{-1}, μstrain y^{-2}, $\mu m y^{-1}$, $\mu m y^{-2}$
when $(1-\alpha) \geq 95\%$

value of $(1-\alpha)$ in percent is given when $(1-\alpha) < 95\%$

* denotes $\hat{\sigma}_o^2 = \sigma_o^2$ at 0.95

Table 6.6 Hollister Relative Network: Sample of Modelling Attempts

parameters or derived quantities. This data was being analysed more in the context of comparison with others of the F.I.G. "ad hoc" Committee because of its peculiarities as real data and in showing the application of the method. As mentioned above, in Chen (1983), and in Chrzanowski et al., (1982a), the investigation of a deformation entails the analysis as only a part of the whole effort. Meaningful analysis of data in some specific application, e.g. the Hollister network as an earthquake precursor, requires ample dialogue with other specialists, even at the outset of the investigation for proper design of the scheme.

The diffusion of fault traces (figure 6.7) would cast doubt on the gathering of stations together to act as a homogeneously straining body and also render a difficult comparison of very local creepmeter behaviour with that described by the network. The possibility of station mark instability in its reaction to the moisture content of the surrounding soil (Savage et al., 1979) would detract from the ability of the network of measurements to reflect the behaviour of the underlying bedrock of which the plates are comprised.

Thus, as a precursory mechanism, the trilateration network may not be as effective as other types of observables (e.g. creepmeters (Evans et al., 1981), deep borehole strainmeters, radon content of ground water) partly because of its situation by having only a small portion (SW) on the Pacific plate and partly because of the nature of the scheme of measuring only annually. Also, as some indication of tectonic plate movement, the network may not extend far enough beyond the fault zone to yield relative movement as might be gained from GPS or VLBI (e.g. Savage et al., 1981).

Especially in the case of areas similar to Hollister and elsewhere in California, a plethora of measurements of observables other than the geodetic survey described here has amassed over the last two decades. Collected by numerous agencies and research institutes, the variety has remained segregated, e.g. measurements of alignment (Burford and Harsh, 1981), of creep (Schulz et al., 1982, 1983), of strain (Slater and Burford, 1979; Johnston et al., 1978), and of tilt (Mortensen and Johnston, 1975; Sylvester, 1981), and geodetic micronetworks (Lisowski and Prescott, 1981), often with somewhat isolated analyses. As revealed in the discussion of observation equations (section 4.2), the generalized method would be such a means for an integrated analysis, similar to that advocated by Reilly (1981).

7. CONCLUSIONS AND RECOMMENDATIONS

In the development of the generalized method, several objectives were achieved in order to render it generalized. Although rigorously developed, the method is relatively uncomplicated and is readily adaptable to the variety of circumstances met in deformation surveys. Together with the several examples of Chen (1983) and those of Chrzanowski and Secord (1983a, b) and of Chrzanowski et al. (1982c, 1983a, b), this thesis has shown how these objectives were met and how easily the method may be applied to an assortment of conditions.

The generality is reflected in the objectives as given in the introduction. Basically the same procedure is applied to any intended style of network or deformation problem and the generalized method dissolves into many common methods as special cases. The same method was applied in the line fitting of the trend analysis of the Hollister relative network as was done in the overall analysis. Also, it was applied to both basic types of networks, but with modelling appropriate to the situation. As revealed in the forms of the observation equations, the method is equally comfortable in three, two, or one dimension with or without temporal parameters. Also, the observation equations show the possibilities for considering all forms of observables including not only geodetic angular and linear measurement and photogrammetry, but

also geotechnical measurements of tilt, strain, pressure, etc. Extending the concept of being generalized even further encompasses the ability of the model parameter estimation to utilize other data, e.g. coordinates or coordinate differences as from photogrammetry for example, along with their covariances and this may be done simultaneously with the customary observables. This has not been fully illustrated in these examples, but the exercise is presently underway. Any sort of configuration, whether defective or incomplete to any extent, may be accommodated, as, for example, in the Hollister network. The datum independence of the depiction of trend, and of the deformation parameter estimation allows the use of any choice of minimal constraints at the outset of the analysis and also to create data for later use in the estimation. The variety of routes, shown in figure 2.2, most of which were followed in the two examples here, reflects the variability and adaptability of this generalized method.

The Lohmuehle reference network example has shown how the intended stable reference was salvaged and a reasonable analysis obtained. A more meaningful effort would have resulted from more campaigns of measurements and more information on secondary circumstances. The facility is available in the generalized method. The only deficiency is in the supply of data and the wherewithal for its analysis. Some efforts at an integrated analysis are underway; but the data has been simulated, both physically and analytically.

The example of the Hollister relative network illustrates how the defect problem can be overcome and how many campaigns can be processed. In this particular case, the complications of the situation

of the network did not allow a clear analysis. But the statistical guidance has ensured that, at least, false conclusions would not be drawn readily from the analysis. Establishing dialogue with other experts, e.g. geophysicists, and the use of other data would enhance the analysis and more likely lead to some meaningful description of the behaviour of the Hollister area. The generalized method possesses the flexibility and capability for an analysis integrating other information. The only limit is the basis for choosing the models. The analysis of only the trilateration network does not seem suitable for the purposes of either the prediction of earthquakes or the description of tectonic movement. Nonetheless, the purpose of the analysis here was to illustrate the applicability of the generalized method and not to present an analysis of the behaviour of the network.

The present constriction on the full application of the generalized method has been the availability of data and interest external to the University. This has been slowly coming forth - several agencies in hydro-electric power, coal mining, and petroleum extraction, have expressed interest, most notably of which has been a contract with Maraven, S.A. in the monitoring of an oil field in Venezuela. The experiences with the applications here and with those cited in the references have convinced this author that the method will readily prove its worth, if given the opportunity to exercise. Present activities include the analysis of other networks, but they are very much similar to the examples already presented.

In the full sense of being generalized, this method would not be limited to the analyses of deformations, but to any circumstance in which coordinates or points would be compared or matched together. In photogrammetry, for example, several different sets of photographs could be considered together with various control to obtain overall information with regard to ground point positions, not necessarily of their change. Also, this method could be applied to the consolidation of cadastral survey records by recognizing various sources, e.g. digitized cadastral maps or an assortment of segregated surveys. In a similar sense, the method can easily envelope the more contemporary forms of positioning and relative positioning, e.g. Global Positioning System, Very Long Baseline Interferometry, Inertial Survey System, with the appropriate observation equations used for positioning and position change monitoring.

REFERENCES

Anderson, D.L. (1971). "The San Andreas Fault", Scientific American 1971, 11, 87-102.

Armenakis, C.; W. Faig (1982). "Photogrammetric monitoring of mining subsidence", Proceedings of the Centennial Convention 1982 04 19-23, Canadian Institute of Surveying, Ottawa, 278-286.

Bibby, H.M. (1973). "The Reduction of Geodetic Survey Data for the Detection of Earth Deformation", New Zealand, Dept. of Scientific and Industrial Research, Geophysics Division, Report No. 84, Wellington 1973 08, 34 pp.

Bibby, H.M. (1982). "Unbiased estimate of strain from triangulation data using the method of simultaneous reduction", Tectonophysics 82 (1982), 161-174.

Blaha, G. (1971). Inner Adjustment Constraints with Emphasis on Range Observations, Ohio State University, Dept. of Geodetic Science, Report No. 148, 1971 01, 85 pp.

Brunner, F.K. (1979). "On the analysis of geodetic networks for the determination of the incremental strain tensor", Survey Review XXV, 192, 1979 07, 56-67.

Brunner, F.K.; R. Coleman; B. Hirsch (1981). "A comparison of computational methods for crustal strains from geodetic measurements" in P. Vyskocil, R. Green, H. Malzer (edit), Recent Crustal Movements 1979, Tectonophysics 71 (1981), 281-298.

Burford, R.O.; P. Harsh (1980). "Slip along the San Andreas fault in central California from alinement array surveys", Bulletin of the Seismological Society of America 70 (4), 1233-1261.

Chen, Yong-qi (1983). Analysis of Deformation Surveys - A Generalized Method, University of New Brunswick, Dept. of Surveying Engineering, Technical Report 94, 1983 04, 262 pp.

Chen, Y-q; M. Kavouras; A. Chrzanowski (1984). "A strategy for the detection of outliers using a generalized approach", submitted to Manuscripta Geodaetica, 16 pp.

Chen, Y-q; M. Kavouras; J.M. Secord (1983). "Design considerations in deformation monitoring", F.I.G. XVII International Congress, Sofia, 1983 06 19-28, paper 603.2, 14 pp.

Chrzanowski, A. (1981). "A comparison of different approaches into the analysis of deformation measurements", F.I.G. XVI International Congress, Montreux 1981 08 09-18, paper 602.3, 24 pp.

Chrzanowski, A.; Chen, Y-q. (1981). "A systematic analysis of tectonic deformations from fault-crossing geodetic surveys", University of New Brunswick, Dept. of Surveying Engineering, Internal Report, 20 pp.

Chrzanowski, A.; J.M. Secord (1983a)."Report on the deformation analysis of the monitoring network at the Lohmuehle Dam", circulated to members of F.I.G. Commission 6 Study Group C Committee on the Analysis of Deformation Surveys, 18 pp.

Chrzanowski, A.; J.M. Secord (compile)(1983b). "Report of the ad hoc committee on the analysis of deformation surveys", F.I.G. XVII International Congress, Sofia, 1983 06 19-28, paper 605.2, 15 pp.

Chrzanowski, A.; Chen, Y-q.; J.M. Secord (1982a). "A general approach to the interpretation of deformation measurements", Proceedings of the Centennial Convention 1982 04 19-23, Canadian Institute of Surveying, Ottawa, 247-266.

Chrzanowski, A.; Chen, Y-q.; J.M. Secord (1982b). "On the analysis of deformation surveys", Proceedings of the Fourth Canadian Symposium on Mining Surveying and Deformation Measurements, Banff, 1982 06 07-09; Canadian Institute of Surveying, 431-452.

Chrzanowski, A.; Chen, Y-q.; J.M. Secord (1982c). "A generalized approach to the geometric analysis of deformation surveys", F.I.G. III International Symposium on Deformation Measurements by Geodetic Methods, Budapest, 1982 08 25-27; in Joo, I.; A. Detrekoi (edit), Deformation Measurements/Deformationsmessungen, Akademiai Kiado, Budapest, 349-371.

Chrzanowski, A.; Chen, Y-q.; J.M. Secord (1983a). "Analysis of the simulated monitoring network using the Fredericton approach", Proceedings of the F.I.G. Commission 6 Study Group C Seminar on Geometric Analysis and Interpretation of Geodetic Deformation Surveys, Munich, 1983 04 22 in W. Welsch (edit) Deformationsanalysen '83, HSBw, Munich, 95-117.

Chrzanowski, A.; Chen, Y-q.; J.M. Secord (1983b). "On the strain analysis of tectonic movements using fault crossing geodetic surveys", in P. Vyskocil, A.M. Wassef, R. Green (edit) Recent Crustal Movements 1982, Tectonophysics 97 (1983), 297-315.

Evans, K.F.; R.O. Burford; G.C.P. King (1981). "Propogating episodic creep and the aseismic slip behaviour of the Calaveras fault north of Hollister, California, Journal of Geophysical Research, V. 86, n. B5 1981 05 10, 3721-3735.

Goulty, N.R.; P.M. Davis; R. Gilman; N. Motta (1979). "Meteorological noise in wire strainmeter data from Parkfiled, Calif.", Bulletin of the Seismological Society of America, v. 69, no. 6, 1979 12 1983-1988.

Harrison, J.C. (1976). "Cavity and topographic effects in tilt and strain measurement", Journal of Geophysical Research, v. 81, 319-336.

Heck, B. (1981). "Der Einfluss einzelner Beobachtungen auf das Ergebnis einer Ausgleichung und die Suche nach Ausreissern in den Beobachtungen", Allgemeine Vermessungs-nachrichten 1, 17-34.

Herd, D.G. (1979). "Neotectonic framework of central coastal California and its implications to microzonation of the San Francisco Bay region", in E.E. Brabb (edit), Progress on Seismic Zonation in the San Francisco Bay Region, United States Geological Survey, Circular 807, 12 pp.

Himmelblau, D.M. (1970). Process Analysis by Statistical Methods, McGraw-Hill, New York.

Jaeger, J.C. (1969). Elasticity, Fracture, and Flow, Methuen, London.

Jennings, C.W.; R.G. Strand (compile) (1958). Geologic Map of California Santa Cruz Sheet, State of California, Dept. of Natural Resources, Division of Mines.

Johnston, M.J.S.; A.C. Jones; C.E. Mortensen; B.E. Smith (1978). "Continuous tilt, strain, and magnetic field measurements near four earthquakes (M_l = 3.6 to 3.8) on the San Andreas fault, California", United States Geological Survey, Open File Report 78-987, 22 pp.

King, N.E.; J.C. Savage; M. Lisowski; W.H. Prescott (1981). "Preseismic and coseismic deformation associated with the Coyote Lake, Calif., earthquake", Journal of Geophysical Research, v. 86, 892-898.

Lazzarini, T. (1974). "Determination of displacements and deformation of structures and their environment by geodetic means", University of New Brunswick, Dept. of Surveying Engineering, unpublished lectures, 40 pp.

Leick, A. (1982). "Minimal constraints in two-dimensional networks", American Society of Civil Engineers, Journal of Surveying and Mapping Division, v. 108, n. SU2, 1982 08, 53-68.

Lisowski, M.; W.H. Prescott (1981). "Short range distance measurements along the San Andreas fault system in central California", Bulletin of the Seismological Society of America 71(5), 1607-1624.

Mortensen, C.E.; M.J.S. Johnston (1975). "The nature of surface tilt along 85 km of the San Andreas fault - preliminary results from a 14-instrument array", Pure and Applied Geophysics, v. 113, 237-249.

Polak, M. (1978). "Examination of the stability of reference points in distance and combined angle-distance networks", F.I.G. II International Symposium on Deformation Measurements by Geodetic Methods, Bonn, 10 pp.

Pope, A.J. (1966). Strain Analysis of Repeated Triangulation for the Investigation of Crustal Movement, Ohio State University, Dept. of Geodetic Science, M.Sc. thesis, 95 pp.

Pope, A.J. (1971). "Transformation of covariance matrices due to changes in minimal control", American Geophysical Union, Fall Meeting, San Francisco, 1971 12 09, 25 pp.

Pope, A.J. (1976). The Statistics of Residuals and the Detection of Outliers, United States Dept. of Commerce, NOAA Technical Report NOS 65 NGS1, 22 pp.

Prescott, W.H. (1981). "The determination of displacement fields from geodetic data along a strike slip fault", Journal of Geophysical Research, v. 86, n. B7, 1981 07 10, 6067-6072.

Prescott, W.H.; J.C. Savage (1974). Effects of the Bear Valley and San Juan Bautista earthquakes of 1972 on geodimeter line lengths", Bulletin of the Seismological Society of America, v. 64, n. 1, 1974 02, 65-72.

Prescott, W.H.; J.C. Savage; W.T. Kinoshita (1979). "Strain accumulation rates in the western United States between 1970 and 1978", Journal of Geophysical Research, v. 84, n. B10, 1979 09 10, 5423-5435.

Reilly, W.I. (1981). "Complete determination of local crustal deformation from geodetic observations", in P. Vyskocil, R. Green, H. Malzer (edit) Recent Crustal Movements 1979, Tectonophysics 71 (1981), 111-123.

Reilly, W.I. (1982). "Three dimensional kinematics of earth deformation from geodetic observations", I.A.G. Proceedings of the International Symposium on Geodetic Networks and Computations, Munich, 1981 08 31 - 09 05, v.V Network Analysis Models, Deutsche Geodatische Kommission, Heft Nr. 258/V, 207-221.

Rogers, T.H. (compile) (1966). Geologic Map of California San Jose Sheet, State of California, Resources Agency, Dept. of Conservation, Division of Mines and Geology.

Rueger, J.M. (1980). Introduction to Electronic Distance Measurement, University of New South Wales, School of Surveying, Monograph No. 7, 2nd edn. 1980 03, 128 pp.

Savage, J.C.; W.H. Prescott (1973). "Precision of geodetic distance measurements for determining fault movements", Journal of Geophysical Research, v. 78, n. 26, 1973 09 10, 6001-6008.

Savage, J.C.; M.A. Spieth; W.H. Prescott (1976). "Preseismic and coseismic deformation associated with the Hollister, California earthquake of November 28, 1974", Journal of Geophysical Research v. 81, n. 20, 1976 07 10, 3567-3574.

Savage, J.C.; W.H. Prescott; M. Lisowski; N.E. King (1979). "Geodolite measurements of deformation near Hollister, California, 1971-1978", Journal of Geophysical Research, v. 84, n. B13, 1979 12 10, 7599-7615.

Savage, J.C.; W.H. Prescott, M. Lisowski; N.E. King (1981). "Strain accumulation in southern California, 1973-1980", Journal of Geophysical Research, v. 86, n.B8, 1981 08 10, 6991-7001.

Schlossmacher, E.J. (1973). "An iterative technique for absolute deviations curve fitting", Journal of the American Statistical Association, v. 68, 857-859.

Schneider, D. (1982). Complex Crustal Strain Approximation, University of New Brunswick, Dept. of Surveying Engineering Technical Report 91, 1982 09, 221 pp.

Schulz, S.; R.O. Burford; B. Mavko (1983). "Influence of seismicity and rainfall on episodic creep on the San Andreas fault system in central California", Journal of Geophysical Research, v. 88, n. B9, 1983 09 10, 7475-7484.

Schulz, S.S.; G.M. Mavko; R.O. Burford; W.D. Stuart (1982). "Long-term fault creep observations in central California", Journal of Geophysical Research, v. 87, n. B8, 1982 08 10, 6977-6982.

Slater, L.E.; R.O. Burford (1979). "A comparison of long-baseline strain data and fault creep records obtained near Hollister, California", Tectonophysics, 52 (1979), 481-496.

Snay, R.A.; M.W. Cline; E.L. Timmerman (1983). "Regional deformation of the earth model for the San Diego region, California", Journal of Geophysical Research, v. 88, n. B6, 1983 06 10, 5009-5024.

Sokolnikoff, I.S. (1956). Mathematical Theory of Elasticity, McGraw-Hill, New York.

Spectra-Physics (1969). Geodolite Laser Distance Measuring Instrument, Spectra-Physics, Mountain View, California, data sheet 1969 02.

Sylvester, A.G. (1981). "Dry tilt and nearfield geodetic investigations of crustal movements; southern California", United States Geological Survey, Open File Report 81-293, 92 pp.

Thapa, K. (1980). Strain as a Diagnostic Tool to Identify Inconsistent Observations and Constraints in Horizontal Geodetic Networks, University of New Brunswick, Dept. of Surveying Engineering Technical Report 68, 162 pp.

Tobin, P. (1983). Examination of Deformation Measurements using Invariant Functions of Displacements, University of New Brunswick, Dept. of Surveying Engineering M.Sc.E. thesis, 72 pp.

Vanicek, P.; E.J. Krakiwsky (1982). Geodesy: The Concepts, North-Holland Pub. Co., Amsterdam, 691 pp.

Vanicek, P.; M.R. Elliott; R.O. Castle (1979). "Four dimensional modelling of recent vertical movements in the area of the southern California uplift", Tectonophysics 52(1979), 287-300.

Veress, S.A. (1981). "Measurement of structural deformation of electric transmission towers", F.I.G. XVI International Congress, Montreux, 1981 08 09-18, paper 604.1, 10 pp.

Welsch, W. (1979). "A Review of the adjustment of free networks", Survey Review, v. XXV, n. 194, 1979 10, 167-180.

Welsch, W.M. (1983). "Finite element analysis of strain patterns from geodetic observations across a plate margin", in P. Vyskocil, A.M. Wassef, R. Green (edit) Recent Crustal Movements 1982, Tectonophysics 97 (1983), 57-71.

A.1 NOTATION

A	first order design or configuration matrix
B	design matrix in the deformation model
C	variance-covariance matrix
D	design matrix for imposing constraints
D	superscript to derived or generated observation values
E	infinitesimal non-translational deformation tensor
F	Fisher distribution
H	datum defect description matrix
H_o	null hypothesis
H_A	alternative hypothesis
N	matrix of normal equations
P	typical occupied station (figure 4.2)
P	weight matrix
Q	typical second station (figure 4.2)
Q	cofactor matrix
S	space spanned by the subscript
S	segregating matrix
T^2	statistic
$\underline{c}$	vector of parameters in the deformation model
d	defect
$\underline{d\ell}$	vector of observation differences
$\underline{dx}$	vector of displacement components
$\vec{dx}$	vector of displacement
e	element of E
k	scale factor

$\underline{\ell}$ vector of observations

n number of elements

p number of stations or points

q element of Q

$\underline{r}$ vector of direction cosines (figure 4.2; section 4.2)

s spatial distance

t student's t distribution

$\underline{u}$ vector of "constants"

u displacement component parallel to x-axis

$\underline{v}$ vector of residuals

v displacement component parallel to y-axis

w displacement component parallel to z-axis

x

y coordinates (figure 4.2)

z

Δ large change

Δ dilatation (section 4.1)

Σ summation

α horizontal azimuth (figure 4.2)

α level of significance; probability of a type I error

β zenith angle (figure 4.2)

γ shear (section 4.1)

$\underline{\delta}$ vector of outlying observations

δ small change

ε strain (section 4.1)

ε "belongs to"; "is an element of"

ν	degrees of freedom
ξ	abscissa of a distribution
$\underline{\xi}$	vector of nuisance parameters
ρ	correlation coefficient
σ	element of C
σ_o^2	variance factor
τ	tau-distribution (Pope, 1976)
χ^2	chi-squared distribution
ψ	subscript denoting "pseudo" or false
ω	rotation
~	approximately; in the order of
^	superscript: least squares estimate
·	superscript: rate or first derivative against time
¨	superscript: acceleration or second derivative againt time
-	superscript: mean value
_	subscript: vector

A.2 Example of the Weighted Projection

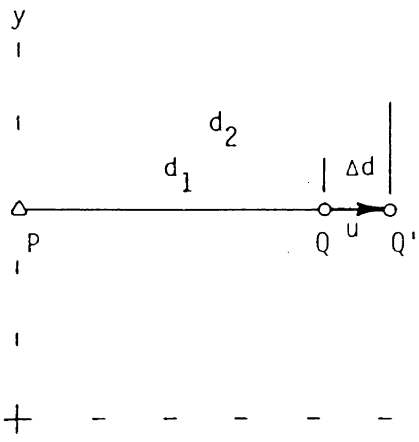

P(0, y);

Q(x, y);

Q'(x+u, y);

$\Delta d = d_2 - d_1$

The datum dependent displacement, u, of Q was determined from the repeated measurement of the distance PQ and by considering P as fixed. The datum independent relative displacement is obtained by the weighted projection as follows.

$$\text{adjustment yielded } \underline{dx} = \begin{bmatrix} \hat{u}_Q \\ \hat{v}_Q \\ \hat{u}_P \\ \hat{v}_P \end{bmatrix} = \begin{bmatrix} u \\ v \\ 0 \\ 0 \end{bmatrix} \text{ with } C_{dx} = \begin{bmatrix} \sigma_u^2 & \sigma_{uv} & 0 & 0 \\ \sigma_{vu} & \sigma_v^2 & 0 & 0 \\ 0 & 0 & 0 & 0 \\ 0 & 0 & 0 & 0 \end{bmatrix}$$

generally

$$H = \begin{array}{c} \begin{matrix} \delta x & \delta y & k & \omega \end{matrix} \\ \begin{bmatrix} 1 & 0 & x_Q-\bar{x} & -y_Q+\bar{y} \\ 0 & 1 & y_Q-\bar{y} & x_Q-\bar{x} \\ 1 & 0 & x_P-\bar{x} & -y_P-\bar{y} \\ 0 & 1 & y_P-\bar{y} & x_P-\bar{x} \end{bmatrix} \end{array} ; \quad H = \begin{array}{c} \begin{matrix} \delta x & \delta y & \omega \end{matrix} \\ \begin{bmatrix} 1 & 0 & 0 \\ 0 & 1 & x/2 \\ 1 & 0 & 0 \\ 0 & 1 & -x/2 \end{bmatrix} \end{array}$$

since scale already determined by d_i.

$P_0 = \text{diag}(1,\ 1,\ 1,\ 1) = I;\ \underline{dx}_0 = [u,\ 0,\ 0,\ 0]^T$ since $v = 0$

$$\underline{dx}_1 = [I - H(H^T P_0 H)^{-1} H^T P_0]\underline{dx}_0$$

$$= [I - H(H^T H)^{-1} H^T]\underline{dx}_0$$

$$= [I - H\begin{bmatrix} 2 & 0 & 0 \\ 0 & 2 & 0 \\ 0 & 0 & x^2/2 \end{bmatrix}^{-1} H^T]\underline{dx}_0$$

$$= [I - H\begin{bmatrix} \frac{1}{2} & 0 & 0 \\ 0 & \frac{1}{2} & 0 \\ 0 & 0 & \frac{2}{x^2} \end{bmatrix} H^T]\underline{dx}_0$$

$$= [I - H\begin{bmatrix} \frac{1}{2} & 0 & \frac{1}{2} & 0 \\ 0 & \frac{1}{2} & 0 & \frac{1}{2} \\ 0 & \frac{1}{x} & 0 & -\frac{1}{x} \end{bmatrix}]\underline{dx}_0$$

$$= [I - \begin{bmatrix} \frac{1}{2} & 0 & \frac{1}{2} & 0 \\ 0 & 1 & 0 & 0 \\ \frac{1}{2} & 0 & \frac{1}{2} & 0 \\ 0 & 0 & 0 & 1 \end{bmatrix}]\underline{dx}_0$$

$$= \begin{bmatrix} \frac{1}{2} & 0 & -\frac{1}{2} & 0 \\ 0 & 0 & 0 & 0 \\ -\frac{1}{2} & 0 & \frac{1}{2} & 0 \\ 0 & 0 & 0 & 0 \end{bmatrix}\begin{bmatrix} u \\ 0 \\ 0 \\ 0 \end{bmatrix} = \begin{bmatrix} \frac{u}{2} \\ 0 \\ -\frac{u}{2} \\ 0 \end{bmatrix}$$

$P_1 = \text{diag}(\frac{2}{u} \quad 0 \quad \frac{2}{u} \quad 0)$, so, say $P_1 = \text{diag}(\frac{200}{u} \quad 1 \quad \frac{200}{u} \quad 1)$

for numerical stability.

$$\underline{dx}_2 = [I - H(H^T P_1 H)^{-1} H^T P_1]\underline{dx}_1$$

$$= [I - H(H^T \begin{bmatrix} \frac{200}{u} & 0 & 0 \\ 0 & 1 & \frac{x}{2} \\ \frac{200}{u} & 0 & 0 \\ 0 & 1 & -\frac{x}{2} \end{bmatrix})^{-1} H^T P_1]\underline{dx}_1$$

$$= [I - H \begin{bmatrix} \frac{400}{u} & 0 & 0 \\ 0 & 2 & 0 \\ 0 & 0 & \frac{x^2}{2} \end{bmatrix}^{-1} H^T P_1]\underline{dx}_1$$

$$= [I - H \begin{bmatrix} \frac{u}{400} & 0 & 0 \\ 0 & \frac{1}{2} & 0 \\ 0 & 0 & \frac{2}{x^2} \end{bmatrix} H^T P_1]\underline{dx}_1$$

$$= [1 - H \begin{bmatrix} \frac{u}{400} & 0 & \frac{u}{400} & 0 \\ 0 & \frac{1}{2} & 0 & \frac{1}{2} \\ 0 & \frac{1}{x} & 0 & -\frac{1}{x} \end{bmatrix} P_1]\underline{dx}_1$$

$$= [I - H \begin{bmatrix} \frac{1}{2} & 0 & \frac{1}{2} & 0 \\ 0 & \frac{1}{2} & 0 & \frac{1}{2} \\ 0 & \frac{1}{2} & 0 & -\frac{1}{x} \end{bmatrix}]\underline{dx}_1$$

$$= [I - \begin{bmatrix} \frac{1}{2} & 0 & \frac{1}{2} & 0 \\ 0 & 1 & 0 & 0 \\ \frac{1}{2} & 0 & \frac{1}{2} & 0 \\ 0 & 0 & 0 & 1 \end{bmatrix}] \underline{dx}_1$$

$$= \begin{bmatrix} \frac{1}{2} & 0 & -\frac{1}{2} & 0 \\ 0 & 0 & 0 & 0 \\ -\frac{1}{2} & 0 & \frac{1}{2} & 0 \\ 0 & 0 & 0 & 0 \end{bmatrix} \begin{bmatrix} \frac{u}{2} \\ 0 \\ -\frac{u}{2} \\ 0 \end{bmatrix} = \begin{bmatrix} \frac{u}{2} \\ 0 \\ -\frac{u}{2} \\ 0 \end{bmatrix}$$

so convergence has occurred. Therefore,

$$C_{dx_w} = [I - H(H^T P_1 H)^{-1} H^T P_1] \, C_{dx} [I - H(H^T P_1 H)^{-1} H^T P_1]^T$$

$$= \begin{bmatrix} \frac{1}{2} & 0 & -\frac{1}{2} & 0 \\ 0 & 0 & 0 & 0 \\ -\frac{1}{2} & 0 & \frac{1}{2} & 0 \\ 0 & 0 & 0 & 0 \end{bmatrix} C_{dx} [I - H(H^T P_1 H)^{-1} H^T P_1]^T$$

$$= \begin{bmatrix} \frac{\sigma_u^2}{2} & \frac{\sigma_{uv}}{2} & 0 & 0 \\ 0 & 0 & 0 & 0 \\ \frac{\sigma_u^2}{2} & \frac{-\sigma_{uv}}{2} & 0 & 0 \\ 0 & 0 & 0 & 0 \end{bmatrix} [I - H(H^T P_1 H)^{-1} H^T P_1]^T$$

$$= \frac{1}{4} \begin{bmatrix} \sigma_u^2 & 0 & -\sigma_u^2 & 0 \\ 0 & 0 & 0 & 0 \\ -\sigma_u^2 & 0 & \sigma_u^2 & 0 \\ 0 & 0 & 0 & 0 \end{bmatrix}$$